Yianni Mavrikios
Joao G. de Oliveira

Design Against Collision for Offshore Structures

MIT Sea Grant
College Program

Massachusetts
Institute of Technology
Cambridge
Massachusetts 02139

MITSG 83-7
April 1983

DESIGN AGAINST COLLISION FOR OFFSHORE STRUCTURES

by

Yianni Mavrikios

Joao G. de Oliveira

Sea Grant College Program
Massachusetts Institute of Technology
Cambridge, Massachusetts 02139

Report No. MITSG 83-7
Grant No. NA81-D-0069
Project No. R/O-2
April 1983

RELATED SEA GRANT REPORTS

Chryssostomidis, Marjorie. OFFSHORE PETROLEUM ENGINEERING: A BIBLIOGRAPHIC GUIDE TO PUBLICATIONS AND INFORMATION SOURCES. MITSG 78-5. New York: Nichols Publishing Company, 1978. 366 pp. $45.00.

Moan, Torgeir. THE ALEXANDER L. KIELLAND ACCIDENT: PROCEEDINGS FROM THE FIRST ROBERT BRUCE WALLACE LECTURE. MITSG 81-8. NTIS PB82 160987. Cambridge: Massachusetts Institute of Technology, Department of Ocean Engineering, 1981. 20pp. No charge.

De Oliveira, Joao G. THE BEHAVIOR OF STEEL OFFSHORE STRUCTURES UNDER ACCIDENTAL COLLISIONS. Reprint from 1981 Offshore Technology Conference in Houston, TX, May 4-7, 1981. 12 pp. No charge.

The Sea Grant Marine Information Center maintains an inventory of technical publications. We invite orders and inquiries to:

Sea Grant Marine Information Center
MIT Sea Grant College Program
Massachusetts Institute of Technology
Building E38-302
Cambridge, Massachusetts 02139
(617)253-5944

ACKNOWLEDGMENTS

The authors are grateful to the American Bureau of Shipping for providing the matching funds for this project. Special thanks are due to Mr. Stanley G. Stiansen, Vice President, Dr. Donald Liu, Chief Research Engineer, and Dr. Youl-Nan Chen, Assistant Chief Research Engineer, for their encouragement during the course of this work.

The authors are also indebted to Professor Tomasz Wierzbicki for the useful suggestions and criticism contributed during various stages of this work.

This research was sponsored by the MIT Sea Grant College Program under grant number NA79AA-D-00101 from the Office of Sea Grant, National Oceanic and Atmospheric Administration, U.S. Department of Commerce.

TABLE OF CONTENTS

Page

Acknowledgments ii

Table of Contents iii

List of Figures vi

List of Tables ix

Abstract x

Foreward xi

Introduction 1

Chapter 1: Local Deformation of Cylinders Under Transverse Loading

1.1 Introduction 9

1.2 Assumptions and Basic Geometry 11

1.2.1 Assumed Deformation Field 11

1.2.2 Definition of Coordinate Axes 14

1.2.3 Equations Describing the Deformation Field 16

1.3 Internal Energy Dissipation 19

1.3.1 Hoop Strain Dissipation 19

1.3.2 Bending Energy Dissipation 22

1.3.3 Membrane Extension Energy Dissipation 25

1.4 External Work 26

1.5 Load Calculation 27

1.6 Discussion 28

Chapter 2: Load Carrying Capacity of a Tubular Member Loaded Transversely

2.1 Introduction 32

2.2 Model for the Deformation Mode Interaction 34

2.3 Energy Dissipation due to Membrane Extension of Compression of the Middle Hinge 38

2.4 Calculation of the Crushing Load for a Simply Supported Tubular Beam 41

2.4.1 Analytical Expression for the Load Versus Deflection and Several Geometric Parameters 41

Page

2.4.2 Minimization Procedure 42

2.4.3 Numerical Results 43

2.5 Effect of Axial Restrain at the Supports 43

2.6 Discussion 51

Chapter 3: Dynamic Modelling of a Collision

3.1 Introduction 56

3.2 Simplified Collision Dynamics Model 57

3.3 Numerical Solutions of the Differential Equations 59

3.3.1 Formulation of the Recursive Relations Used for the Solution 59

3.3.2 Required Input for the Solution 61

3.3.3 Description of the Computer Program Used for the Solution of the Differential Equations 63

3.4 Numerical Examples 64

3.4.1 Cases Examined 64

3.4.2 Results 64

3.5 Discussion 65

Chapter 4: Cost Benefit Analysis for Minor Collisions

4.1 Introduction 80

4.2 Risk Analysis of Offshore Collisions 84

4.2.1 Collision Probability Based on Past Experience 85

4.2.2 Collision Probability Based on Simulation Techniques . . 86

4.3 Cost-Benefit Analysis 88

4.4 Conclusions 93

List of References 95

Page

Appendix A

A.1 Calculation of Angular Rotation ω' 98

A.2 Evaluation of the Equation Describing the Parabolic Approximation of the Cross-Section of the Plasticized Zone 99

A.3 Evaluation of the First Moment of Area of the Cross-Section Between the Inner and the Outer Hinge 102

A.4 Relation Between θ' and w_L 102

A.5 Relation Between λ' and γ' 104

A.6 Calculation of the Rate of Membrane Extension 105

A.7 Complete Numerical Results. 107

Appendix B

B.1 Calculation of the Location of the Plastic Neutral Axis for an Indented Section Subject to Both Global Bending and Local Tension 121

B.2 Evaluation of the Integrals Over the Sectional Areas Under Tension and Under Compression 123

B.3 Maximum Load that an Indented Section can Sustain Under Compression 124

B.4 Listing of the Minimization Program Used for the Calculations of the Total Load Capacity of a Tube. 125

B.5 Complete Numerical Results. 128

Appendix C

C.1 Method for Combining In Series two Non-Linear Springs which are Defined by Force-Deflection Curves Consisting of Linear Segments. 134

C.2 Calculation of the Initial Critical Time Step 135

C.3 Calculation of the Equivalent Mass and Added Mass of a Bottom-Supported Structure. 136

C.4 Listing of the Program Used for the Solution of the Collision Equations 138

C.5 Complete Numerical Results. 143

LIST OF FIGURES

		Page
1.1	Longitudinal Section of Hinge Planes	12
1.2	Coordinate Systems	15
1.3	Parabolic Approximation of the Cylinder's Cross Section	17
1.4	Cross Section of the Plasticized Region Between the Two Hinges	20
1.5	Deformation Pattern Caused by a Rectangular Indenter	24
1.6	Variation of the Local Crushing Load with the Loading Beam's Width	29
1.7	Comparison with Experiments	31
2.1	Load Deflection Curve Showing Transition from Local to Global Mode	33
2.2	Tubular Member's Cross Section	35
2.3	Superposition of Local and Global Strain and Strain Rates	36
2.4	Definition of the Local and the Global Deflection Rates	37
2.5	Regions of Integration	39
2.6	Crushing Curves for a S.S. Beam with R/h = 10.	44
2.7	Crushing Curves for a S.S. Beam with R/h = 17.65	45
2.8	Crushing Curves for a S.S. Beam with R/h = 25.	46
2.9	Crushing Curves for a S.S. Beam with L/R = 10.	47
2.10	Crushing Curves for a S.S. Beam with L/R = 15	48
2.11	Crushing Curves for a S.S. Beam with L/R = 20	49
2.12	Crushing Curves for a S.S. Beam with R/h = 17.65 and L/R = 6.11	50

Page

2.13 Increase in the Load Carrying Capacity Due to Axial Support Restraint 52

2.14 Global Load vs Global Deflection for an Axially Restrained Tubular Beam 53

2.15 Effect of Local Crushing Load on the Calculated Overall Load-Deflection Curve 55

3.1 Collision Model 58

3.2 Typical Load-Deformation Curve for Jacket's Cylindrical Leg 66

3.3 Typical Load-Deformation Curve for Jacket's Brace 67

3.4 Typical Load-Deformation Curve for a "Stiff" Bow 68

3.5 Typical Load-Deformation Curve for a "Soft" Bow 69

3.6 Typical Load-Deformation Curve for a Supply Vessel's Side 70

3.7 Typical Load-Deformation Curve for a Supply Vessel's Stern 71

3.8 Collision Scenario I 72

3.9 Collision Scenario II 73

3.10 Collision Scenario III 74

3.11 Collision Scenario IV 75

3.12 Collision Scenario V 76

3.13 Collision Scenario VI 77

3.14 Variation of Contact Force for Several Collision Scenarios 79

4.1 Distribution of Movements of Supply Vessels to and From Scottish East Coast Ports in July 1975 90

4.2 Distribution of the Tonnage of Supply Vessels Involved in Collisions in 1974-76 in the Northern North Sea 92

Page

A1 Coordinate System and Notation. 119

A2 General Longitudinal Vertical Cut at Subsequent Points During Deformation 120

B1 Different Regions in Tube's Cross Section 133

C1 Combination of Non-Linear Spring Characteristics. 161

C2 Combination of Non-Linear Spring Characteristics. 162

C3 Combination of Non-Linear Spring Characteristics When the Slope of One or More of the Linear Segments is Negative 163

C4 Notation for Collision Model 164

LIST OF TABLES

		Page
I.1	Fatal Accidents Offshore	2
I.2	Lives Lost in Structural Accidents Offshore	3
I.3	Structural Losses in Accidents Offshore	5
IV.1	Probability of Collisions at Sea	81
IV.2	Incidents Involving UK Offshore Installations in the North Sea in 1974/6	83

ABSTRACT

The force deflection curve for a rigid-plastic circular cylinder subjected to transverse loading applied by a sharp wedge is derived following an energy approach. A local deformation field is assumed and global deformation of the cylinder acting as a beam is neglected. The concept of the moving hinge with no slope discontinuity is used. The effects of the global deformation of the cylinder are then taken into consideration, and the overall force-deflection curve of the member acting as a beam is calculated.

The above obtained force-deflection curve, in combination with the equivalent curve for a ship's bow, and also the foundation stiffness of a platform are used as spring data for a simplified two-mass dynamic model with linear and nonlinear springs. This model is then used to determine numerically the plastic deformation on one platform member (leg or brace) due to a collision with a ship.

Finally a method is outlined for a cost-benefit analysis of a minor collision vs. strength of a platform, using probabilistic data on the risk of such a collision, and the platform's damage calculation method presented above.

FOREWORD

As offshore oil and gas exploration and production activities expand, industry and the public in general have become more aware of potential hazards which might seriously affect the safety of offshore operations. One such hazard is the possibility of collision between ships and offshore platforms. This is an area in which considerable attention has been devoted in Europe, particularly in Norway, Denmark and the United Kingdom. In the United States the project reported here was to our best knowledge the first attempt at studying this problem from an engineering point of view.

One of the main difficulties in studying the problem of collisions offshore is that these accidents can take a variety of forms, depending on many factors, such as the type of vessel and platform involved, the relative velocity and angle at impact and the environmental conditions. In extreme situations there is hardly anything the designer can do, except to try to improve navigation and handling capabilities and safety and evacuation procedures. Thus if a supertanker runs at 20 knots into a fixed platform a complete loss of the platform's structure probably cannot be avoided, and it would be unreasonable to modify the design to allow for such an extreme case. The very low probability of occurrence of such an accident is in general the main reason for ignoring it, as far as the platform design is concerned. It is then reasonable to concentrate on collision scenarios involving typical offshore supply vessels, for which the displacement is of the order of a few thousand tons. In such cases the probability of occurrence of collision accidents is not negligible, and it is possible to design the platform's structure so as to limit the extent of collision damage, improving as a result its survivability and performance under accidental load conditions.

In simple terms the purpose of this project is to develop a set of techniques capable of assisting the designer in assessing the behavior of an offshore platform when subjected to collision loads. These techniques can then be used to modify the structural design in such a way as to improve the collision damage survivability of the platform. A short discussion on cost-benefit considerations is also included in the present report.

This study cannot claim to cover in a comprehensive way all the aspects of collisions offshore. This is an area in which research work can still be done, and some suggestions regarding those aspects which can be considered as more critical are included in the present report.

Introduction

Although very detailed analytical methods have been developed and employed in the design of offshore platforms so that they will be able to withstand all the operational and environmental loads imposed on them during their expected life, not much work has yet been done in the area of protection against collision.

One reason for the above is that usually only a few collision accidents result in loss of life as compared to other accidents like blow-outs or explosions. Table I.1 shows the number of total accidents occuring in connection with platforms in world-wide operation during the 1/1/80 to 12/31/80 period. We can see that only 4 out of 62 fatal platform accidents were due to collision. In addition, each fatal collision accident has far less fatalities than accidents like capsizings. Table I.2 shows the number of lives lost in structural accidents for platforms in worldwide operation during the above mentioned eleven year period. We can see that capsizings average over 12 fatalities per accident as compared to 4 for collisions.

Unless the collision results in great structural damage, in addition to a few deaths, the accident is treated more or less as equivalent to a car accident and does not receive substantial coverage in the news media. From all collision accidents which occurred during the above mentioned period, only one resulted in total structural loss (a tanker with an old deserted platform in the Gulf of Mexico) and had only one fatality. The remaining collisions were small scale with supply boats. The fact that, most of the time, work on safety issues is initiated after a large scale accident has received considerable attention in the

TABLE I.1

Number of fatal accidents occurring in connection with platforms in world-wide operation during 70.01.01. - 80.12.31. according to initiating event and extent of structural damage.

ALL PLATFORMS (MOBILE PLATFORMS)					
Initiating event	Structural Loss				SUM
	Total	Severe	Damage	Minor	
Weather	1 (1)	-	-	-	1 (1)
Collision	1 (1)	1 (1)	-	1 (1)	3 (3)
Blow - out	4 (1)	6 (4)	2 (2)	1 (0)	13 (7)
Leakage	-	1 (1)	-	-	1 (1)
Machine etc.	-	-	1 (1)	-	1 (1)
Fire	-	1 (0)	1 (0)	2 (0)	4 (0)
Explosion	1 (0)	4 (2)	5 (2)	5 (4)	15 (0)
Out - of - pos	-	-	-	-	-
Foundering	-	-	1 (1)	-	1 (1)
Grounding	-	1 (1)	-	-	1 (1)
Capsizing	4 (4)	3 (3)	1 (1)	-	8 (88)
Structural strength	1 (1)	-	1 (0)	6 (4)	8 (5)
Other	-	-	-	4 (2)	4 (2)
SUM	12 (8)	17 (12)	12 (7)	19 (11)	60 (38)

Source: Lloyds' List

Adopted from Ref. [33]

TABLE I.2

Number of lives lost in structural accidents for platforms in world-wide operating during 70.01.01 - 80.12.31 according to initiating event and extent of structural damage

Initiating event	ALL PLATFORMS (MOBILE PLATFORMS)				SUM
	Structural Loss				
	Total	Severe	Damage	Minor	
Weather	13(13)	-	-	-	13(13)
Collision	1(1)	8(8)	-	4(4)	13(13)
Blow-out	12(5)	35(26)	20(20)	3(0)	70(51)
Leakage	-	1(1)	-	-	1(1)
Machine etc.	-	-	1(1)	-	1(1)
Fire	-	7(0)	2(0)	8(0)	17(0)
Explosion	4(0)	8(2)	11(2)	11(8)	34(12)
Out-of-phase	-	-	-	-	-
Foundering	-	-	1(1)	-	1(1)
Grounding	-	6(6)	-	-	6(6)
Capsizing	93(93)	6(6)	1(1)	-	100(100)
Structural strength	123(123)	-	3(0)	10(7)	136(130)
Other	-	-	-	4(2)	4(2)
SUM	246(235)	71(49)	39(25)	40(21)	396(33)

Source: Lloyd's list

Adopted from Ref. [33]

media might explain why so little work has been done on the collision protection of offshore platforms. Still, collisions occupy the third place in platform accidents after the ones due to environmental load and blowouts. (Table I.3). As a result, considerable capital losses occur in structural damages because of collisions.

In the following Chapters a simple method of estimating the structural damage to a platform resulting from a minor platform-ship collision (like the ones with supply boats) is presented. In the first Chapter, an upper bound calculation of the force-deflection curve is performed for a rigid-plastic circular cylinder under transverse loading applied by a wedge. A local deformation field is assumed and any global deformation of the cylinder acting as a beam is neglected. In the second Chapter, the effects of the global deformation of the cylinder are taken into consideration and the overall force-deflection curve of the cylindrical beam is calculated. In the third Chapter, the above obtained force-deflection curve, in combination with the equivalent curve for a ship's bow and side, and also the foundation stiffness of a platform are used as spring data for a simplified two-mass dynamic model with linear and non-linear springs. This model is used to calculate numerically the plastic deformation on one of the platform's members (leg or brace) due to a collision with a ship. Finally, in the fourth Chapter, a method is outlined for a cost-benefit analysis of a minor-collision-damage vs. strengthening of the platform using probabilistic data on the risk of such a collision and the platform's damage calculation method presented in the first three Chapters.

TABLE I.3

Number of accidents for platforms in world - wide operation during 70.01.01. - 80.12.31. according to initiating event and extent of structural damage.

ALL PLATFROMS (MOBILE PLATFORMS)					
Initiating event	Structural Loss				SUM
	Total	Severe	Damage	Minor	
Weather	7(3)	12(10)	30(22)	21(17)	70(52)
Collision	4(2)	5(2)	17(11)	21(18)	47(32)
Blow-out	15(5)	13(7)	15(9)	14(7)	57(28)
Leakage	-	2(2)	3(3)	-	5(5)
Machine etc.	1	2(1)	5(4)	5(6)	13(11)
Fire	3(1)	6(2)	20(12)	19(12)	48(27)
Explosion	2(0)	3(2)	10(4)	9(6)	24(12)
Out-of-pos	-	-	3(2)	-	3(2)
Foundering	4(1)	-	-	-	4(1)
Grounding	2(1)	6(6)	3(2)	5(2)	16(11)
Capsizing	11(11)	4(4)	3(1)	1(1)	19(17)
Structural strength	1(1)	6(4)	20(14)	25(20)	52(39)
Other	2(0)	3(0)	1(0)	12(8)	18(8)
SUM	52(25)	62(40)	130(84)	132(97)	376(246)

Source: Lloyds' list

Adopted from Ref. [33]

This research cannot claim to cover in a comprehensive way all the aspects of collisions offshore. Some areas certainly need further work, and the most relevant aspects of recommended research are summarized below.

(a) Local Structural Behavior

Interaction curves defining the magnitudes of axial force, bending moment and crushing force required for plastic deformation should be developed. The effects of shear force and torsion should also be considered, as well as inplane versus out of plane bending.

(b) Material Ultimate Strength

The energy absorption capability of structural elements is determined by the material's capacity to suffer large strains without fracture. Methods for assessing material ultimate strength when very large plastic deformations are involved should be developed. The effect of strain hardening should also be studied.

(c) Support Flexibility

Tubular joints do not provide a perfect degree of end fixity. A varying degree of end fixity, in terms of end translations and rotations, has a strong influence on the energy absorption capability of tubular members. Methods for taking this effect into account in the analysis should be developed. Consideration should be given to the adjacent members in performing such a study.

(d) Redundancy and Overall Structural Behavior

The survivability of any structure is to a very large extent determined by its degree of redundancy. No systematic way for assessing the optimum degree of redundancy is available in the literature, and this is a very important area of research.

(e) Collision Mechanics Models

The collision problem cannot be completely isolated from its own scenario. The way the impacting and impacted structure interact with each other and the environment is very important when studying collision effects. The collision model included in this report is a very crude representation of reality and is acceptable for initial estimates of structural behavior. However, for a more complete understanding of the problem and its implications it is necessary to develop a more sophisticated approach.

(f) Reliability Studies

Collision studies should be considered within the more general context of structural reliability. Most existing codes of practice for structural design, and those being currently developed for the offshore industry, are based on reliability considerations. This trend should also be reflected in the way collision studies should be carried out in the future.

(g) Data Collection

Collision accidents are occurring quite often in offshore operations. However, in most cases the information which is made available is very limited, mainly because of the reluctance industry has in publicizing accidents. It would be extremely beneficial to researchers if technical information regarding such accidents could be collected, since this is the best way to close the gap between theory and practice.

(h) Experimental Studies

Analytical and numerical studies are not enough to cover all the aspects involved in the structural behavior of tubular members.

These should whenever possible be complemented by careful experimental studies. Some tests have already been performed in Norway and the United Kingdom. Due to the magnitude of the investments involved this is an area in which an international university/industry cooperative effort would be most welcome.

(i) Fendersystems for Offshore Structures

A natural extension of the structural studies suggested above is the development of fendersystems for offshore installations. These should include not only systems capable of protecting the structure from direct impact, but also systems capable of preventing the impacting ship from passing below the floating platform's deck, and damaging for example the risers.

CHAPTER 1

LOCAL DEFORMATION OF CYLINDERS UNDER TRANSVERSE LOADING

1.1 Introduction

Tubular members are extensively used in offshore structures. Consequently, an offshore collision will most probably involve transverse concentrated loading of a cylindrical beam and will result in either local damage of the shell or in global deformation of the cylinder as a beam. In both cases, the extent of local damage will be of great importance since it will affect the strength of the structural member by decreasing its moment of inertia and introducing an eccentricity. In order to assess the extent of such a crumpling due to a collision we need the force-deformation relation for such a local deformation.

Although some work has been done in the area of large deformation of shells of revolution loaded axisymmetrically (Ref. [1] to [7]), not much of that work has been extended for the case of non-axisymmetric loading. The reason is that because of the non-axisymmetric nature of the loading, the resulting deformation field is asymmetric. Thus, its modelling and the analytical solution of the problem can become very complicated, requiring several (sometimes relatively crude) approximations.

In this Chapter, an attempt is made to extend an existing method of analysis so that the problem of the transverse loading of a cylinder under a concentrated load can be solved and a force-deformation relation can be obtained. Most of the work done with respect to that problem is experimental (Ref. [8] to [12]). Morris and Calladine have presented in [13] an upper-bound calculation method for the indentation of cylindrical shells but their analysis was limited to relatively small deflections. The method presented in this chapter involves the concept

of the isometric transformation of surfaces, first applied in mechanics problems by Pogorielov in [14]. According to this , we say that a surface has undergone an isometric transformation if its Gaussian curvature* is the same before, during and after the deformation. As the word isometric indicates, all linear dimensions along the surface are preserved and no extension is required during the transformation. Instead, the surface is folded. In the case of a thin shell, which is easier to deform by bending rather than extension, the choice of an isometric transformation to describe the assumed deformation field (in an upper bound calculation) becomes the logical one. The above approach was successfully used in [15] to analyse the crushing of rotationally symmetric plastic shells undergoing large deflections.

In employing the above concept of isometric transformation for the solution of the problem of the transversely loaded cylinder, we observe that it is impossible to have a local deformation that is strictly isometric.** Instead, we can assume a deformation field that requires an isometric transformation in the transverse direction and a quasi-isometric transformation in the longitudinal direction (where the shell transforms isometrically but some extension is required). As in the case of plastic axisymmetric shells, a distinctive feature of such a deformation mechanism is that the energy dissipation function is concentrated in narrow zones (hinge lines) while the remainder of the structure is undergoing a rigid body motion. To obtain an expression for the load vs. deflection, the rate of internal energy dissipation

* The Gaussian curvature of a surface is the product of its curvatures along any arbitrary pair of principal axes.

** Only if the crushing of the cylinders is uniform along its length (case of a ring crushing mode). The conditions for such a mode of deformation are very small length-to-radius ratio and ends free to ovalize and they make this mode of deformation of no practical use in our problem.

due to the imposed deformation field is calculated and equated to the rate of external work performed by the moving load as deformation proceeds. Then, the resulting expression is minimized with respect to several geometric parameters. Because of some simplifications made with respect to the kinemetics (in order to be able to obtain an analytical closed form final solution), the obtained load cannot strictly be called an upper bound but the analysis is essentially along the same lines.

In the following section, a detailed description of the assumed deformation field is given together with other assumptions made during the present analysis.

1.2 Assumptions and Basic Geometry

1.2.1 Assumed Deformation Field

In defining the deformation field, the cylinder is divided in three regions (Fig. 1.1):

(i) The deforming plasticized region bounded by two closed curved hinges called from now on outer and inner hinge lines.

(ii) The undeformed rigid region outside the outer hinge line.

(iii) The already deformed rigid region inside the inner hinge line.

We should note that these hinge lines and regions are symmetric about the transverse plane that is perpendicular to the cylinder's axis and also contains the line of application of the load. Because of the above symmetry, we can consider only half of the cylinder.

The hinge lines are assumed to lie on a plane. In order to have local deformation only, that plane has to be at an angle with the cylinder's generators.*

* As compared to the ring crushing mode where the hinges will lie on a plane parallel to the cylinder's generators.

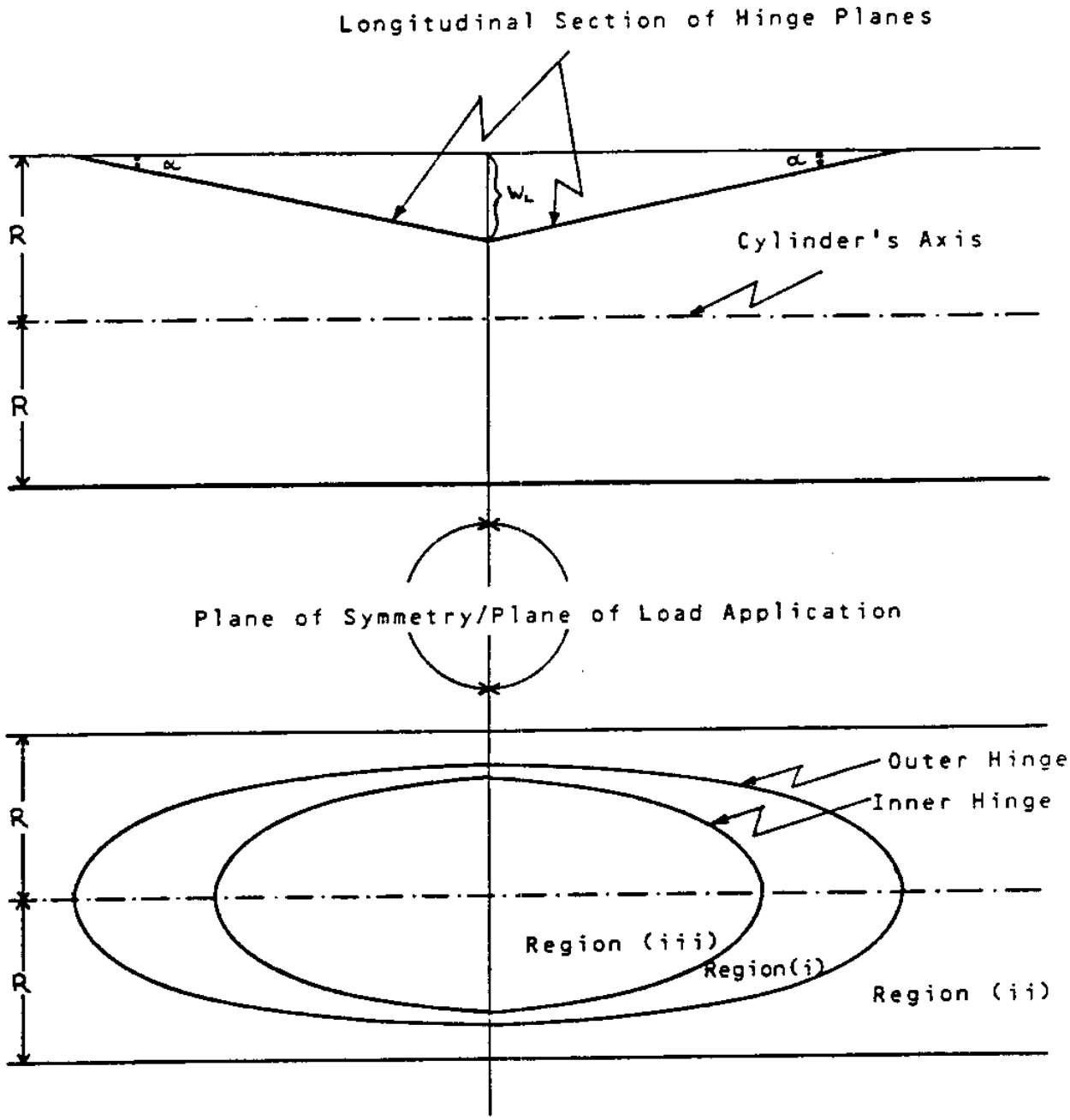
Longitudinal Section of Hinge Planes
α
α
W_L
R
R
Cylinder's Axis
Plane of Symmetry/Plane of Load Application
Outer Hinge
Inner Hinge
R
R
Region (iii)
Region(i)
Region (ii)

FIGURE 1.1

We call that angle α (Fig. 1.2). Thus, because of the existing symmetry, the above inclined plane forms an angle 2α with the inclined plane of the other half of the cylinder. It follows that the two hinge lines have points of slope discontinuity (A, B, A', B':Fig. 1.2) lying on the line of intersection of the two inclined planes.

Another assumption is that the transverse cross-sections of the cylinder remain circular outside the deformed region. Further, an isometric transformation is assumed in the transverse direction. This requires that the region inside the inner hinge is the mirror image, about the inclined plane, of the intact cylinder before any deformation has occurred. As a result, the region inside the inner hinge is a cylindrical section of reversed curvature and with generators forming an angle of 2α with the generators of the undeformed cylinder. Such a deformation pattern requires a certain extension of the material along the longitudinal direction. The existence of that extension is the main conceptual difference between the analysis of an axisymmetric case and the present one.

During deformation and as deflection increases, the planes of the hinges move downwards and the hinges themselves move outwards through the material. In order to satisfy the conditions of kinematic continuity on the moving hinges (presented in [15] and [16]) the deforming shell should have no slope discontinuities at the hinges as they propagate through the material. Thus, the only effect of the hinges as they move through the material is to impose a change of curvature. In addition to that mode of energy dissipation, the material that lies between the outer and the inner hinge lines is in a plastic state undergoing extension in the

hoop direction* relative to the hinges.

In order to calculate the dissipation due to hoop extension we need to have an expression defining the form of the plasticized zone that lies between the inner and outer hinges. Approximating the perpendicular, to the outer hinge line, cross-section of the plasticized zone by a parabola was proved in [15] to give very satisfactory results. As mentioned earlier, the material outside the outer hinge and inside the inner hinge line is rigid, with the latter moving downwards in a rigid body motion as deformation progresses.

1.2.2 Definition of Coordinate Axes

Now that we have described the kinematics we should define the several coordinate systems used.

From Figure 1.2 we have:

(i) X,Y,Z: Global coordinate system fixed on the cylinder with the X-axis coinciding with the cylinder's axis and the Y-axis being in the negative direction of the applied load.

(ii) X',Y',Z': Global coordinate system fixed on the inclined plane of the hinges and moving with it as the deformation progresses. X' and Z' are on the inclined plane and Z' is also parallel to the Z-axis.

(iii) λ',x',y': Local coordinate system. λ' is tangent to the outer hinge, and λ'-x' plane coincides with the inclined plane. Consequently, y' is perpendicular to the inclined plane.

* The term hoop will be used throughout here to describe a direction parallel to the hinge lines.

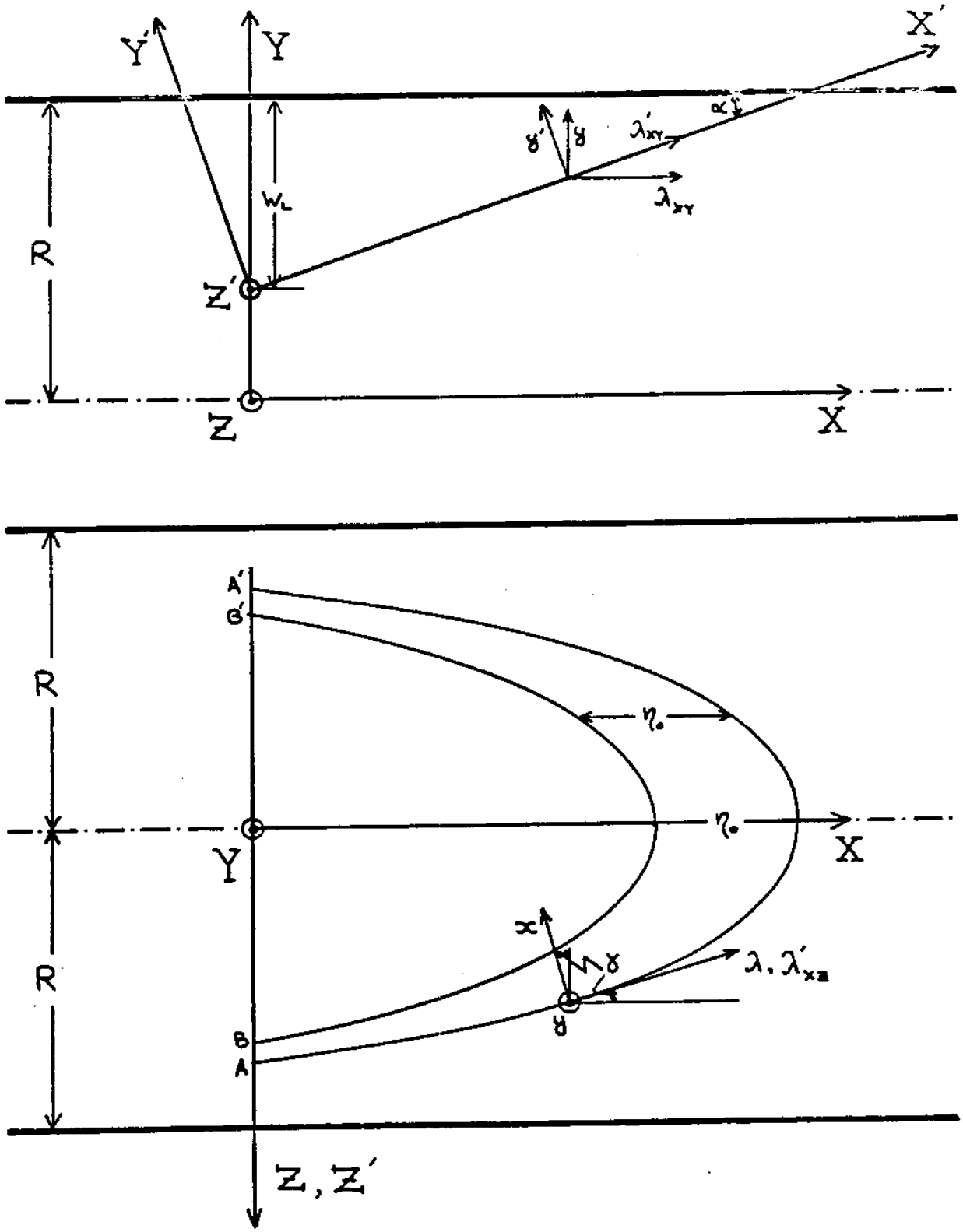

FIGURE 1.2

As it can be seen with the used notation, a prime (') denotes a variable that is associated with the moving inclined plane. In the following calculations variables without a prime should be interpreted as the projections of the ones with the prime on the fixed coordinate system.

1.2.3 Equations Describing the Deformation Field

Before proceeding with writing of equations we should make another simplification. In order to have compatible kinematics, the outer hinge line, which lies on the inclined plane, should be the intersection of a plane with a cylinder. The resulting ellipse, however, prohibits the closed form evaluation of (the further along) required integrals around the outer hinge. In order to obtain a closed form solution the cylinder's circular cross section is approximated by a parabolic expansion (Fig. 1.3). As a result of that simplification the obtained hinge lines are parabolas. Further, we assume that the inner hinge is the outer one shifted by η_0 towards the negative X direction. This is consistent with the previous assumption that both inner and outer hinge lines lie on the same plane.

We can now write the equations that describe the assumed deformation field in terms of the plastic deflection at the point of application of the load and various geometric parameters:

- equation of the inclined plane:

$$Y = (R - w_L) + X \tan\alpha \tag{1.1}$$

where w_L = deflection of the point of load application

R = radius of the cylinder

- equation of the parabolic expansion of the cylinder

$$Y = R - \frac{1}{2R} Z^2 \tag{1.2}$$

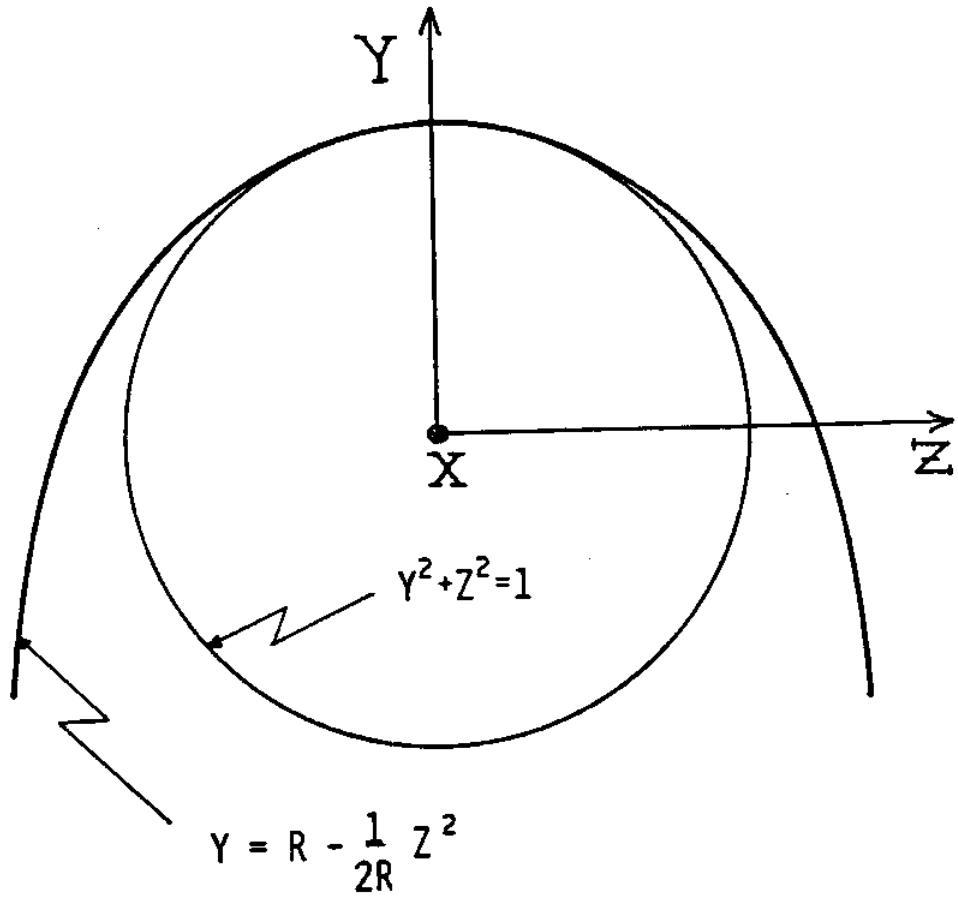

PARABOLIC APPROXIMATION
OF THE CYLINDER'S CROSS-SECTION

FIGURE 1.3

Combining (1.1) and (1.2) we get the equations for the parabolic outer hinge line:

$$X = \frac{w_L - \frac{Z^2}{2R}}{\tan\alpha}$$

$$Y = (R - w_L) + X \tan\alpha \qquad (1.3)$$

Relative to the X', Y', Z', coordinate system the two equations become:

$$X' = \frac{w_L - \frac{Z'^2}{2R}}{\sin\alpha}$$

$$Y' = 0 \qquad (1.4)$$

By requiring that there is a material continuity at both the outer and inner hinge and that there is also a slope continuity at the outer hinge and approximating the cross section of the plasticized zone by a parabola (as discussed earlier) we obtain the following equation for the cross section:

$$y' = \frac{\tan\alpha}{\sin\gamma}\left[-\left(\frac{\cos\alpha}{\eta_o \sin\gamma'}\right)x'^2 + x'\right] \qquad (A.5)^*$$

where γ' = angle between the tangent at an arbitrary point on the outer hinge and the X' axis.

η_o = distance between the inner and outer hinge lines measured along X. η_o is assumed constant and independent of γ'.

The angle γ' can take values between θ' and $\frac{\pi}{2}$ along the outer hinge, where θ' is the value of γ' at the point of slope discontinuity of the outer hinge (on the intersection line of the two symmetric inclined planes). θ' is related to w_L and α by the following expression:

* In order to avoid clustering the main text with unnecessary detailed derivations, all equations that require such involved derivations are given in the appendix. The letter preceding the label of these equations refers to the respective appendix (A for Chapter 1, B for Chapter 2, etc.).

$$\cot\theta' = \frac{\sqrt{2\frac{W}{R}}}{\sin\alpha} \tag{A19}$$

We are now ready to proceed with the calculation of the internal energy dissipation due to the above described deformation field. An idealized rigid-plastic material model will be used so that no strain hardening or Baushinger effects are considered.

1.3 Internal Energy Dissipation

The rate of energy dissipation during plastic deformation of a rigid-plastic continuum can be written as:

$$D = \iiint_V \sigma_o \dot{\varepsilon} dV \tag{1.5}$$

where V: volume of the deforming material

$\dot{\varepsilon}$: sum of all the strain rates corresponding to a particular dissipation mechanism

σ_o: yield stress of the material

In order to evaluate the rate of internal energy dissipation due to hoop and bending strain rates the concept of the instantaneous rotation of a section presented by Calladine in [16] will be used. In doing so, a general, perpendicular to the outer hinge, section of the plasticized zone between the two hinges (shown in Fig. 1.4).will be considered. As already discussed, the shape of the section is approximated by a parabola and its equation in terms of the local coordinate system x', y' is given by (A5). In Figure 1.4, A represents the outer hinge, B the inner hinge, and I the center of instantaneous rotation.

1.3.1 Hoop Strain Dissipation

For a shallow arc section $\widehat{AB}$ we can write dV approximately as:

$$dV = dx'dy'd\lambda' \tag{1.6}$$

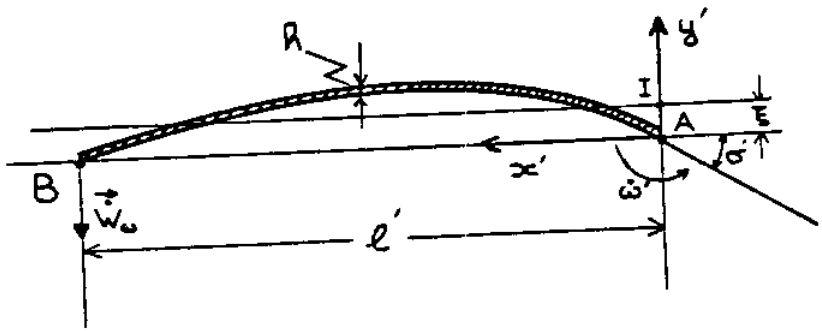

CROSS-SECTION OF THE PLASTICIZED
REGION BETWEEN THE TWO HINGES

FIGURE 1.4

Also, $\dot{\varepsilon}$ is given by:

$$\dot{\varepsilon} = \dot{\omega}' \frac{(y'-\xi)}{(\rho'-x')} \tag{1.6}$$

Where $\dot{\omega}'$ = rate of angular rotation about the outer hinge

ρ' = radius of curvature of the outer hinge

ξ = distance of the center of instantaneous rotation from the x'-axis

For a shallow arc section, and in order to simplify calculations we can approximate $\dot{\varepsilon}$ as:

$$\dot{\varepsilon} = \dot{\omega}' \frac{y'}{\rho'} \tag{1.7}$$

Also, $d\lambda'$ can be written as:

$$d\lambda' = \rho' d\gamma' \tag{1.8}$$

Substituting (1.6), (1.7) and (1.8) in (1.5) we obtain:

$$\dot{D}^{hoop} = 4\sigma_o \int_{\theta'}^{\pi/2} \dot{\omega}' \int_{o}^{\ell'} \int_{-\frac{h}{2}}^{\frac{h}{2}} y'dy'dx'd\gamma'$$

where ℓ' is the width of the plasticized zone.

Since $\omega' = \frac{|\vec{\dot{W}}_\omega|}{\ell'}$ we get:

$$\dot{D}^{hoop} = 4\sigma_o \int_{\theta'}^{\pi/2} |\vec{\dot{W}}_\omega| \frac{M'}{\ell'} d\gamma' \tag{1.9}$$

$$\text{with } M' = \int_{o}^{\ell'} \int_{-\frac{h}{2}}^{\frac{h}{2}} y'dy'dx' \tag{1.10}$$

where $|\vec{\dot{W}}_\omega|$: rate of displacement of the inner hinge in the negative y' direction.

M': first moment of area of the plasticized zone's section

For a shallow arc section it can be shown that $\frac{M'}{\ell'}$ is given approximately by:

$$\frac{M'}{\ell'} = h\frac{\eta_o}{6}\frac{\tan\alpha}{\cos\alpha} \tag{A14}$$

and

$$|\dot{\vec{W}}_\omega| = 2\dot{w}\cos\alpha \qquad \text{(From A1)}$$

where $\dot{w}$ is the rate of displacement of the point of application of the load along the negative Y direction.

Substituting (A1) and (A14) in (1.9) we obtain:

$$D^{hoop} = \frac{4}{3}\sigma_o\, h\, \eta_o \tan\alpha\, \dot{w}\int_{\theta'}^{\pi/2} d\gamma'$$

Evaluating the integral and subtituting the expression relating θ' to w_L and α, (A19), we arrive at the final expression for the rate of internal energy dissipation due to hoop extension, in terms of $\frac{\eta_o}{h}$, $\dot{w}$, α, and $\tilde{w}_L$.

$$\dot{D}^{hoop} = \frac{16}{3} M_o \dot{w}\left(\frac{\eta_o}{h}\right)\tan\alpha\, \tan^{-1}\left(\frac{\sqrt{2\tilde{w}_L}}{\sin\alpha}\right) \tag{1.11}$$

where

$$M_o = \frac{\sqrt{2\tilde{w}_L}}{\tan\alpha} \tag{1.12}$$

$$\tilde{w}_L = \frac{w_L}{R} \tag{1.13}$$

1.3.2 Bending Energy Dissipation

In evaluating the rate of internal energy dissipation due to bending we assume that all bending is concentrated at the outer hinge.*

The bending strain rate then can be written as:

$$\dot{\varepsilon} = \dot{\omega}'\,\frac{y'}{\ell' h} \tag{1.14}$$

* This assumption is consistent with the concept of the instantaneous rotation of a section as presented by Calladine [16].

where ℓ'_h is the width of the plastic hinge.

The rate of angular rotation can be shown to be:

$$\dot{\omega}' = \frac{2\dot{w}\cos^2\alpha}{\eta_o \sin\gamma'} \tag{A4}$$

As before dV is given by:

$$dV = dx'dy'd\lambda' \tag{1.6}$$

Substituting (1.14), (A4), and (1.6) in (1.5) and evaluating the integrals over the thickness of the shell and over the width of the plastic hinge we arrive at:

$$\dot{D}^{bend} = 8\,\sigma_o \frac{h^2}{4}\dot{w}\frac{1}{\eta_o}\cos^2\alpha \int_{\lambda'} \frac{d\lambda'}{\sin\gamma'} \tag{1.15}$$

$d\lambda'$ is related to $d\gamma'$ by the following expression:

$$d\lambda' = \frac{R\sin\alpha}{\sin^3\gamma'}\,d\gamma' \tag{A21}$$

Substituting (A21) in (1.15) evaluating the integral, and rearranging we get the expression for the rate of internal energy dissipation due to bending in terms of M_o, $\frac{R}{h}$, $\frac{\eta_o}{h}$, α, $\dot{w}$, and $\tilde{w}_L$

$$\dot{D}^{bend} = 8M_o\dot{w}\frac{\left(\frac{R}{h}\right)}{\left(\frac{\eta_o}{h}\right)}\sqrt{2\tilde{w}_L}\left[\cos^2\alpha + \frac{2\tilde{w}_L}{3\tan^2\alpha}\right] \tag{1.16}$$

The above expression is for wedge loading only. If the load is not exerted through a wedge but through a beam of width B the deformation changes as shown in Fig. (1.5). A constant, along the length, cross-section (Fig. 1.5b) region replaces the line hinge between the two parabolically shaped plastic zones. The only energy dissipation mechanism along this region is due to bending since, as the straight hinge lines AC and A'C' move through the material the radial curvature of the cyliner is reversed from $\frac{1}{R}$ to $-\frac{1}{R}$. The expression for the energy dissipation due

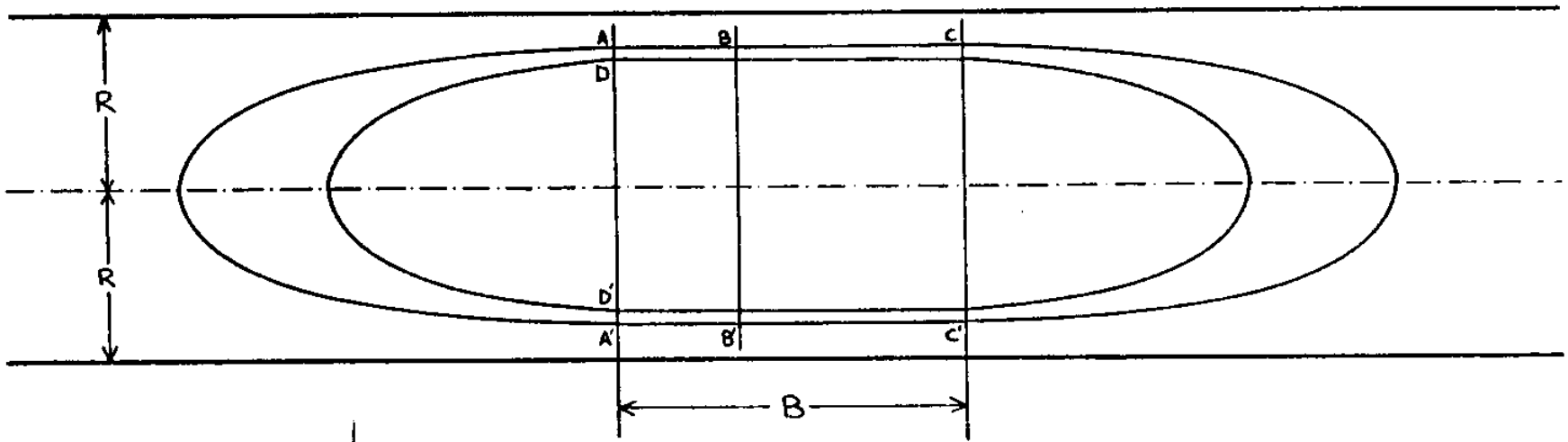

(5A)

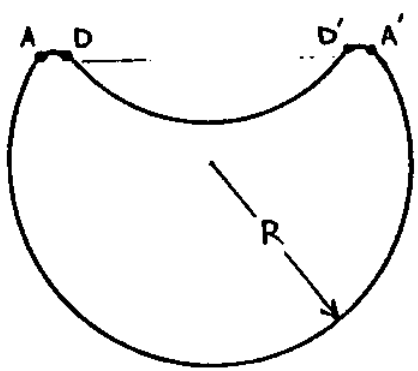

(5B):Sections AA', BB', CC'

FIGURE 1.5

to bending for the above case is the same with the one given in [15] for the crushing of rotationally symmetric shells if the circumferential length is replaced by the loading beam's width B. It can be written:

$$\dot{D}^B = 4M_o\dot{\omega}\, B \tag{1.17}$$

with

$$\dot{\omega} = \frac{2\dot{w}}{\eta_o \tan\theta} \tag{1.18}$$

Combining the above two expressions we obtain:

$$D^B = 8M_o\dot{w}\,\frac{\tilde{B}\,\frac{R}{h}}{\frac{\eta_o}{h}}\,\frac{\sqrt{2\tilde{w}_L}}{\tan\alpha} \tag{1.19}$$

with

$$\tilde{B} = \frac{B}{R} \tag{1.20}$$

Then, by combining (1.16) and (1.19) we arrive at the general expression for the rate of internal energy dissipation due to bending in terms of M_o, $\frac{R}{h}$, $\frac{\eta_o}{h}$, $\frac{B}{R}$, α, $\dot{w}$, and $\tilde{w}_L$

$$\dot{D}^{bend}_{tot} = 8M_o\dot{w}\,\frac{\left(\frac{R}{h}\right)}{\left(\frac{\eta_o}{R}\right)}\sqrt{2\tilde{w}_L}\left[\cos^2\alpha + \frac{2\tilde{w}_L}{3\tan^2\alpha} + \frac{\tilde{B}}{\tan\alpha}\right] \tag{1.21}$$

1.3.3 Membrane Extension Energy Dissipation

As discussed earlier we do not have any extension in the transverse direction but only along the longitudinal direction. The extension strain rate along that direction can be written then as:

$$\dot{\varepsilon} = \frac{\dot{W}_e}{\ell' h} \tag{1.22}$$

where $\dot{W}_e$ is the rate of membrane extension along the longitudinal direction. Since $\dot{\varepsilon}$ is independent of the location along the hinge and along the cylinder's thickness the energy dissipation due to membrane extension is given by:

$$\dot{D}^{ext} = 2h\sigma_o \, W_e \, 2R\beta\Big|_{\gamma=\theta} \tag{1.23}$$

where $2R\beta\Big|_{\gamma=\theta}$ represents the length of the cylinders arc over which the membrane extension is exerted. β is shown in Fig. (2.5) and given by:

$$\beta = \cos^{-1}(1 - \tilde{w}_L) \tag{1.24}$$

It can be shown that $\dot{W}_e$ can be written as:

$$\dot{W}_e = \dot{w} \tan 2\alpha \tag{A23}$$

Substituting (1.24) and (A23) in (1.23) and rearranging we arrive at the final expression for the rate of internal energy dissipation due to the membrane extension in terms of M_o, $\frac{R}{h}$, $\dot{w}$, α, and $\tilde{w}_L$.

$$\dot{D}^{ext} = 16 \, M_o \dot{w} \left(\frac{R}{h}\right) \tan 2\alpha \cdot \cos^{-1}(1 - \tilde{w}_L) \tag{1.25}$$

1.4 External Work

The external work performed by the moving load as the deformation proceeds depends on the type of loading member used. If a wedge or beam is used the point of application of the load is moving along the negative Y direction with velocity $\dot{w}$. Thus, the external work is given by:

$$\dot{D}^{B}_{ext} = P_B \cdot \dot{w} \tag{1.26}$$

where P_B is the applied load.

If a point load is applied through a boss in the middle of the deformed rigid region, the point of application of the load is moving along the negative Y direction with velocity $\dot{w} \frac{\tan 2\alpha}{\tan\alpha}$ [see (A22)]. Thus, the external work is given by:

$$\dot{D}^{p}_{ext} = P_p \dot{w} \frac{\tan 2\alpha}{\tan\alpha} \tag{1.27}$$

We should note, that the above expression for boss loading holds even if the load is not applied in the middle of the deformed rigid region, as long as it is applied on that region (since its points move downwards with the same velocity).

1.5 Load Calculation

Combining equations (1.11), (1.21), (1.25) we obtain the following expression for the rate of total internal energy dissipation

$$\dot{D}_{int} = 8M_o\dot{w}\left[\left(\frac{\eta_o}{h}\right) \cdot C_1 + \frac{1}{\left(\frac{\eta_o}{h}\right)} C_2 + 2C_3\right] \tag{1.28}$$

with $C_1 = \frac{2}{3} \tan\alpha \cdot \tan^{-1}\left(\frac{\sqrt{2\tilde{w}_L}}{\sin\alpha}\right)$ (1.29a)

$$C_2 = \left(\frac{R}{h}\right)\sqrt{2\tilde{w}_L}\left[\cos^2\alpha + \frac{2\tilde{w}_L}{3\tan^2\alpha} + \frac{\tilde{B}}{\tan\alpha}\right] \tag{1.29b}$$

$$C_3 = \left(\frac{R}{h}\right) \tan 2\alpha \cdot \cos^{-1}(1 - \tilde{w}_L) \tag{1.29c}$$

Since neither of the expressions for the external work performed by the load are functions of $\frac{\eta_o}{h}$ we can minimize (1.28) with respect to $\frac{\eta_o}{h}$. We obtain:

$$\left(\frac{\eta_o}{h}\right) = \sqrt{\frac{C_2}{C_1}}$$

Substituting that back in (1.28) we get:

$$D_{int} = 16M_o\dot{w}\left[\sqrt{C_1C_2} + C_3\right] \tag{1.30}$$

Equating (1.30) with (1.26) or (1.27) we arrive at the final expression for the applied load in terms of $\frac{R}{h}$, α, and $\tilde{w}_L$.

- For a beam of wedge loading:

$$P_B = 16M_o \sqrt{\frac{2}{3}\left(\frac{R}{h}\right)\sqrt{2\tilde{w}_L}\,\tan\alpha\cdot\tan^{-1}\left(\frac{\sqrt{2\tilde{w}_L}}{\sin\alpha}\right)\left[\cos^2\alpha + \frac{2\tilde{w}_L}{3\tan^2\alpha} + \frac{\tilde{B}}{\tan\alpha}\right]}$$

$$+ \left(\frac{R}{h}\right)\tan 2\alpha\cdot\cos^{-1}(1 - \tilde{w}_L) \qquad (1.31a)$$

- For a point loading:

$$P_p = \frac{1}{2}\,\frac{\cos 2\alpha}{\cos^2\alpha}\,P_B \qquad (1.31b)$$

Both (31a) and (31b) have only one minimum with respect to α. Since it looks impossible to minimize them analytically we will minimize them numerically.

Appendix A, section 7 contains the numerical results for the $\left(\frac{P_B}{M_o}\right)_{min}$ and α_{min} at various $\tilde{w}_L$'s and for several combinations of the geometric parameters $\left(\frac{R}{h}\right)$ and $\left(\frac{B}{R}\right)$. Figure 6a,b,c shows the variation of the load, for several values of the thickness ratio, $\left(\frac{R}{h}\right)$.

1.6 Discussion

The presented analysis is valid only if ovalization of the cylinder does not occur and the transverse sections outside the deforming region remain circular. To obtain a deformation that satisfies this condition we should have a cylinder with small length-to-radius ratio and fixed ends The only experiments that tried to satisfy the no-ovalization condition were done by Morris in [11]. Unfortunately, the investigation was limited to deflections up to $\tilde{w}_L = 0.057$ for a thickness-to-radius ratio of 53. Therefore, no direct comparison can be made between our analysis and these experiments.

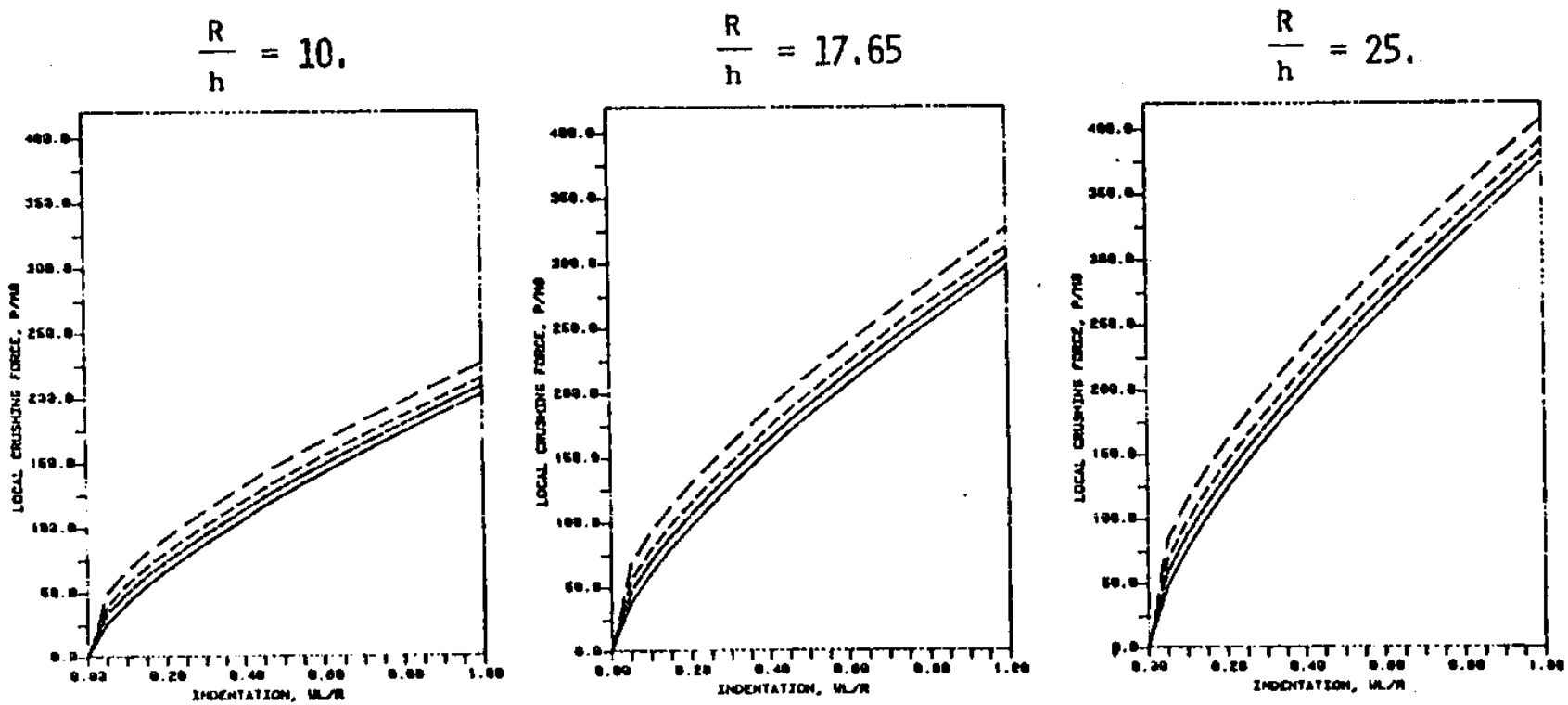

(a) (b) (c)

VARIATION OF THE LOCAL CRUSHING LOAD
WITH THE LOADING BEAM'S WIDTH

$\frac{B}{R}$ = 0.0 ———
0.465 - - - - -
1.0 — — —
2.0 — —

FIGURE 1.6

If we compare our results with the one from experiments (Ref [12]) where ovalization had occured (Fig. 1.7)* we see that our analysis overestimates the crushing load by approximately a factor of three. Since ovalization is unavoidable for all length-to-radius ratios that are useful for practical applications, we conclude that further studies should include an ovalization mechanism in the assumed deformation field.

---

* Figure 1.7 shows only up to $\tilde{w}_L = 0.4$ because for $\tilde{w}_L > 0.25$ global bending of the tubular beam had started during the experiment. Thus, comparing the corresponding load with the calculated local crushing load has no meaning.

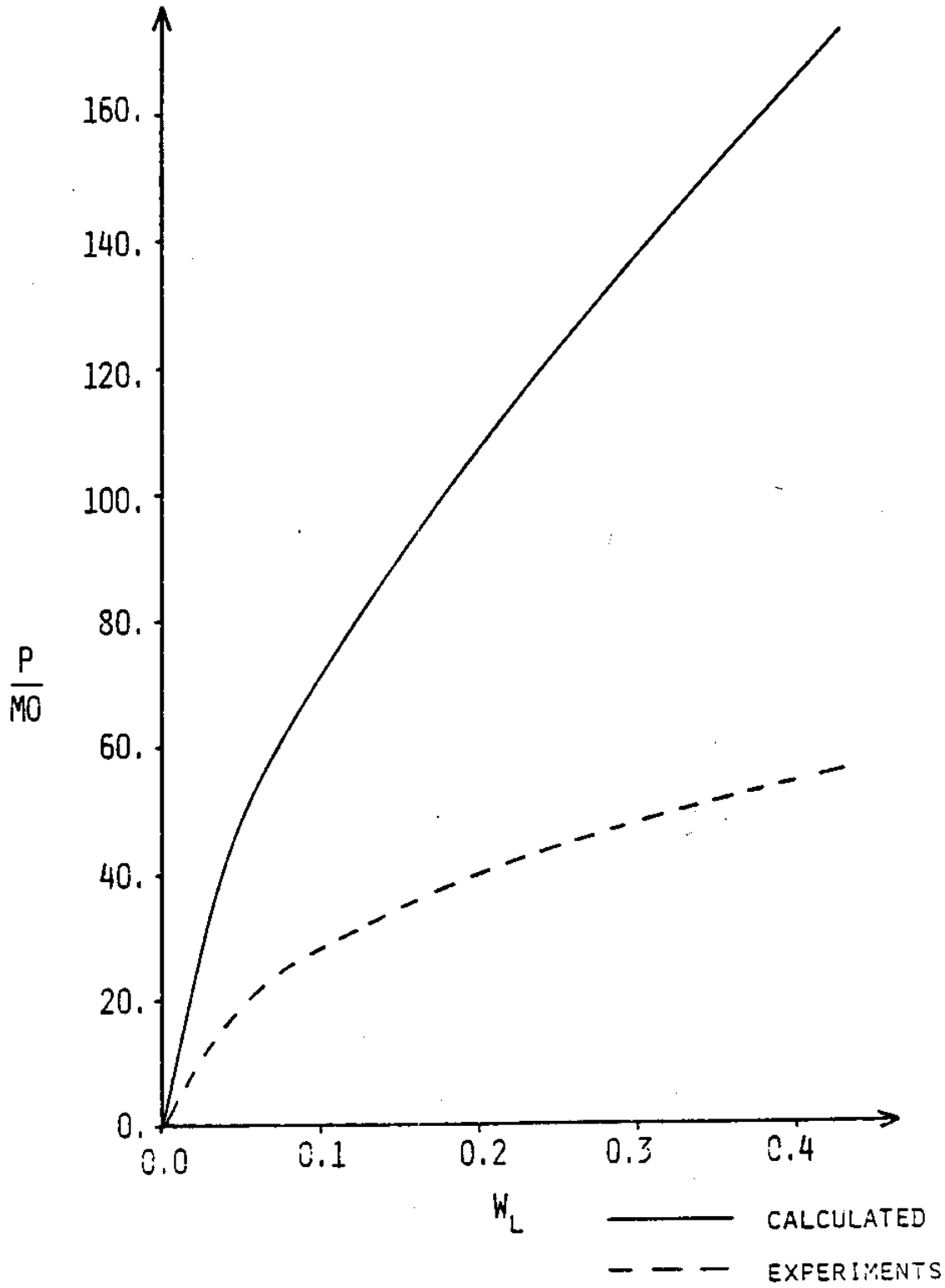
160.
140.
120.
100.
80.
60.
40.
20.
0.
P/MO
0.0
0.1
0.2
0.3
0.4
W_L
CALCULATED
EXPERIMENTS

FIGURE 1.7

Chapter 2

LOAD CARRYING CAPACITY OF A TUBULAR MEMBER LOADED TRANSVERSELY

2.1 Introduction

The expression for the indenting load obtained in the previous chapter holds only if the global deflection of the cylinder acting as a beam is zero. In practice, we have simultaneous local and global deflection. The two deformation modes interact with each other producing a necessary crushing force for a given pair of deflections, local and global, which is a function of these deflections.

To simplify the problem we can separate the cylinder's deformation into two phases as done in [17]. In the first phase, the cylinder is assumed to deform only locally. In this way a local indentation load vs. deflection is obtained (as done in Chapter 1). In the second phase, it is assumed that the local deformation stops and the global bending mechanism takes over. From simple geometry considerations, a function of the global load vs. indentation can be obtained (see Appendix B, Section 3). The indentation where the local load equals the global load is the one at which the switch from the local to the global mode takes effect (Fig. 2.1). This approach, although simple, tends to overestimate both the maximum load sustained during the collision and the local deflection at which this occurs. The overestimation of both these quantities, in a problem where the important variable is the absorbed energy, can very seriously offset the results and conclusions. In the following sections, an attempt is made to model the interaction between the local and the global deformation modes in order to obtain more realistic results.

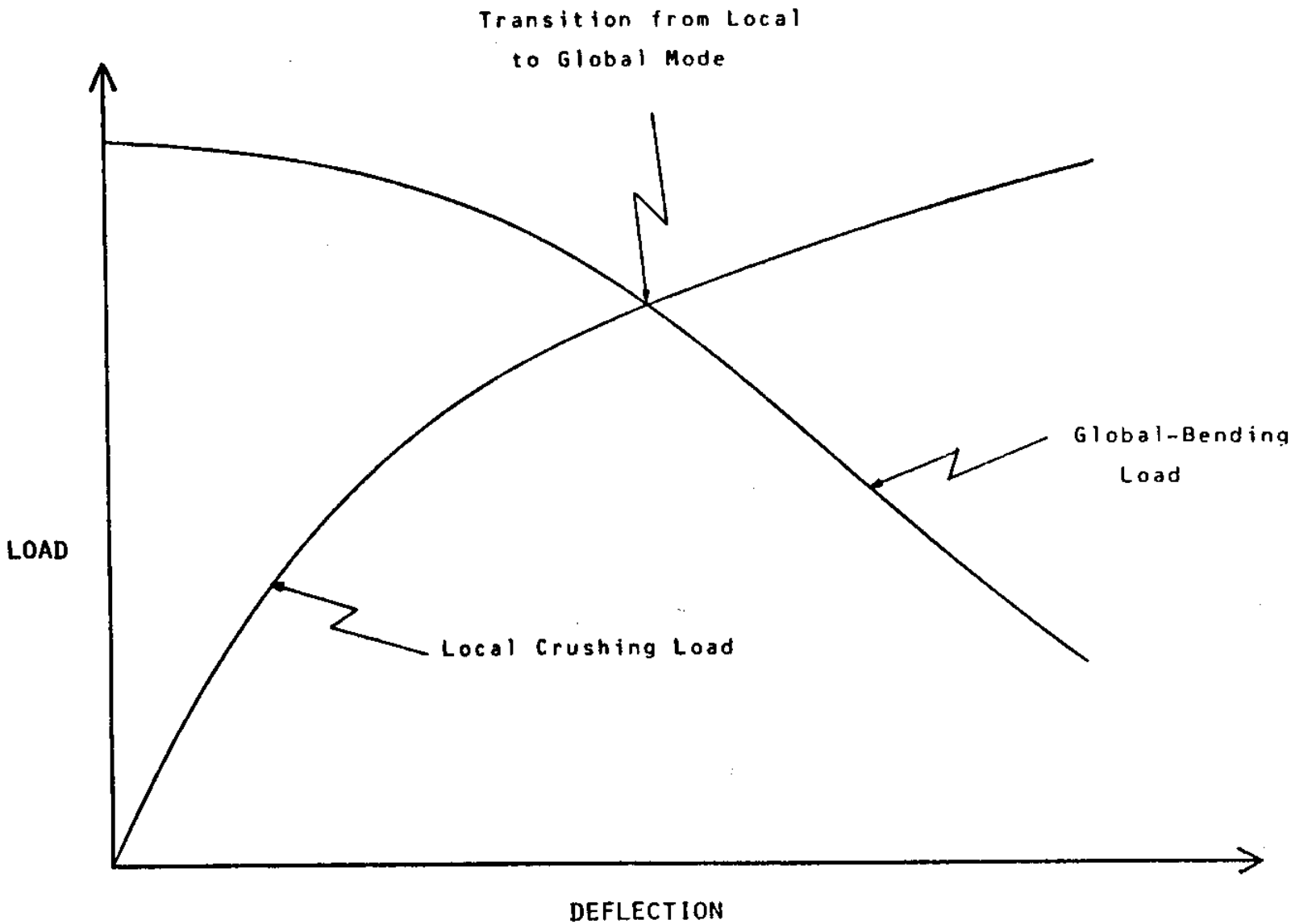
Transition from Local
to Global Mode
Global-Bending
Load
LOAD
Local Crushing Load
DEFLECTION

FIGURE 2.1

2.2 Model for the Deformation Mode Interaction

The deformation due to the global bending deflection can be taken as occurring only in the middle section of the cylinder, where the concentrated hinge in global bending is formed. It is reasonable then to assume that the interaction, if any, between the local and the global deformation fields will occur in that middle section. Fig. 2.2 shows a general case of the middle indented section. As a result of the global bending, arc $\widehat{FDH}$ is in tension and arcs $\widehat{AF}$, $\widehat{CH}$ and $\widehat{ABC}$ are in compression. Also, due to the local deformation arc $\widehat{ABC}$ is in tension. Since we cannot have a section both in tension and compression it is obvious that tension will prevail for part of the $\widehat{ABC}$ arc, say $\widehat{EG}$, and compression will prevail for the rest. Fig. 2.3 shows how the local tensile strain rate is superimposed on the global compressive strain rate over the arc $\widehat{AB}$. At point E the two strain rates are equal and they cancel each other. The position of point E depends on the relative magnitude of the local and global deflection rates $\dot{w}_L$ and $\dot{w}_G$ respectively defined in Fig. 2.4. This position is defined by the angle $\phi + \omega$ (see Fig. B1), which is related to the above rates by the following expression:

$$(1 - \zeta)\,[2(1 - \tilde{w}_L) + \sin(\phi + \omega) - \cos(\phi + \omega)] - \zeta\left[\left(\frac{L}{R}\right)\frac{\tan 2\alpha}{2}\right] = 0 \qquad \text{(B12)}$$

$$\text{with } \zeta = \frac{\dot{w}_L}{\dot{w}} \qquad \text{(B10)}$$

$$1 - \zeta = \frac{\dot{w}_G}{\dot{w}} \qquad \text{(B11)}$$

where $\dot{w}$: total deflection rate

$\dot{w}_L$: local deflection rate

$\dot{w}_G$: global bending deflection rate

$\tilde{w}_L$: local non-dimensional deflection

$2(\phi + \omega)$: angle spanning the arc $\widehat{EBG}$ where local extension prevails

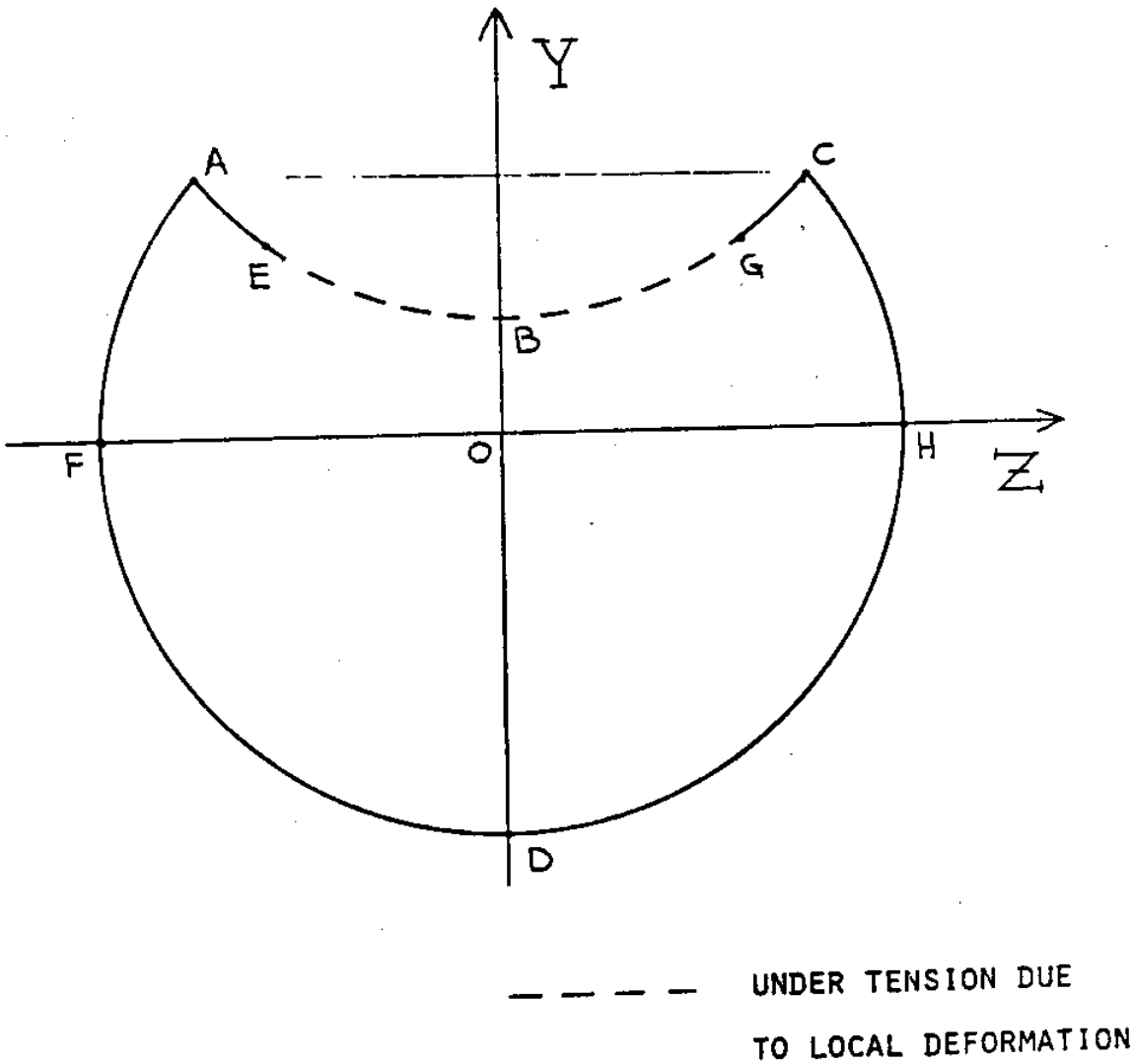

FIGURE 2.2

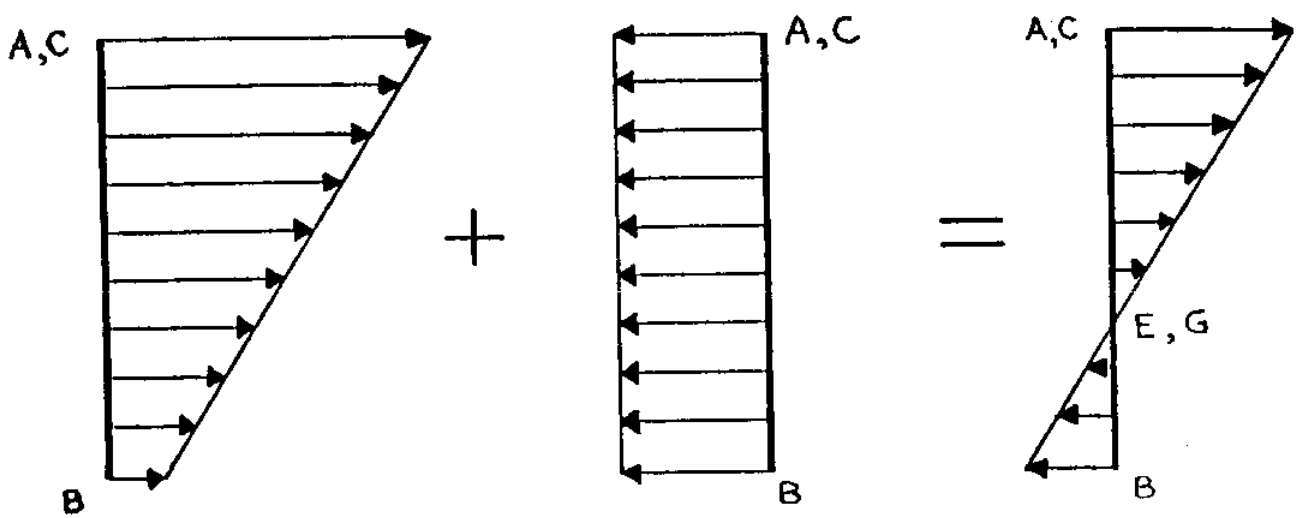

SUPERPOSITION OF THE LOCAL TENSILE STRAIN AND THE GLOBAL-BENDING COMPRESSIVE STRAIN RATE OVER THE DEFORMED ARC AB

FIGURE 2.3

DEFINITION OF THE LOCAL AND THE

GLOBAL DEFLECTION RATE

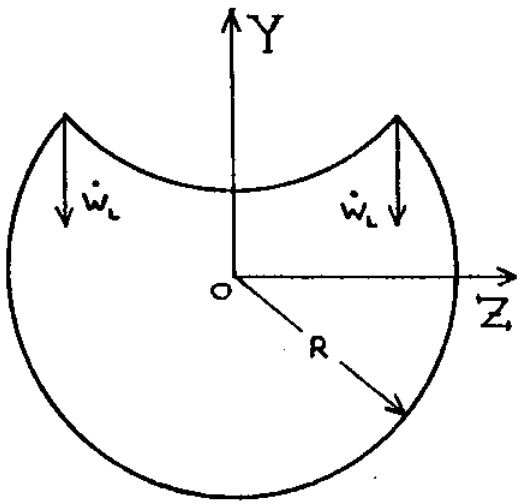

(a)

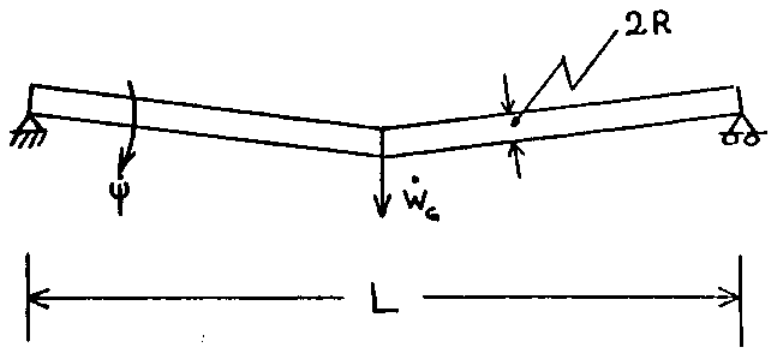

(b)

FIGURE 2.4

Now that it is well defined which parts of the indented middle cross-section are under tension and which are under compression we can find the location of the plastic neutral axis by equating the sectional areas under tension and compression. We obtain the following simple relation:

$$\frac{\xi}{R} = \sin(\phi + \omega) \tag{B5}$$

We note that the location of the neutral axis depends on the amount of material on the deformed part of the indented section which is under tension. Thus it depends on the relative magnitdues of $\dot{w}_L$ and $\dot{w}_G$.

2.3 Energy Dissipation due to Membrane Extension or Compression at the Middle Hinge

For the cross-section of Fig. 2.5 we have:

$$\dot{\varepsilon} = \dot{\varepsilon}_I + \dot{\varepsilon}_{II} + \dot{\varepsilon}_{III} \tag{2.1}$$

where $\dot{\varepsilon}_I$: strain rate over region I
$\dot{\varepsilon}_{II}$: strain rate over region II
$\dot{\varepsilon}_{III}$: strain rate over region III

The above strain rates are given by:

$$\dot{\varepsilon}_I = \frac{1}{\ell_h} \dot{\psi}\, d_I \tag{2.2a}$$

$$\dot{\varepsilon}_{II} = \frac{1}{\ell_h} \dot{\psi}\, d_{II} \tag{2.2b}$$

$$\dot{\varepsilon}_{III} = \frac{1}{\ell_h} \left| \dot{\psi}\, d_{III} - \dot{W}_e \right| \tag{2.2c}$$

$$\text{with } \dot{\psi} = \frac{2\dot{\omega}_G}{L} \tag{B7}$$

where $\dot{\psi}$: rate of angular rotation of the cross-section about the neutral axis

ℓ_h: width of the plastic hinge due to global bending

L: length of the cylinder

$d_{I,II,III}$: distances from the neutral axis (see Fig. 2.5)

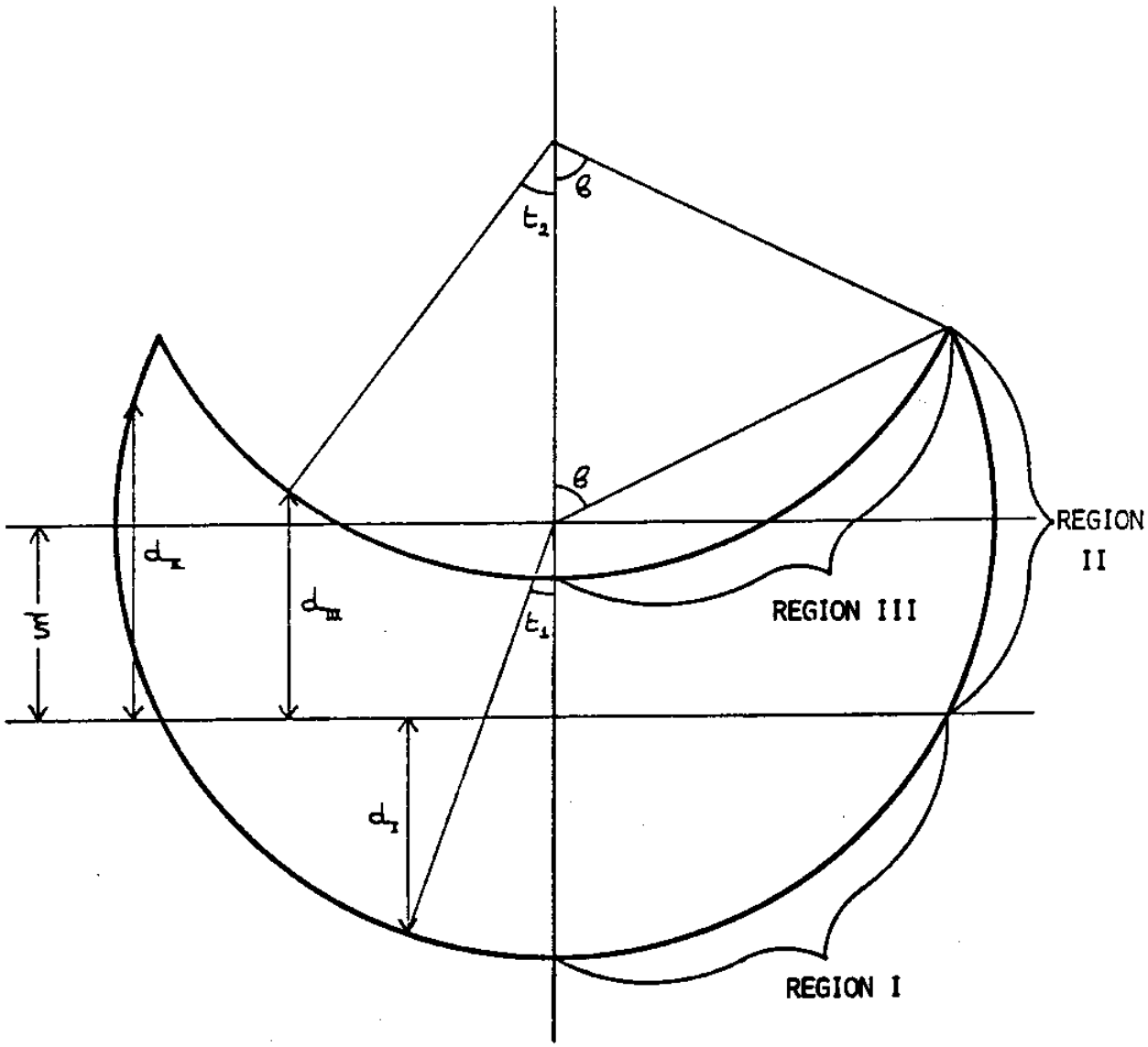

FIGURE 2.5

They are given by the following expressions:

$$\left(\frac{d_I}{R}\right) = \cos t_1 - \left(\frac{\xi}{R}\right) \qquad 0 \le t_1 \le \frac{\pi}{2} - \sin^{-1}\left(\frac{\xi}{R}\right) \tag{2.3a}$$

$$\left(\frac{d_{II}}{R}\right) = \left(\frac{\xi}{R}\right) - \cos t_1 \qquad -\sin^{-1}\left(\frac{\xi}{R}\right) \le t_1 \le \frac{\pi}{2} - \beta \tag{2.3b}$$

$$\left(\frac{d_{III}}{R}\right) = \left(\frac{\xi}{R}\right) + 2\cos\beta - \cos t_2 \qquad 0 \le t_2 \le \beta \tag{2.3c}$$

From (1.5) integrating along the thickness of the cylinder and along the width of the plastic hinge we obtain an expression for the rate of energy dissipation due to local membrane extension and global bending:

$$\dot{D}^H = 4h\ell_h\sigma_o \int_{arcs} \dot{\varepsilon} ds \tag{2.4}$$

By substituting (2.1), (2.2a,b,c), (2.3a,b,c), (A23), (B5), (B7) (B10) and (B11) into (2.4) and integrating over the arcs of the cross-section we obtain the final expression in terms of $\left(\frac{R}{h}\right)$, $\left(\frac{L}{R}\right)$, $\tilde{w}_L$, α, ζ, and $(\phi + \omega)$. (See appendix B, section 2).

$$\begin{aligned} D^H = 16M_o\dot{w}\left(\frac{R}{h}\right)\Bigg\{ & 2\,\frac{(1-\zeta)}{\left(\frac{L}{R}\right)}\Bigg[2\Big[\cos(\phi+\omega) + (\phi+\omega)\sin(\phi+\omega)\Big] \\ & - \sin[\cos^{-1}(1-\tilde{w}_L)] - \cos^{-1}(1-\tilde{w}_L)\sin(\phi+\omega)\Bigg] \\ & + \Bigg| 2\,\frac{(1-\zeta)}{\left(\frac{L}{R}\right)}\Bigg[\Big[2(1-\tilde{w}_L) + \sin(\phi+\omega)\Big]\cos^{-1}(1-\tilde{w}_L) \\ & - \sin\Big[\cos^{-1}(1-\tilde{w}_L)\Big]\Bigg] - \zeta\Big[\tan 2\alpha \cdot \cos^{-1}(1-\tilde{w}_L)\Big]\Bigg|\Bigg\} \end{aligned} \tag{B13}$$

From (B12) we obtain:

$$\zeta = \frac{2(1-\tilde{w}_L) + \sin(\phi+\omega) - \cos(\phi+\omega)}{\left(\frac{L}{R}\right)\frac{\tan 2\alpha}{2} + 2(1-\tilde{w}_L) + \sin(\phi+\omega) - \cos(\phi+\omega)} \tag{2.5}$$

$$(1 - \zeta) = \frac{\left(\frac{L}{R}\right) \frac{\tan 2\alpha}{2}}{\left(\frac{L}{R}\right) \frac{\tan 2\alpha}{2} + 2(1-\tilde{w}_L) + \sin(\phi+\omega) - \cos(\phi+\omega)} \tag{2.6}$$

We substitute (2.5) and (2.6) in (B.13). Noting that the denominator in these equations is always positive we can take it out of the absolute value, to obtain:

$$\dot{D}_H = 16M_o\dot{w} \frac{\left(\frac{R}{h}\right)}{\left(\frac{L}{R}\right) \frac{\tan 2\alpha}{2} + 2(1-\tilde{w}_L) + \sin(\phi+\omega) - \cos(\phi+\omega)} \left\{ \tan 2\alpha \left[2 \left[\cos(\phi+\omega) + (\phi+\omega)\sin(\phi+\omega) \right] - \sin\left[\cos^{-1}(1-\tilde{w}_L)\right] - \cos^{-1}(1-\tilde{w}_L)\sin(\phi+\omega) \right] + \left| \tan 2\alpha \cdot \cos^{-1}(1-\tilde{w}_L)\cos(\phi+\omega) - \sin\left[\cos^{-1}(1-\tilde{w}_L)\right] \right| \right\} \tag{2.7}$$

2.4 Calculation of the Crushing Load for a Simply Supported Beam

2.4.1 Analytical Expression for the Load vs Deflection and Several Geometric Parameters

The above expression is the rate of energy dissipation due to global bending of the cylinder and due to local membrane extension. Thus, by combining it with the hoop and bending term of (1.30) we obtain the total rate of internal energy dissipation. By equating that with the external energy dissipation given in (1.26) and (1.27) we arrive at the final expression for the total applied load, $\bar{P}$:

For a beam or wedge loading:

$$\bar{P}_B = 16M_o \left\{ \frac{\left(\frac{R}{h}\right)}{\left(\frac{L}{R}\right) \frac{\tan 2\alpha}{2} + 2(1-\tilde{w}_L) + \sin(\phi+\omega) - \cos(\phi+\omega)} \left\{ \tan 2\alpha \left[2 \left[\cos(\phi+\omega) + (\phi+\omega)\sin(\phi+\omega) \right] - \sin\left[\cos^{-1}(1-\tilde{w}_L)\right] - \cos^{-1}(1-\tilde{w}_L)\sin(\phi+\omega) \right] + \left| \tan 2\alpha \cdot \cos^{-1}(1-\tilde{w}_L)\cos(\phi+\omega) - \sin\cos^{-1}(1-\tilde{w}_L) \right| \right\} + \sqrt{\frac{2}{3}\left(\frac{R}{h}\right)\sqrt{2\tilde{w}_L}\,\tan\alpha \cdot \tan^{-1}\left(\frac{\sqrt{2\tilde{w}_L}}{\sin}\right)\left[\cos^2\alpha + \frac{2\tilde{w}_L}{3\tan^2\alpha} + \frac{\tilde{P}}{\tan\alpha}\right]} \right\} \tag{2.8a}$$

where ω is given by:

$$\omega = \cos^{-1}\left[(1 - \tilde{w}_L) \pm \sqrt{\tilde{w}_L(2 - \tilde{w}_L) - \frac{1}{2}}\right] \text{for } \tilde{w}_L \geq 0.5 \qquad (B4)$$

$$\omega = 0 \qquad \text{for } \tilde{w}_L \leq 0.5$$

For a point loading:

$$\overline{P}_p = \frac{1}{2}\,\frac{\cos 2\alpha}{\cos^2\alpha}\,\overline{P}_B \qquad (2.8b)$$

The final crushing load vs. total deflection is then given parametrically by (2.8a,b) and (B4) in terms of M_o, $\frac{R}{h}$, ϕ, and α.

2.4.2 Minimization Procedure

Given the geometric parameters $\frac{R}{h}$ and $\frac{L}{R}$, for each value of $\tilde{w}_L$, expressions (2.8a,b) can be minimized with respect to ϕ and α to yield the final crushing load corresponding to that value of $\tilde{w}_L$. From the above process, the function of ϕ values at the minimum load, ϕ_{min}, vs $\tilde{w}_L$ is obtained. Combining $\phi_{min}(\tilde{w}_L)$ with (2.5) and (B4) we obtain a function of the ξ values at the minimum load vs $\tilde{w}_L$, $\zeta_{min}(\tilde{w}_L)$. To obtain the final relation for the load vs total deflection we need to calculate $\tilde{w}$ as follows:

$$\tilde{w} = \int_0^{\tilde{w}_L} \frac{d\hat{w}_L}{\zeta_{min}(\hat{w}_L)} \qquad (2.9)$$

A small computer program was developed to perform the minimization. A very simple grid search scheme was employed. An 11 by 50 point grid was used in most of the cases, and was found adequate. Yet, since the required computer time was minimal, a much more detailed search could be easily performed if better accuracy was needed. The program was constructed to be interactive so that the user could vary the various parameters and search ranges and intervals. A listing of the program is given in Appendix B, section 4.

2.4.3 Numerical Results

The crushing load was calculated for several combinations of the radius-to-thickness ratio, $\frac{R}{h}$, and length-to-radius ratio, $\frac{L}{R}$. Appendix B, section 5 contains the detailed results for the cases examined. For each combination of $\frac{R}{r}$ and $\frac{L}{R}$, the values of $\tilde{w}$, $\frac{P}{M_o}$, ξ_{min}, α_{min}, and ϕ_{min} are given at several deflections, $\tilde{w}_L$. The crushing load vs local deflection are plotted in Fig. 2.6-2.11. In Fig. 2.6-2.8 the crushing load variation with the length-to-radius ratio is shown for three radius-to-thickness ratios. In Fig. 2.9-2.11 the variation of the crushing load with the radius-to-thickness ratio is given for three length-to-radius ratios. Fig. 2.12 gives the maximum load and the load-deflection curve for two cases: when the interaction between the local and the global deformation modes is taken into consideration and when they are assumed (for simplicity) to be independent.

2.5 Effect of Axial Restraint at the Supports

If the ends of the tubular beam are axially restrained the load carrying capacity of the beam will increase compared to the simply supported case presented in the previous sections. This is due to membrane forces developing while the tube deflects globally as a beam. The post-yield behavior of rectangular beams has been analysed in [18] and extended to beams with tubular cross-section by Oliveira in [19]. The following expressions hold:

$$\frac{P_R}{P_B} = \cos \frac{\pi}{2}\frac{N}{N_p} + \frac{\pi}{8}\frac{N}{N_p}\tilde{w}_G$$

$$\frac{d\frac{N}{N_p}}{d(\tilde{w}_G)} = k_s\left|\tilde{w}_G - \sin\frac{\pi}{2}\frac{N}{N_p}\right| \qquad \frac{N}{N_p} \leq 1$$

$$\frac{P_R}{P_B} = \frac{\pi}{8}\tilde{w}_G \qquad \frac{N}{N_p} > 1$$

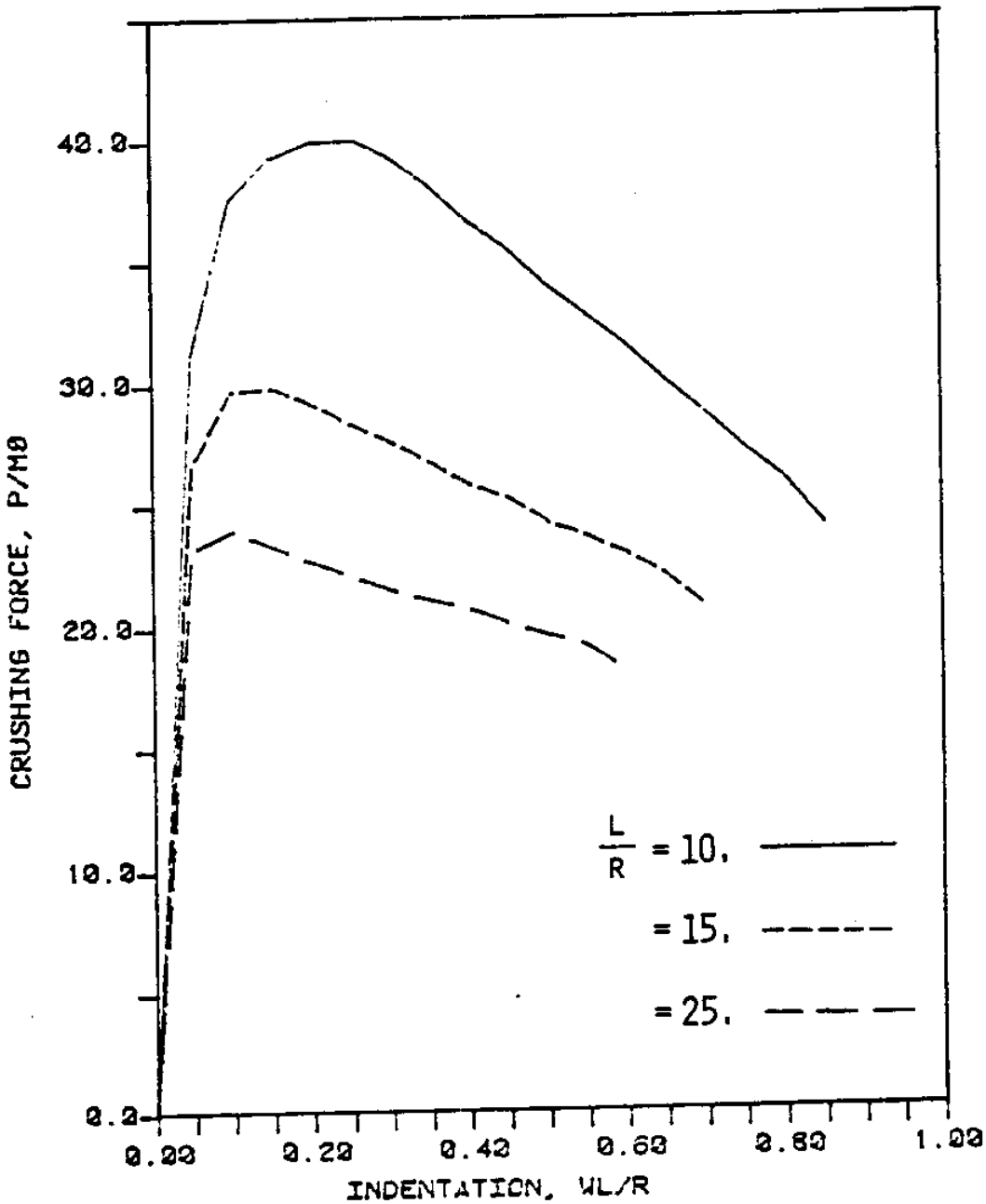

SIMPLY SUPPORTED BEAM : $\frac{R}{h} = 10.$

FIGURE 2.6

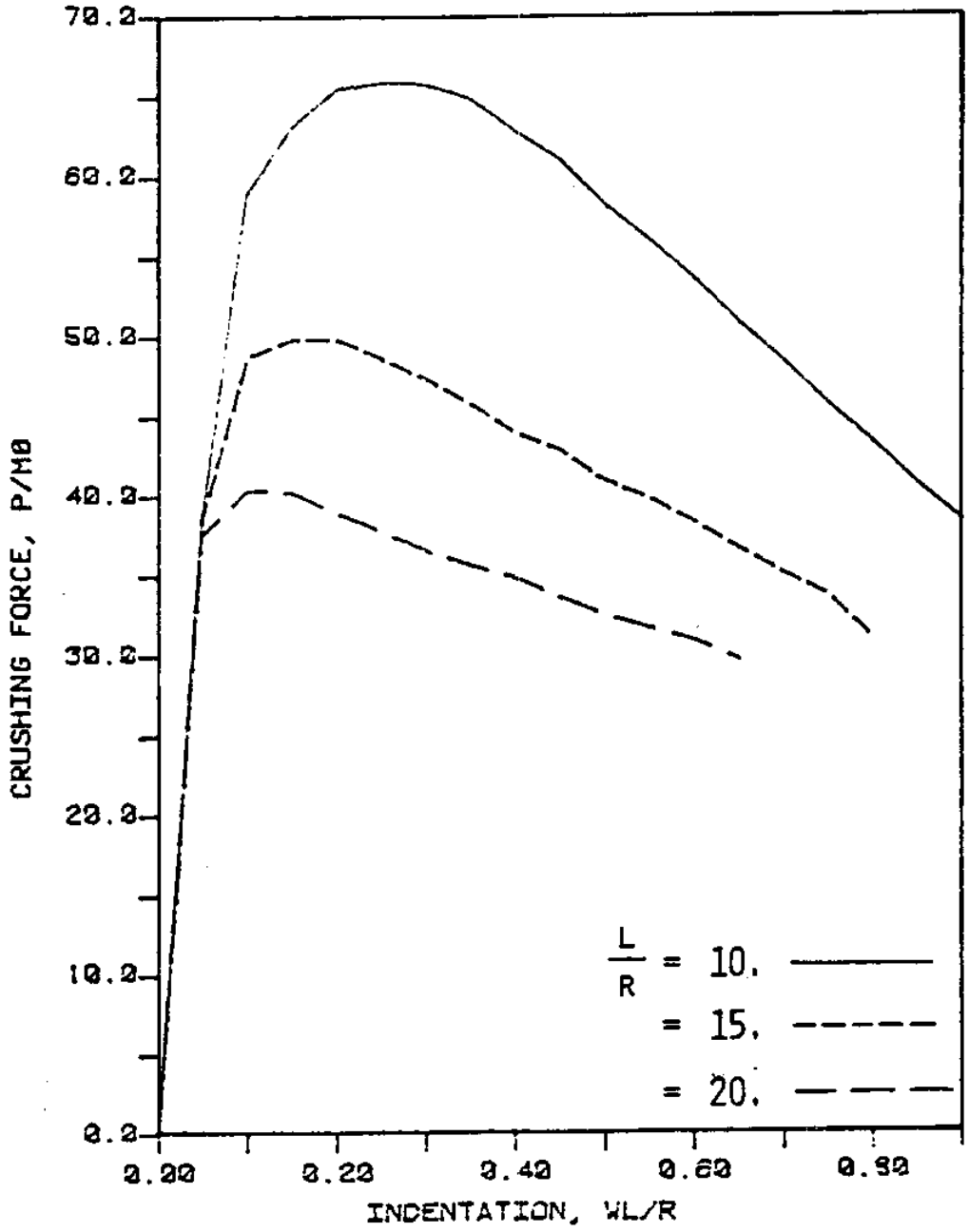

SIMPLY SUPPORTED BEAM : $\frac{R}{h} = 17.65$

FIGURE 2.7

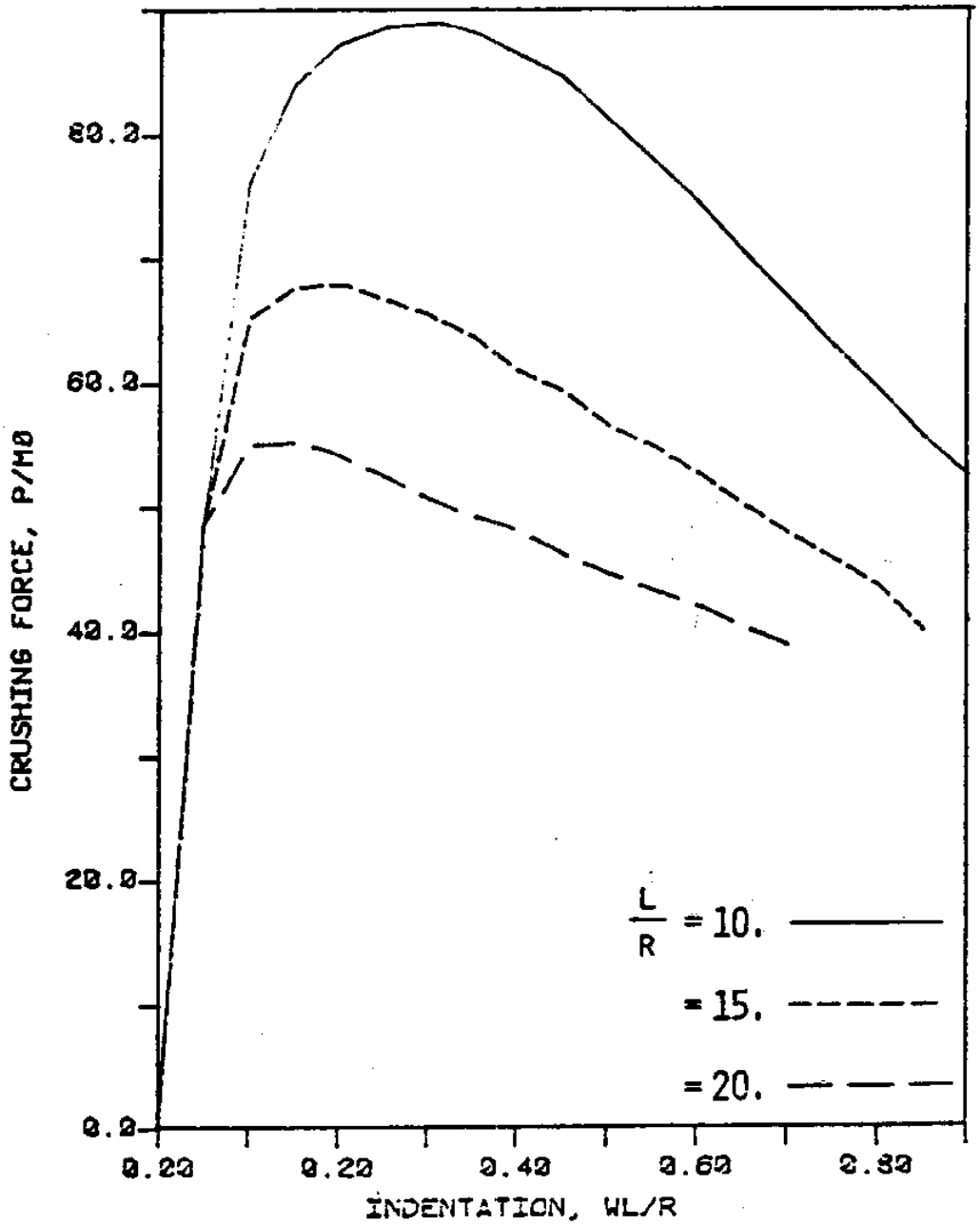

SIMPLY SUPPORTED BEAM : $\frac{R}{h} = 25.$

FIGURE 2.8

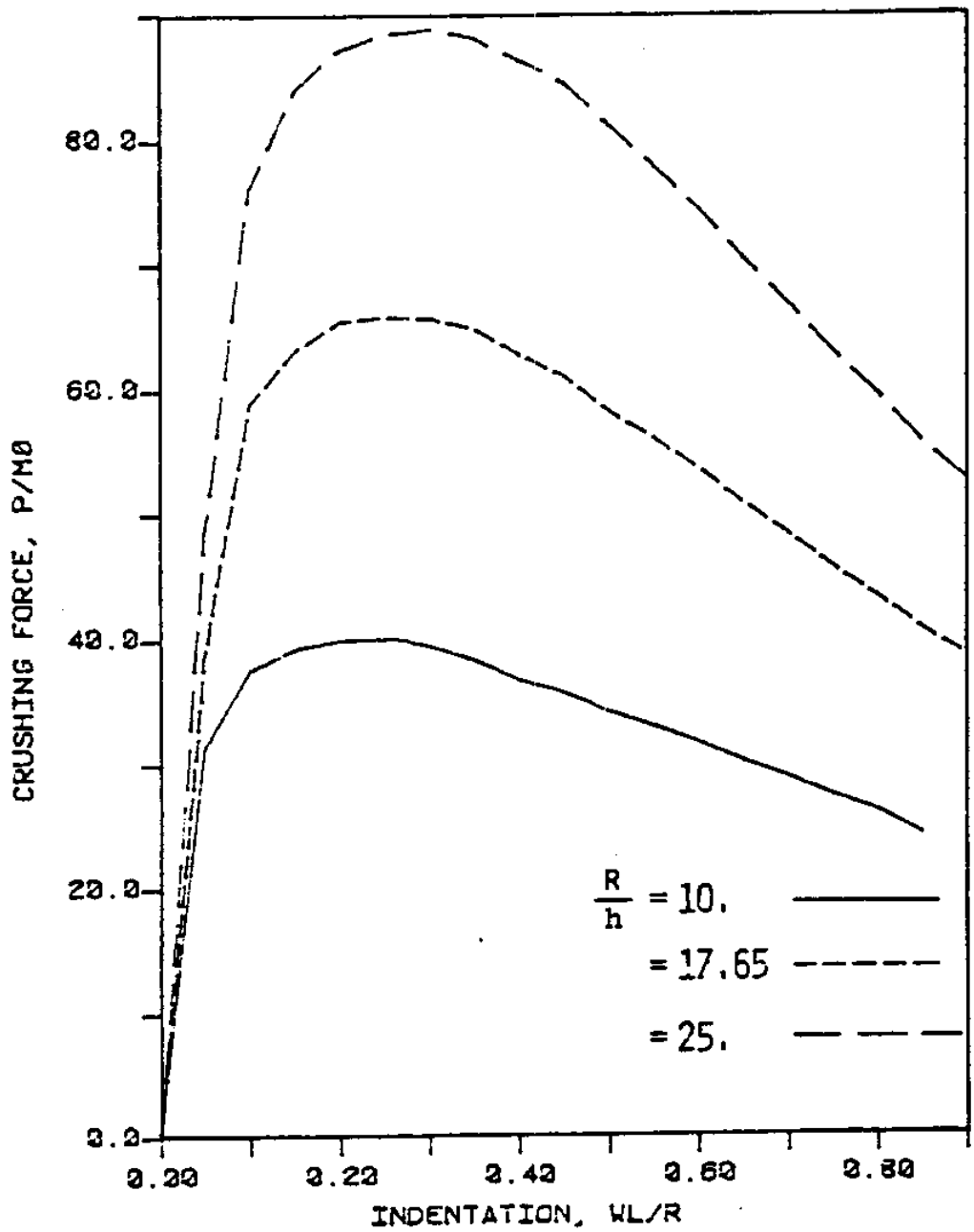

SIMPLY SUPPORTED BEAM : $\frac{L}{R} = 10.$

FIGURE 2.9

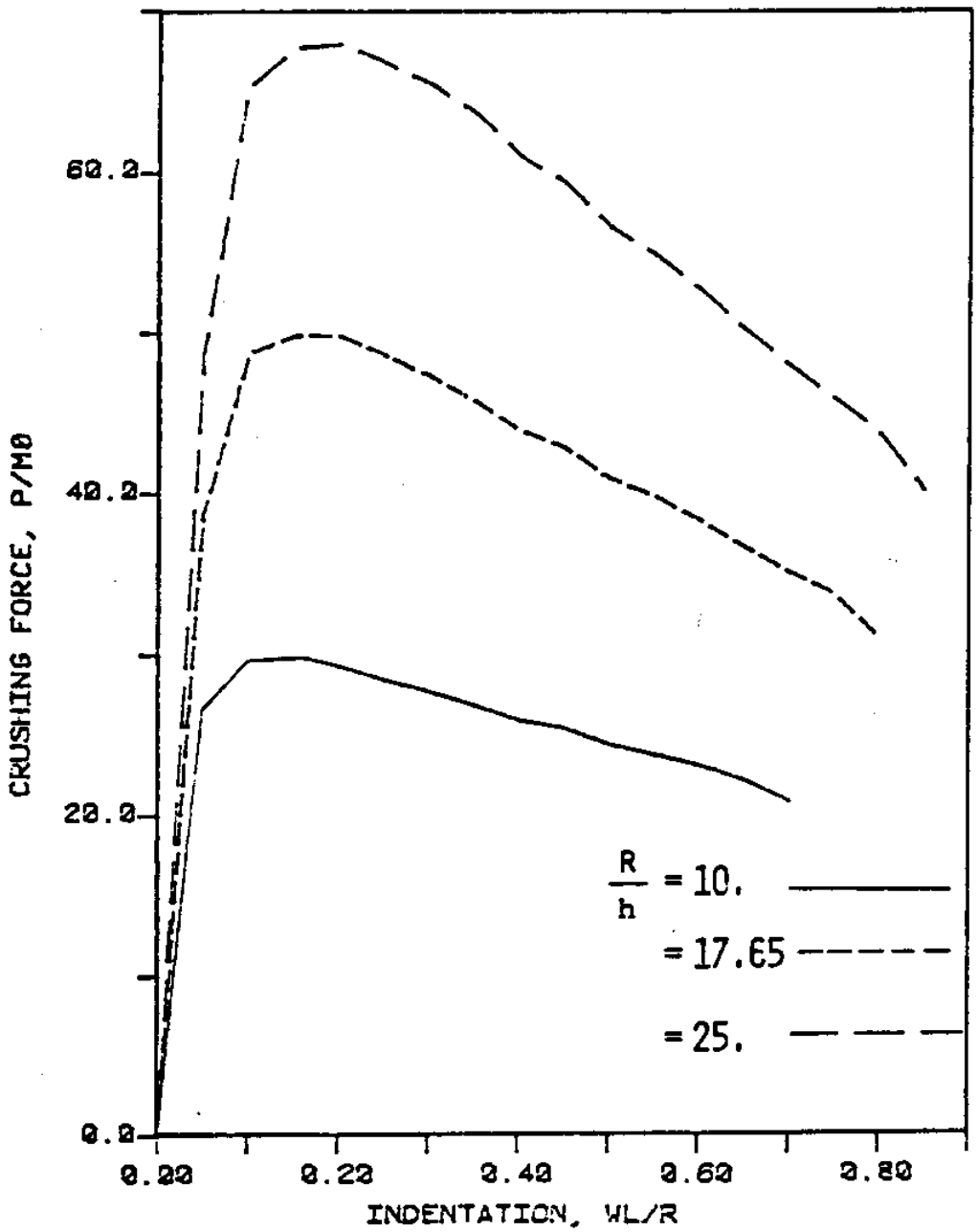

SIMPLY SUPPORTED BEAM : $\frac{L}{R} = 15.$

FIGURE 2.10

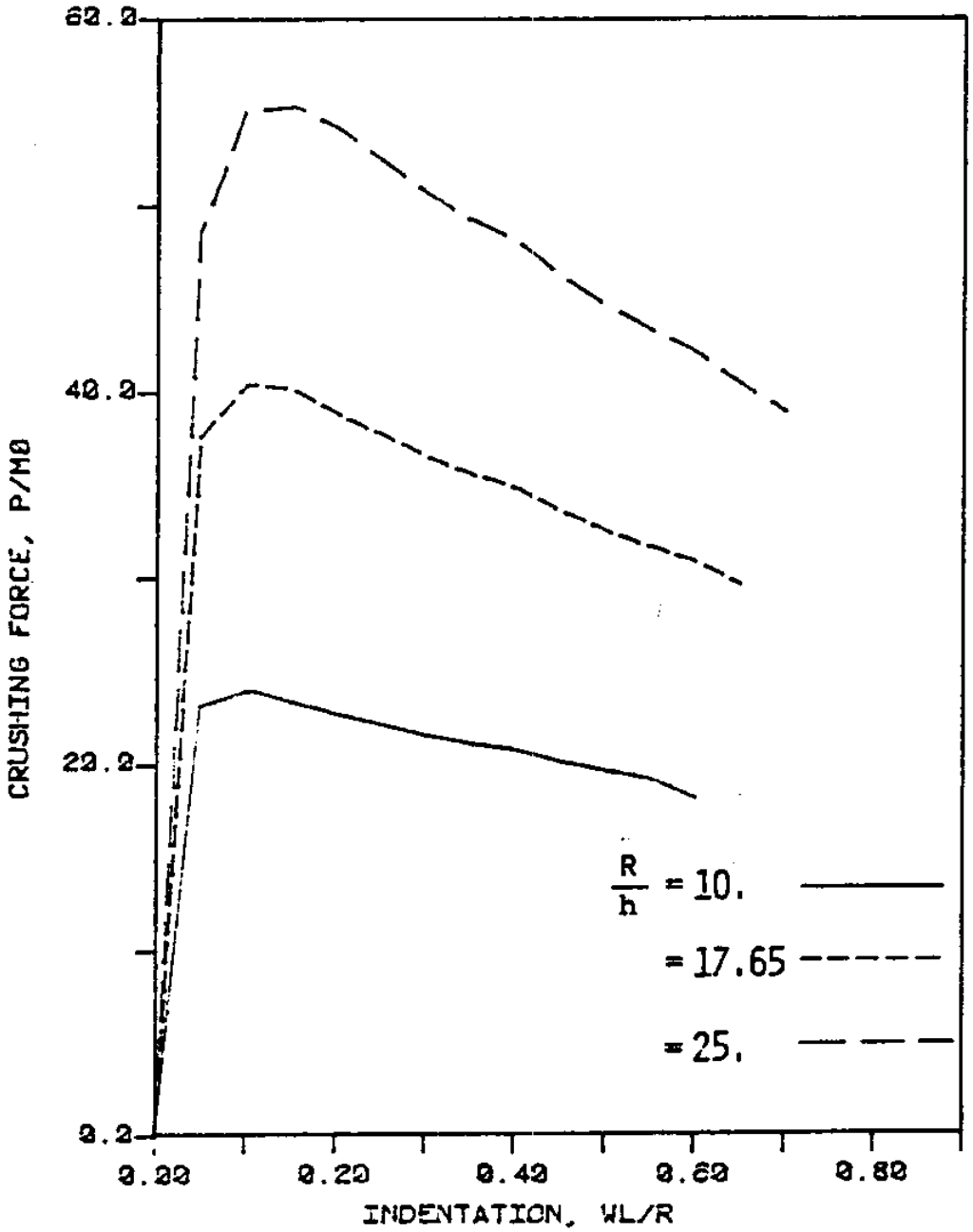

SIMPLY SUPPORTED BEAM : $\frac{L}{R} = 20.$

FIGURE 2.11

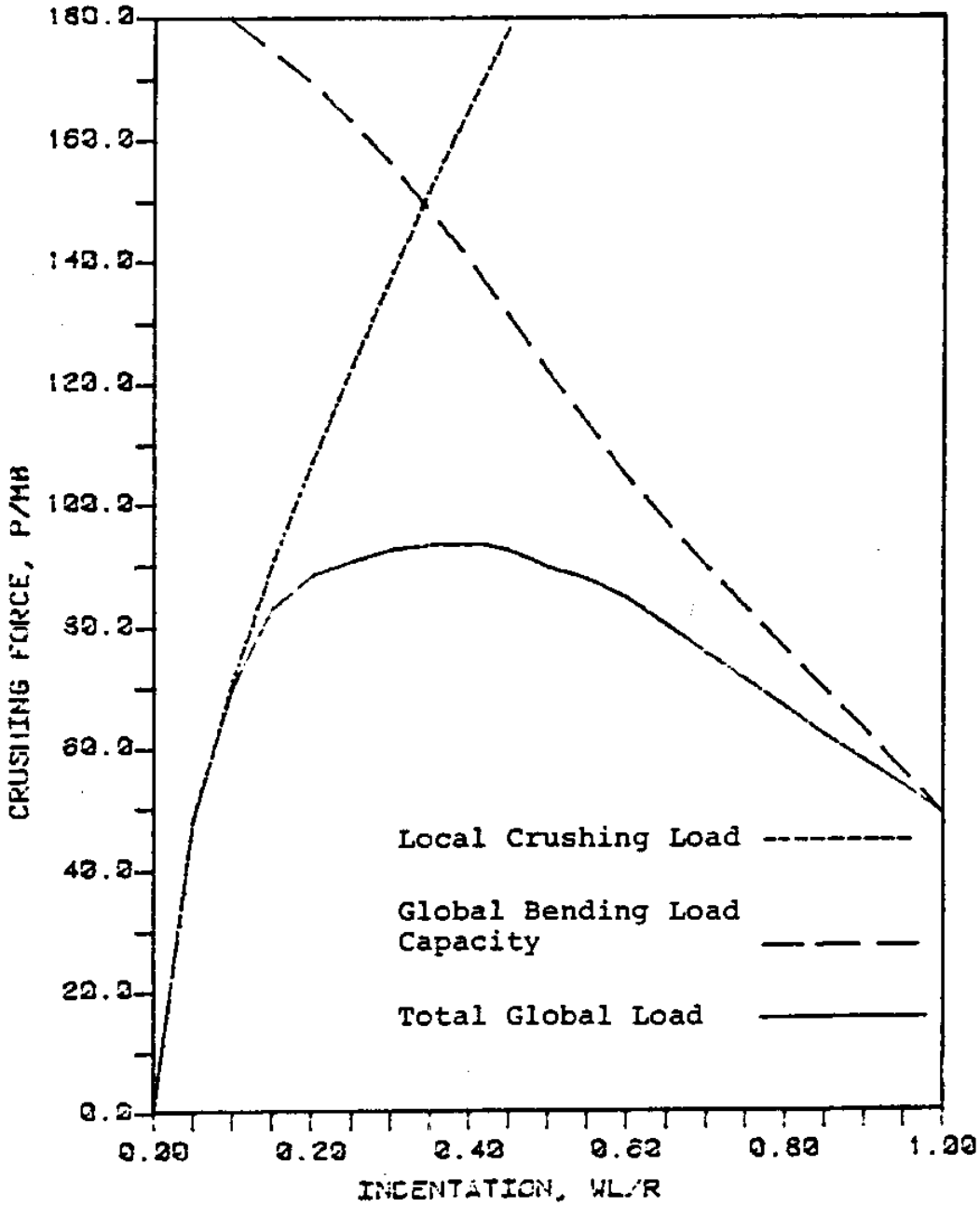

SIMPLY SUPPORTED BEAM : $\frac{R}{h} = 17.65$, $\frac{L}{R} = 6.11$

FIGURE 2.12

with $k_s = \dfrac{\frac{R}{h}\,\frac{K_s}{R}}{\frac{\pi}{2}\,\frac{L}{R}\,\sigma_o}$

where P_R: load carried by a beam axially restrained at the supports

P_B: load carried by a simply supported beam

$\frac{N}{N_p}$: non-dimensional axial force

K_s: axial stiffness at the supports

The above equations were solved by linearizing the yield condition for a particular value of $\frac{N}{N_p}$. Fig. 2.13 shows several curves relating P_R to P_B and w_G for various values of the stiffness parameter k_s. Fig. 2.14 shows the simply supported case of Fig. 2.12 adjusted for an axial support restraint of $k_s = 1$, together with the results from an experiment ([12]). Both are for the same geometric parameters: $\frac{R}{h} = 17.65$, $\frac{L}{R} = 6.11$, $\frac{B}{R} = 0.465$.

2.6 Discussion

In all of the calculated load-deformation curves three separate phases during deformation can be noted. These phases which were also observed during experiments ([8] to [10]) are: (i) a pure crumpling phase during which only local deformation occurs, (ii) a bending and crumpling phase during which both local deformation and global bending occurs simultaneously, and (iii) a phase of structural collapse during which the local deformation is very small and the load drops steeply.

There are several trends that can be deduced from the results. Examining Fig. 2.6-2.8 we can note that the load capacity is reduced as the length-to-radius ratio is increased for constant radius-to-thickness ratio. This behavior, of course, is analogous to the variation with

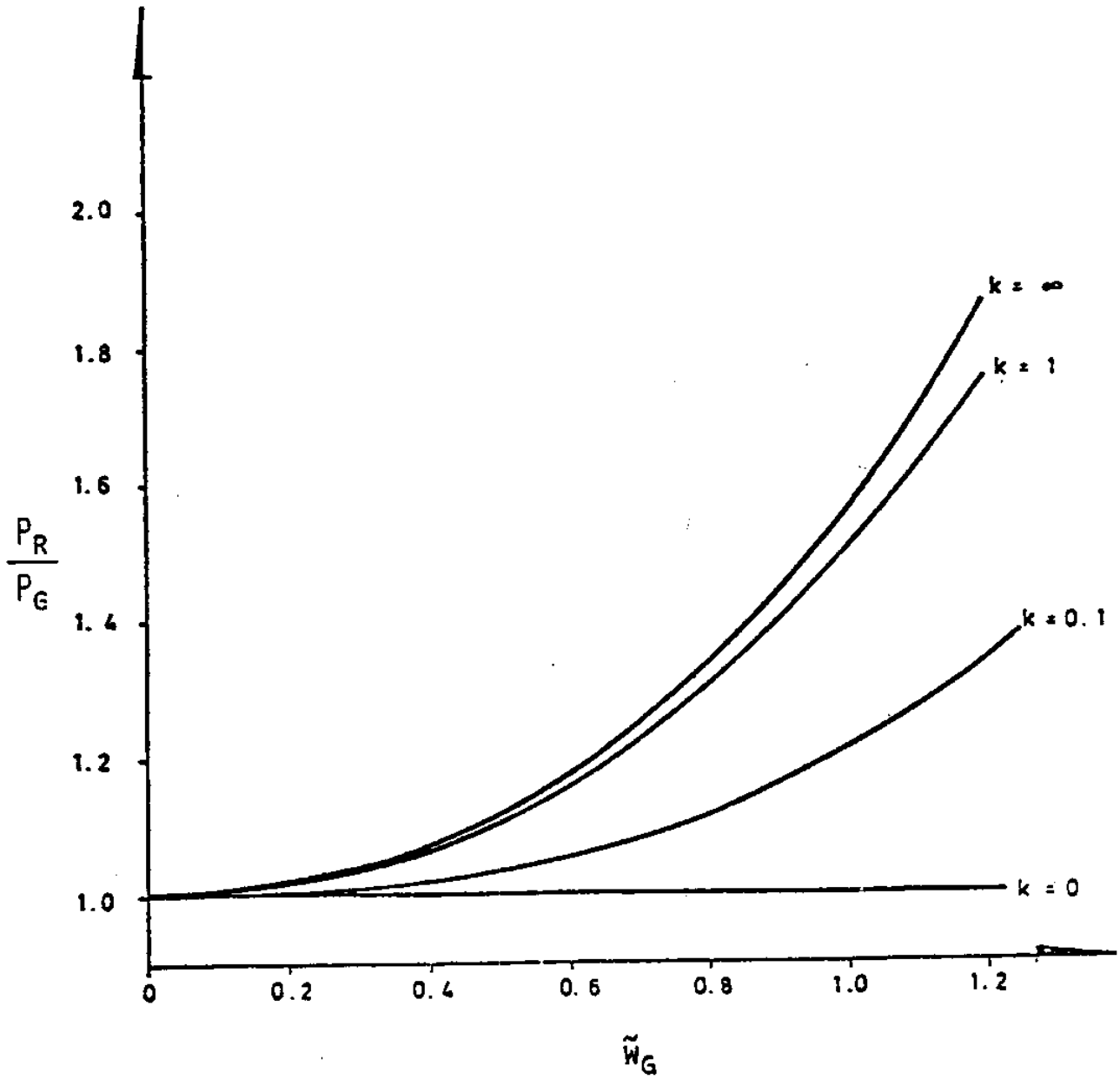

INCREASE IN THE LOAD CARRYING CAPACITY
DUE TO AXIAL SUPPORT RESTRAINT

FIGURE 2.13

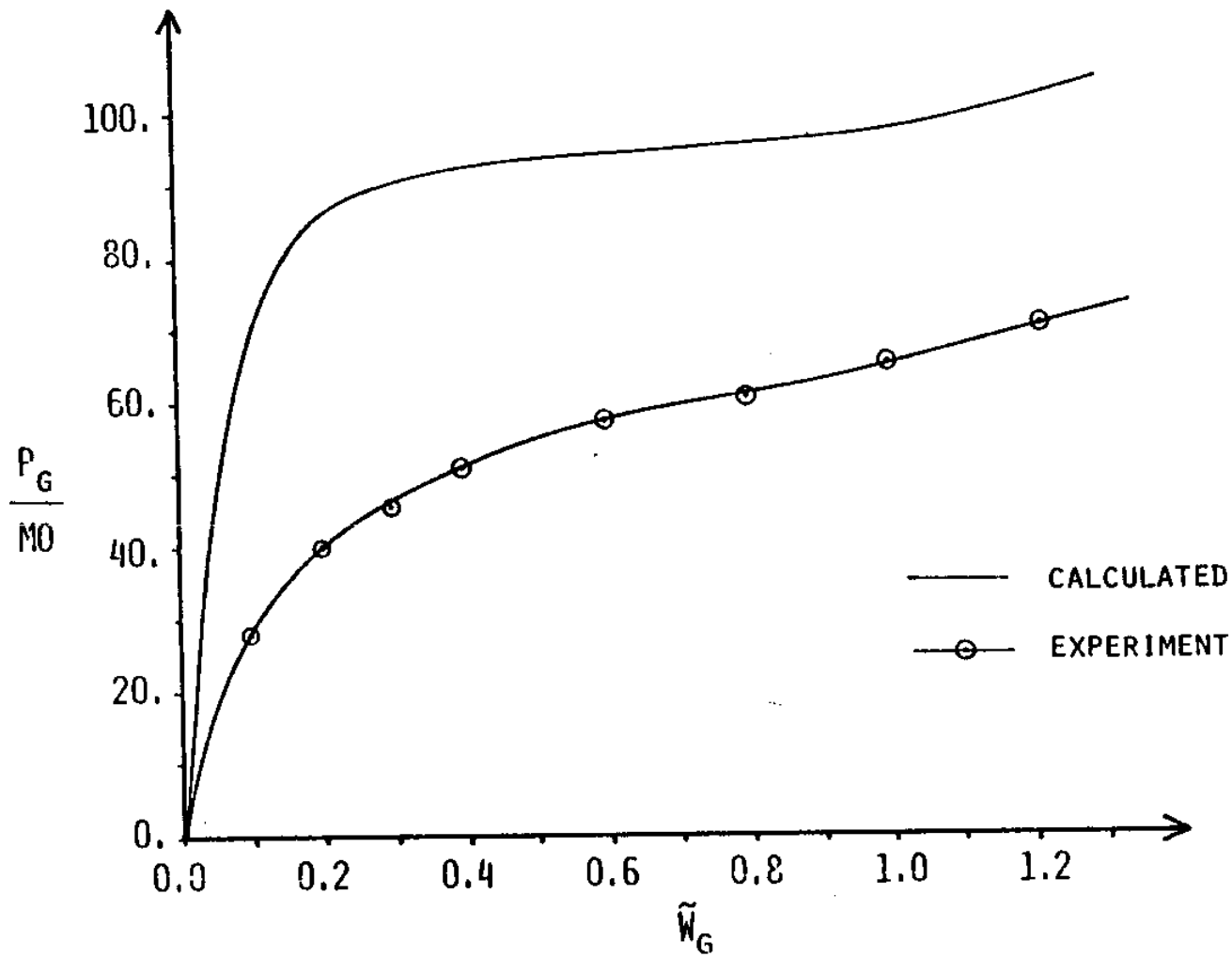

GLOBAL LOAD VS GLOBAL DEFLECTION

FOR AN AXIALLY RESTRAINED TUBULAR BEAM : $\frac{R}{t} = 17.65$, $\frac{L}{R} = 6.11$

$k_s = 1.0$

FIGURE 2.14

length of the collapse load for a rigid-plastic beam. Another observation from the above figures is that the crumpling phase gets shorter as $\frac{L}{R}$ increases. This was also observed during the experiments by Thomas, S.G. et al. in [8] to [10].

In addition to the above we can see from Fig. 2.9 - 2.11 that the load capacity increases as the radius-to-thickness ratio increases for constant length-to-radius ratio. This can also be explained by recalling the rigid-plastic beam case mentioned above. Similarly, it can be seen that the pure crumpling phase becomes longer as $\frac{R}{h}$ increases. Also, we note that the variation of the duration of the above phase with $\frac{R}{h}$ is less than the variation of that phase's duration with $\frac{L}{R}$.

If now we examine Fig. 2.14 we see that the overall pattern of the calculated load-deflection curve is similar to the one obtained by the experiment. However, there is a difference of a factor of two in the two load levels. Also the slope of the experimental curve between $0.4 \leq w_G \leq 1.0$ is larger than the slope of the calculated curve, although a relatively high axial support stiffness was used for the latter (probably higher than the actual one of the experiment). This, I believe, can be explained by the fact that as discussed in the first chapter the expression which is used in this chapter for the load due to local deformation overestimates that load by a factor of around three. Finally, in Fig. 2.15 it is shown schematically how a smaller local crushing load would affect the calculated overall load-deflection curve for a tubular beam.

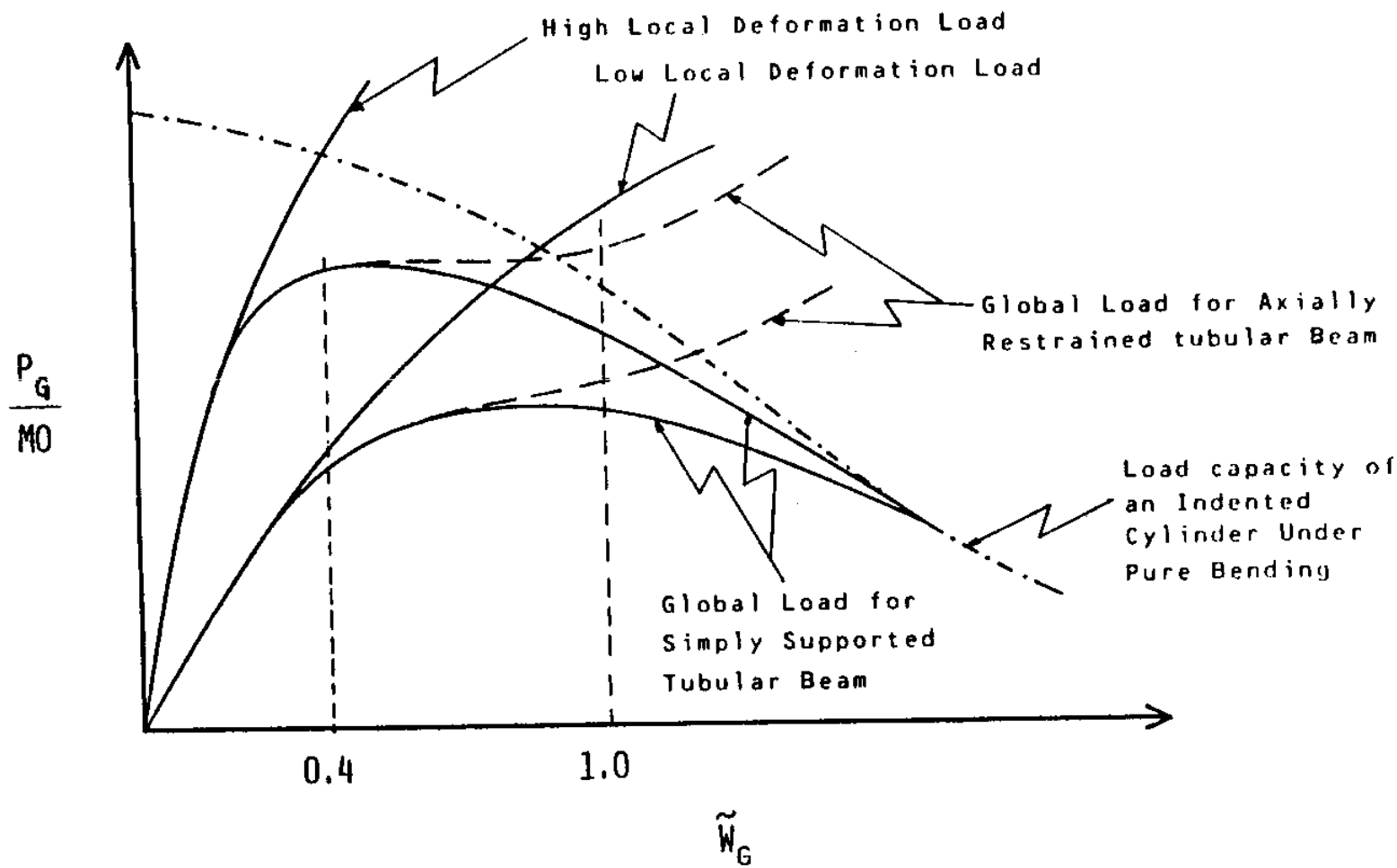
High Local Deformation Load
Low Local Deformation Load
Global Load for Axially Restrained tubular Beam
Load capacity of an Indented Cylinder Under Pure Bending
Global Load for Simply Supported Tubular Beam
$\frac{P_G}{MO}$
0.4
1.0
$\tilde{W}_G$

FIGURE 2.15

Chapter 3

DYNAMIC MODELLING OF A COLLISION

3.1 Introduction

During a collision of a ship with an offshore platform the kinetic energy of the ship is partially absorbed by the platform and partially absorbed by the ship itself. The classification societies and other regulatory bodies have included in their codes clauses that define what percentage of the transformed energy is absorbed by the ship and what by the platform. Since the partitioning of the energy depends on both the masses and the plastic load-deflection characteristics of the ship and the platform, just defining a percentage partitioning might result in considerable errors. To avoid this, most codes specify a percentage that is conservative for the platforms, with the 100% of the energy required to be absorbed by the platform being the extreme.

Sørensen has presented in [20] a simple way of calculating the maximum load that a platform of known stiffness characteristics would withstand during a collision with a ship of also known mass and stiffness characteristics and for a given impact velocity. The load vs. deflection curves for both structures were assumed to be elastic-perfectly plastic and the problem could thus be solved analytically. In addition, the foundation stiffness of the platform was taken as infinite so that no movement of the impacted member was allowed. In this section the above method is extended, so that it can be applied using more realistic load-deflection characteristics. Furthermore, one more degree of freedom was added to the model, so that cases where the platform's foundation stiffness cannot be assumed infinite, could now be analyzed.

3.2 Simplified Collision Dynamics Model

The collision problem can be modelled as a plastic impact involving translational motion only. The following equations can be written:

$$m_1\ddot{x}_1 = -F(\delta_1 + \delta_2) \tag{3.1a}$$

$$m_2\ddot{x} = F(\delta_1 + \delta_2) - F_R(x) \tag{3.1b}$$

where m_1: mass and hydrodynamic added mass of the impacting ship

m_2: equivalent mass and hydrodynamic added mass of the platform (defined further in this section)

x_1: displacement of the center of mass of the impacting ship

x: displacement of the center of mass of the platform

F: contact force between the ship and the platform

F_R: platform's foundation reaction force

δ_1: crushing length of the impacting ship

δ_2: crushing length of the platform

A schematic representation of the impact model is given in Fig.3.1. The following relation between x_1, x and δ_1, δ_2 holds:

$$x_1 - x = \delta_1 + \delta_2 = \delta \tag{3.2}$$

By substituting the above in (3.1a,b) we obtain:

$$m_1\ddot{x}_1 = -F(x_1 - x) \tag{3.3a}$$

$$m_2\ddot{x} = F(x_1 - x) - F_R(x) \tag{3.3b}$$

Defining $X = x_1 - x$ (3.4a)

we have $\ddot{X} = \ddot{x}_1 - \ddot{x}$ (3.4b)

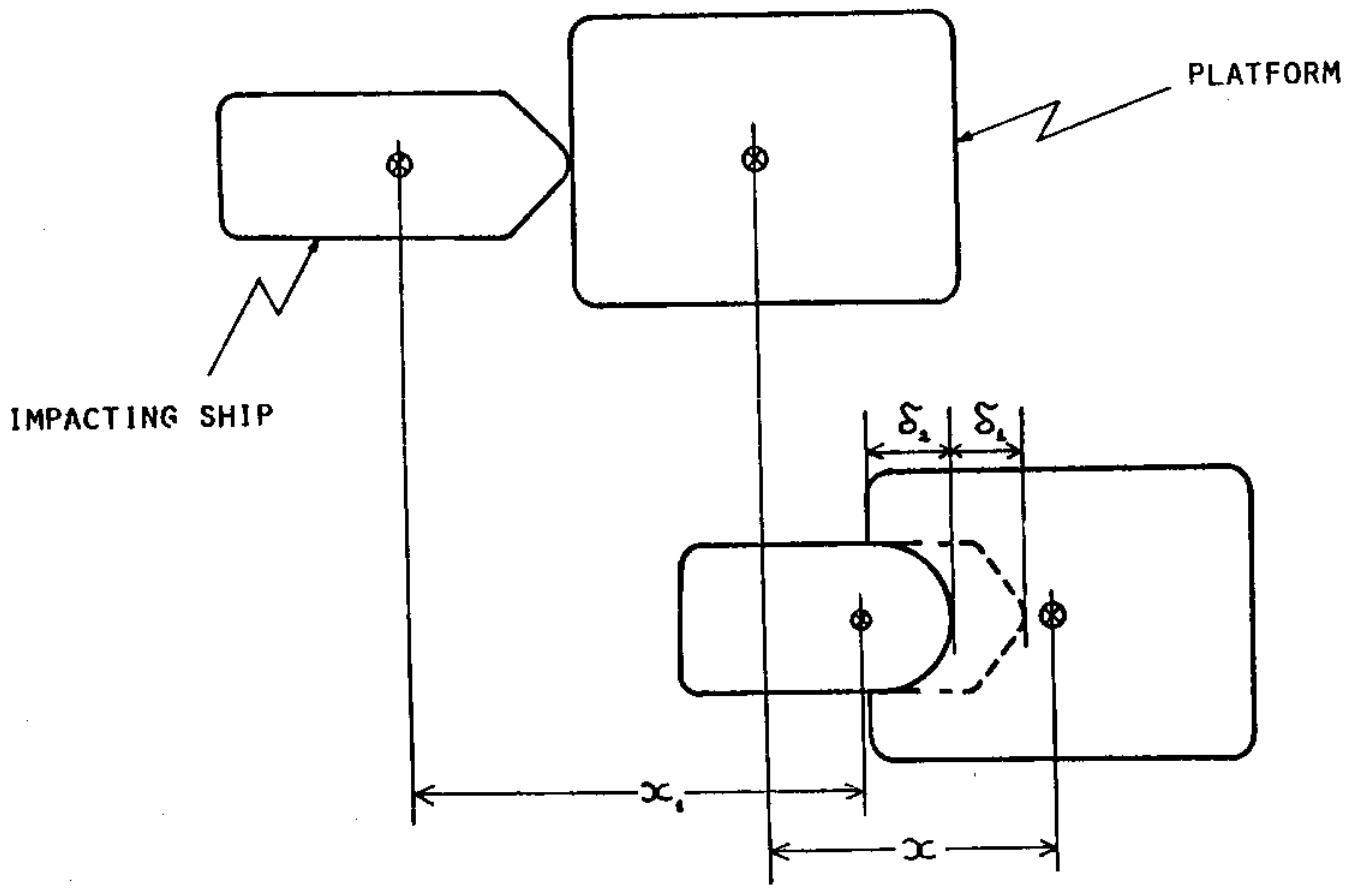

FIGURE 3.1

By substituting in (3.3a,b) we obtain:

$$m_1(\ddot{X}_1 + \ddot{X}) = -F(X) \tag{3.5a}$$

$$m_2\ddot{X} = F(X) - F_R(x) \tag{3.5b}$$

The load-deformation function F(X) can be obtained by combining the two plastic load-deformation functions of the ship and the platform as explained in appendix C, section 1. The platform foundation's load-deformation function, $F_R(x)$, could, for most cases, be substituted by the linear term $(k \cdot x)$. Since F(X) will be non-linear and (3.5a,b) should be solved numerically we can leave $F_R(x)$ in a general force-deflection form. Thus we preserve generality, in case that the foundation support reaction is non-linear.

3.3 Numerical Solution of the Differential Equations

3.3.1 Formulation of the Recursive Relations Used for the Solution

To solve (3.5a,b) we use the Central Difference Method as outlined in [21]. The equations are integrated using a numerical step-by-step procedure. In essence, this method is based on two ideas. First, instead of trying to satisfy (3.5a,b) at any time t, it is aimed to satisfy them only at discreet time intervals Δt apart. Second, a linear variation of displacements, velocities and accelerations within each time interval Δt is assumed. We then have:

$$\ddot{X}_t = \frac{1}{\Delta t^2}\left[X_{t-\Delta t} - 2X_t + X_{t+\Delta t}\right] \tag{3.6a}$$

$$\ddot{x}_t = \frac{1}{\Delta t^2}\left[x_{t-\Delta t} - 2x_t + x_{t+\Delta t}\right] \tag{3.6b}$$

where t denotes position in time.

Substituting back in (3.5a,b) and solving for $X_{t+\Delta t}$ and $x_{t+\Delta t}$ we obtain:

$$X_{t+\Delta t} = \Delta t^2\left[\frac{1}{m_2} F_R\,(x_t) - \left(\frac{1}{m_1} + \frac{1}{m_2}\right) F(X_t)\right] + 2X_t - X_{t-\Delta t} \tag{3.7a}$$

$$x_{t+\Delta t} = \frac{\Delta t^2}{m_2}\,[F(X_t) - F_R(x_t)] + 2x_t - x_{t-\Delta t} \tag{3.7b}$$

To initialize the problem and calculate the solution at time Δt, $X_{-\Delta t}$ and $x_{-\Delta t}$ are needed. They are given by:

$$X_{-\,t} = X_o - \Delta t\cdot\dot{X}_o + \frac{\Delta t^2}{2}\,\ddot{X}_o \tag{3.8a}$$

$$x_{-\Delta t} = x_o - \Delta t\cdot\dot{x}_o + \frac{\Delta t^2}{2}\,\ddot{x}_o$$

where X_o $\dot{X}_o$ $\ddot{X}_o$

and x_o, $\dot{x}_o$, $\ddot{x}_o$ are the initial conditions.

To obtain a valid solution using the central difference method, the time step Δt should be less than a critical value t_{cr} and

$$\Delta t_{cr} = \frac{T_{min}}{\pi}$$

where T_{min} is the smallest period of the system.

The critical time step, Δt_{cr}, at small displacements is evaluated in Appendix C, section 2. Thus we have

$$\Delta t \leq \Delta t_{cr} = \frac{2\sqrt{2}}{\sqrt{\left(\frac{K}{m_1}\right) + \left(\frac{K+k}{m_2}\right) + \sqrt{\left(\frac{K}{m_1}\right)^2 + \left(\frac{K+k}{m_2}\right)^2 + 2\left(\frac{K}{m_1}\right)\left(\frac{K-k}{m_2}\right)}}} \tag{C.7}$$

with $K = \frac{k_1 k_2}{k_1 + k_2}$ (C.4)

$$k_1 = \left.\frac{dF_1}{d\delta_1}\right|_{\delta_1 = \pm 0} \quad \text{(C.3a)}$$

$$k_2 = \left.\frac{dF_2}{d\delta_2}\right|_{\delta_2 = \pm 0} \quad \text{(C.3b)}$$

$$k = \left.\frac{dF_R}{\delta x}\right|_{x = \pm 0} \quad \text{(C.3c)}$$

where $F_1(\delta_1)$: plastic load-deformation relationship of the impacting ship

$F_2(\delta_2)$: plastic load-deformation relationship of the platform

$F_R(x)$: force-deflection relationship for the platform's foundation reaction

Here we should note that a Δt slightly smaller than the critical time step guarantees stability in the results but not accuracy. In many occasions a time step several times smaller than the critical one is required for the results to converge within satisfactorily small errors.

3.3.2 Required Input for the Solution

For the consecutive time step solution a computer program was developed using (3.7a,b), (3.8a,b) and the method of combining (in series) two piecewise linear force-deflection curves (presented in appendix C, section 1). The input of the program consists of:

(i) masses m_1 and m_2

(ii) load deflection relationships $F_1(\delta_1)$, $F_2(\delta_2)$, $F_R(x)$

(iii) initial conditions x_o, $\dot{x}_o$, $\ddot{x}_o$ and X_o, $\dot{X}_o$, $\ddot{X}_o$

Before proceeding with the description of the program and the results the physical meaning of the above quantities should be given:

- The mass m_1 is the mass of the impacting ship plus the added mass which can be taken as 10% of the ship's mass for bow and stern collision and 40% for side collision (Ref. [22]).
- The mass m_2 for a floating structure is the total mass of the structure plus the hydrodynamic added mass. In the case of a bottom-supported structure, m_2 is the equivalent lumped mass plus added mass of the structure taken as a candilever (see appendix C, section 3).
- The load-deformation relationship $F_1(\delta_1)$ can be taken from (2.8 a,b), (2.9), and (B4) for minor collisions. In the case of a major collision, where the deformation of the platform will not be limited at the impacted member, a global analysis of the platform using finite element methods should be performed to complement the above given relationship for large δ_2.
- The load-deformation relationship $F_2(\delta_2)$ can be taken from the literature. Some experimental data and analytical results are given in Ref. [23], [24], and [25].
- The foundation reaction vs. deflection relationship can be calculated for a given platform design.
- Initial conditions will be dictated by the case we want to analyze. For fixed structures, $\dot{x}_0$, $\ddot{x}_0$, and $\ddot{X}_0$ are zero.

3.3.3 Description of the Computer Program used for the Solution of the Differential Equations

The program, which uses double precision variables, was constructed to be interactive so that the user can vary the input masses and initial conditions to examine various cases. In addition, he can vary the time step, Δt, until the results converge within an acceptable margin. The program goes through the following steps during execution:

(i) Reads the stiffness characteristics of the ship, the platform and the platform's foundation.

(ii) Calculates the combined spring characteristics of the ship and platform spring in series.

(iii) Prompts for input of the ship's and platform's masses.

(iv) Calculates and displays the natural periods for the linearized system at time $t = \pm 0$.

(v) Prompts for input of the ship's velocity and acceleration at the moment right before impact.

(vi) Prompts for input of the time step to be used for the calculations, and the time interval at which to print the results*.

(vii) Calculates, displays, and stores in an output file the results consisting of: the time, t, the displacement of the center of gravity of the ship, x_1, the displacement of the center of gravity of the paltform, x, the contact force developed between the ship and the platform, and the platform's foundation reaction.

(viii) Since both the ship's and the platform's deformations are plastic when $(x_1 - x)$ becomes negative the program stops and

---

* For example, if 50 is input as print interval, the results will be printed at every 50 time steps, i.e. at $t = 50\Delta t$, $100\Delta t$, $150\Delta t$, etc.

asks if the user wants to continue with a new time step, new initial conditions, or new masses and goes back to steps (vi), (v), or (iii) accordingly. Otherwise it stops.

A complete listing of the program is given in Appendix C, section 4.

3.4 Numerical Examples

3.4.1 Cases Examined

There were eighteen example cases examined. These consisted of six different collision scenarios for each of the following three types of platforms: an anchored semisubmersible, a jacket, and a tension leg platform. The various collision scenarios are given below:

(i) "Stiff" bow collision on a brace

(ii) "Stiff" bow collision on a leg

(iii) "Soft" bow collision on a leg

(iv) "Soft" bow collision on a brace

(v) Side collision on a leg

(vi) Stern collision on a leg

In the above, "stiff" bow refers to a typical-strength bow of a supply vessel while "soft" bow refers to a specially designed bow that requires a lower crushing load for the same deformation. Typical load deformation curves for the ship are obtained from Ref. [26], while the equivalent curves for a typical installation's brace and leg were calculated from equations (2.8a,b), (2.9), and (B4). They are presented in Fig. 3.2 to 3.7.

3.4.2 Results

The results for the various cases examined are given in Appendix C, section 5. The calculated ship and platform displacements for scenarios (i) to (vi) are plotted in Figures 3.8a through 3.13a. Similarly, the calculated contact forces and the platform's foundation reactions for the

above six scenarios are plotted in Figures 3.8b through 3.13b. Each of the above graphs contains the obtained curves for the three different platform types: the semisubmersible, the fixed jacket, and the tension leg platform. The contact force level is very important in assessing the damages to both the platform and the ship during a collision. Therefore, in Fig. 3.14 the contact forces developed during a collision according to the above six scenarios are compared for each of the examined platforms.

3.5 Discussion

It appears from Figures 3.8a through 3.13a that the displacement of the center of gravity of the impacting ship is independent of the mass or the foundation stiffness of the impacted structure and that it varies with the platform's and ship's structural stiffness. On the other hand, the deflection of the center of gravity of the platform seems to be more dependent on the foundation stiffness and the platform's mass. Thus, we see that the deflection of the semisubmersible, with a relatively small mass and foundation stiffness, is consistently higher than the ones of the fixed jacket, which has a comparable mass but much higher foundation stiffness, and the tension leg platform, which has a comparable foundation stiffness but much higher mass (and consequently inertia).

Examining the forces developed during the various collision set-ups which were studied we note from figures 3.8b through 3.13b that the contact force between the impacting ship and the impacted structures shows trends inverse of the platform's deflection. Hence, the contact force for the case of the semisubmersible is consistently slightly lower than the ones of the jacket and the tension leg platform. Also, we can see that the jacket's deflection is kept small by its large foundation

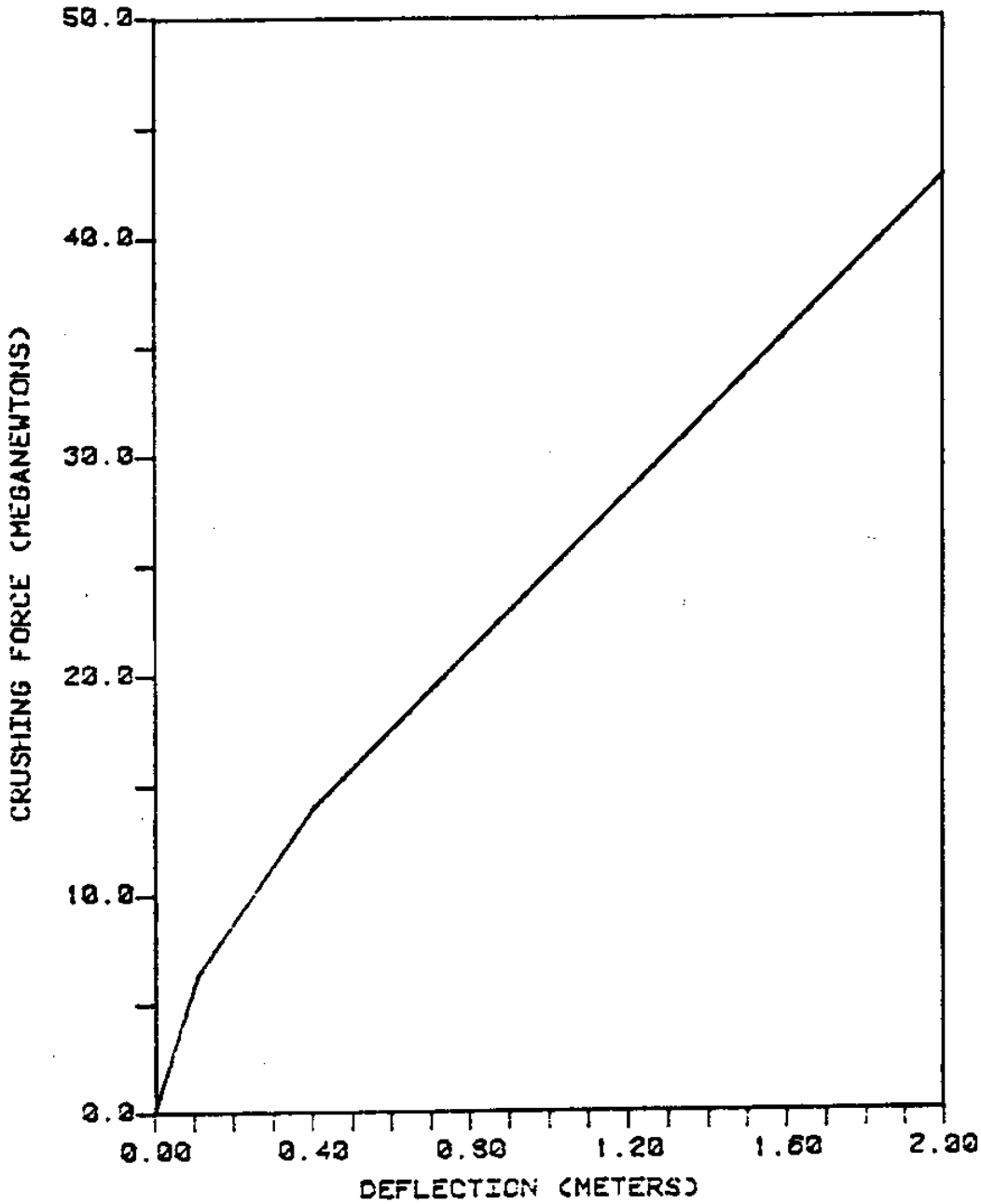

TYPICAL LOAD-DEFORMATION CURVE
FOR JACKET'S CYLINDRICAL LEG

FIGURE 3.2

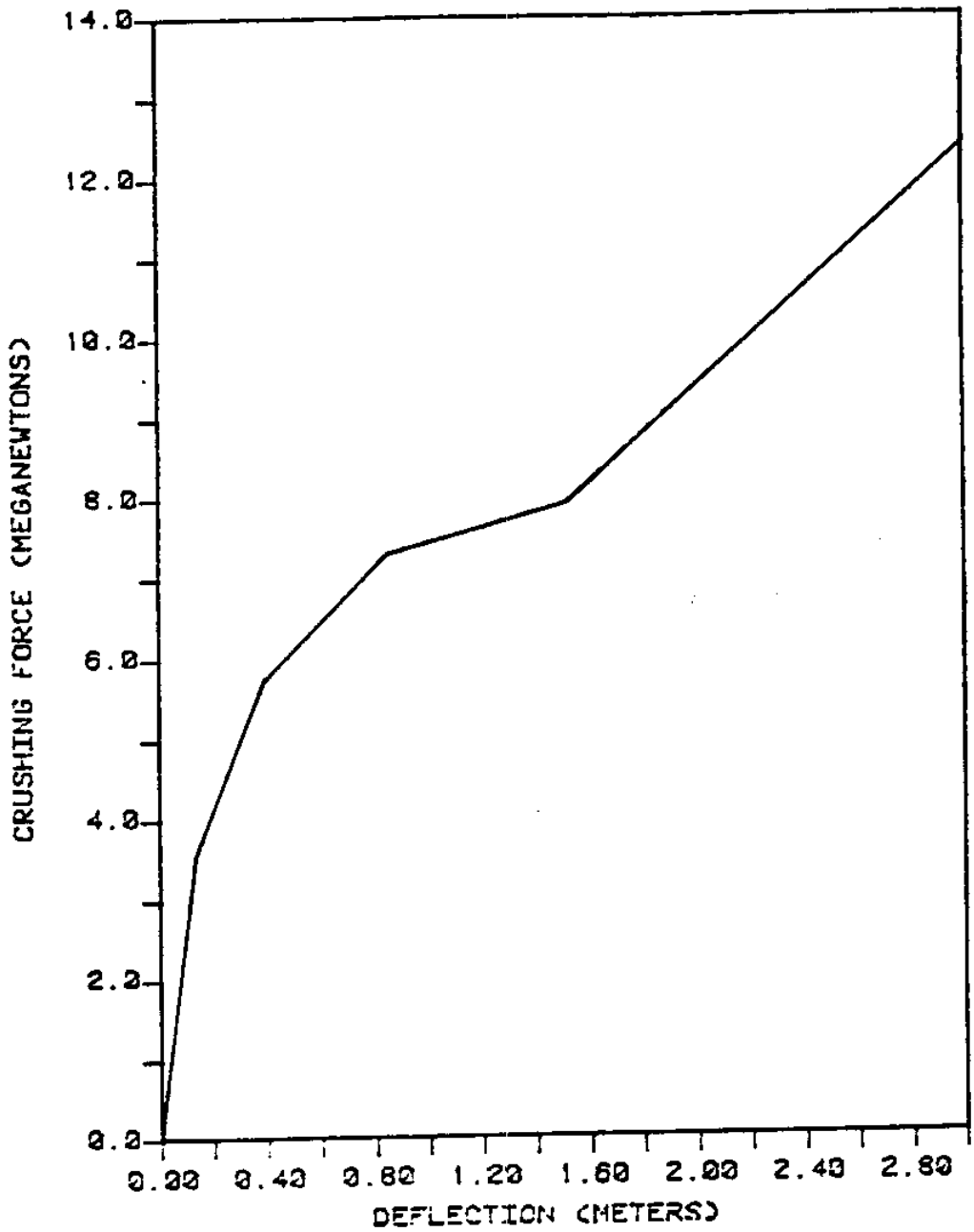

TYPICAL LOAD-DEFORMATION CURVE
FOR JACKET'S BRACE

FIGURE 3.3

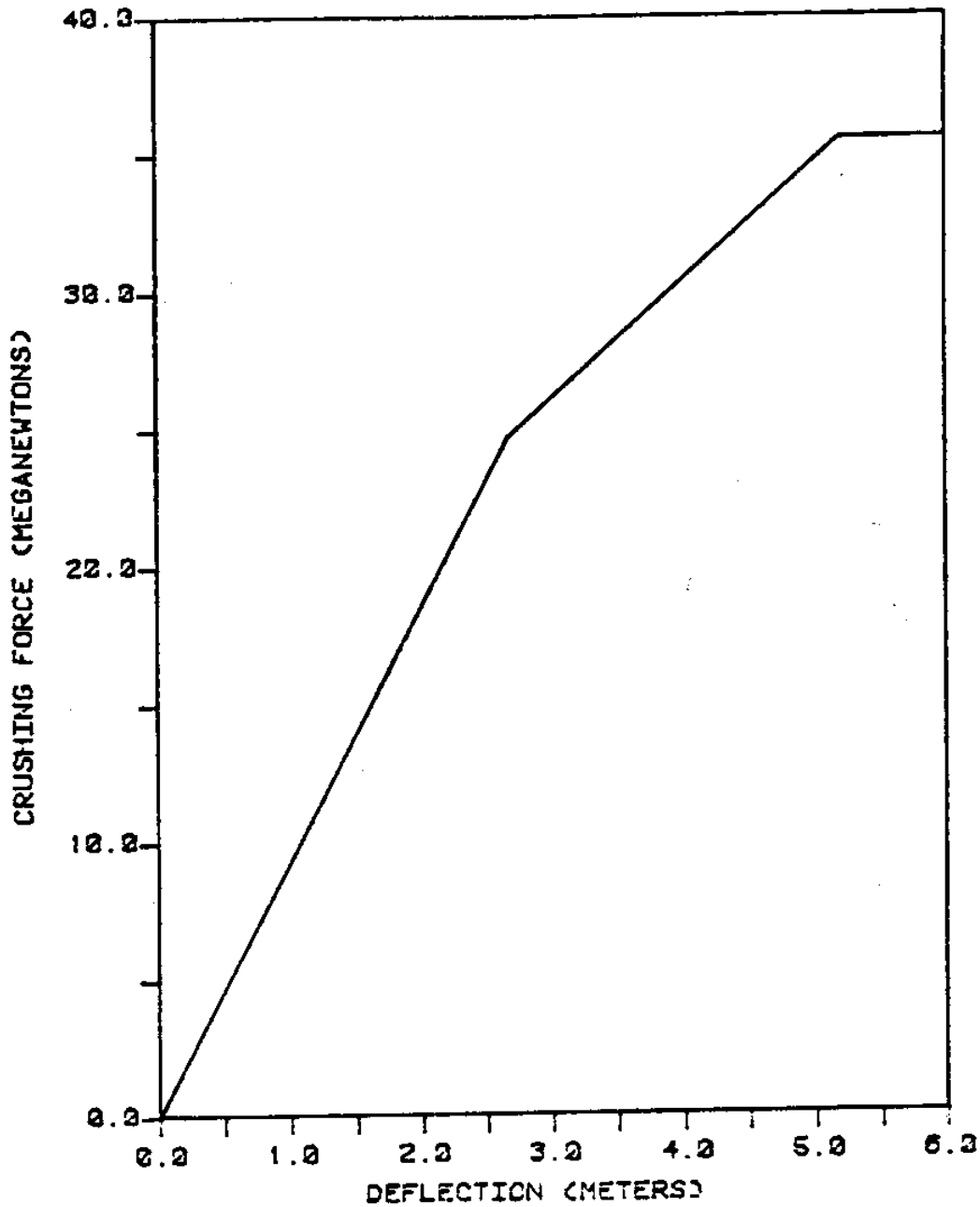

TYPICAL LOAD-DEFORMATION CURVE
FOR A "STIFF" BOW

FIGURE 3.4

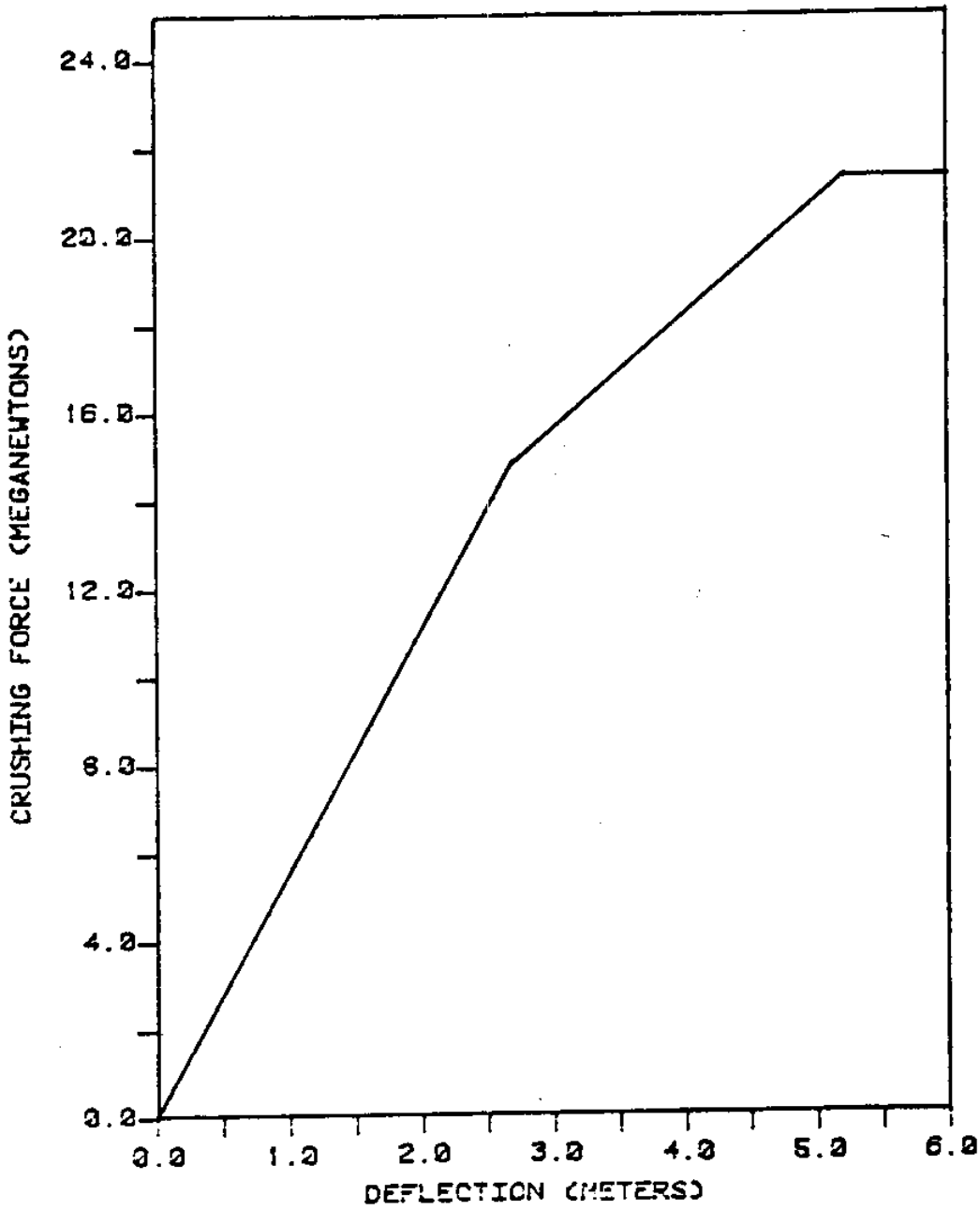

TYPICAL LOAD-DEFORMATION CURVE
FOR A "SOFT" BOW

FIGURE 3.5

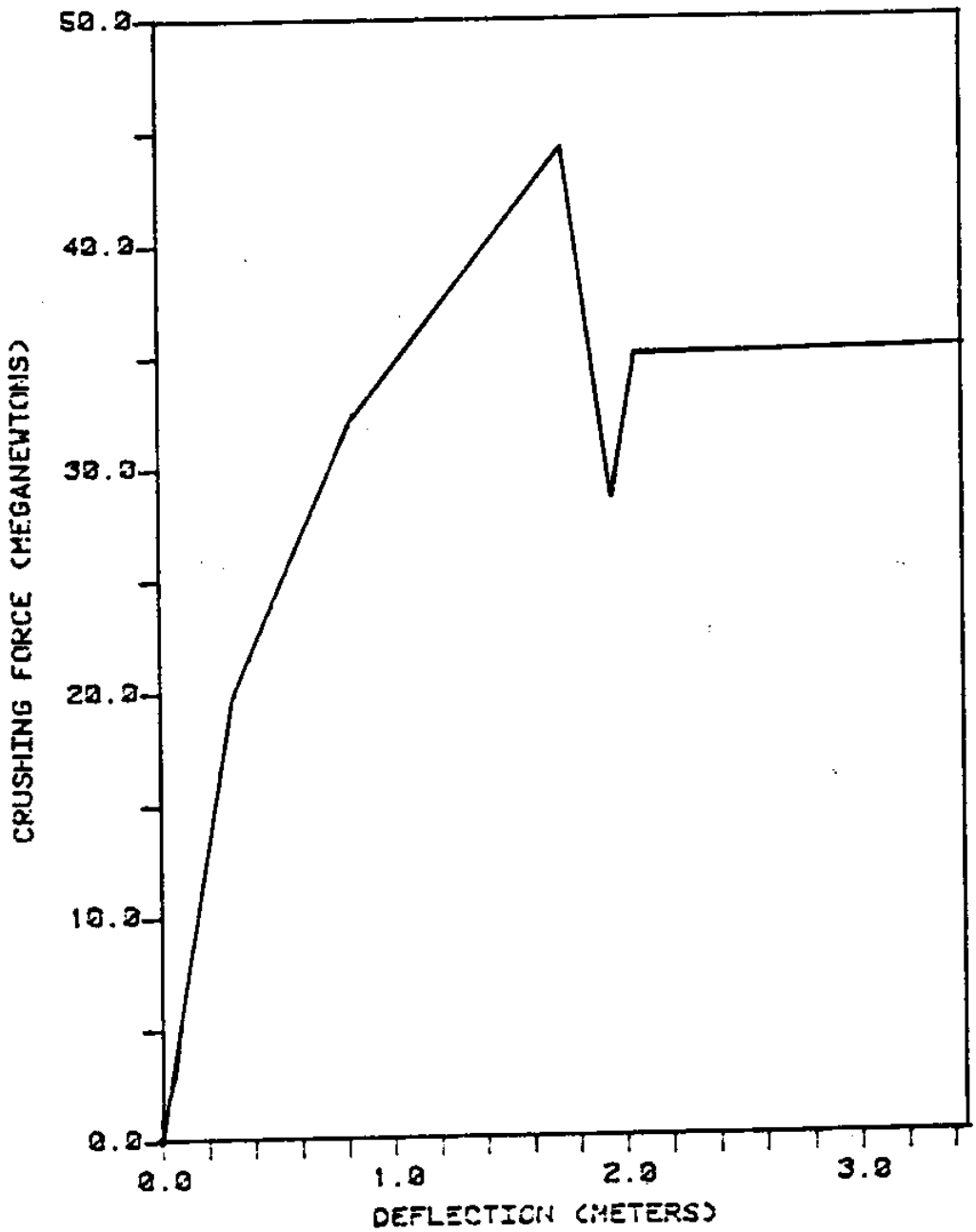

TYPICAL LOAD-DEFORMATION CURVE
FOR A SUPPLY VESSEL'S SIDE

FIGURE 3.6

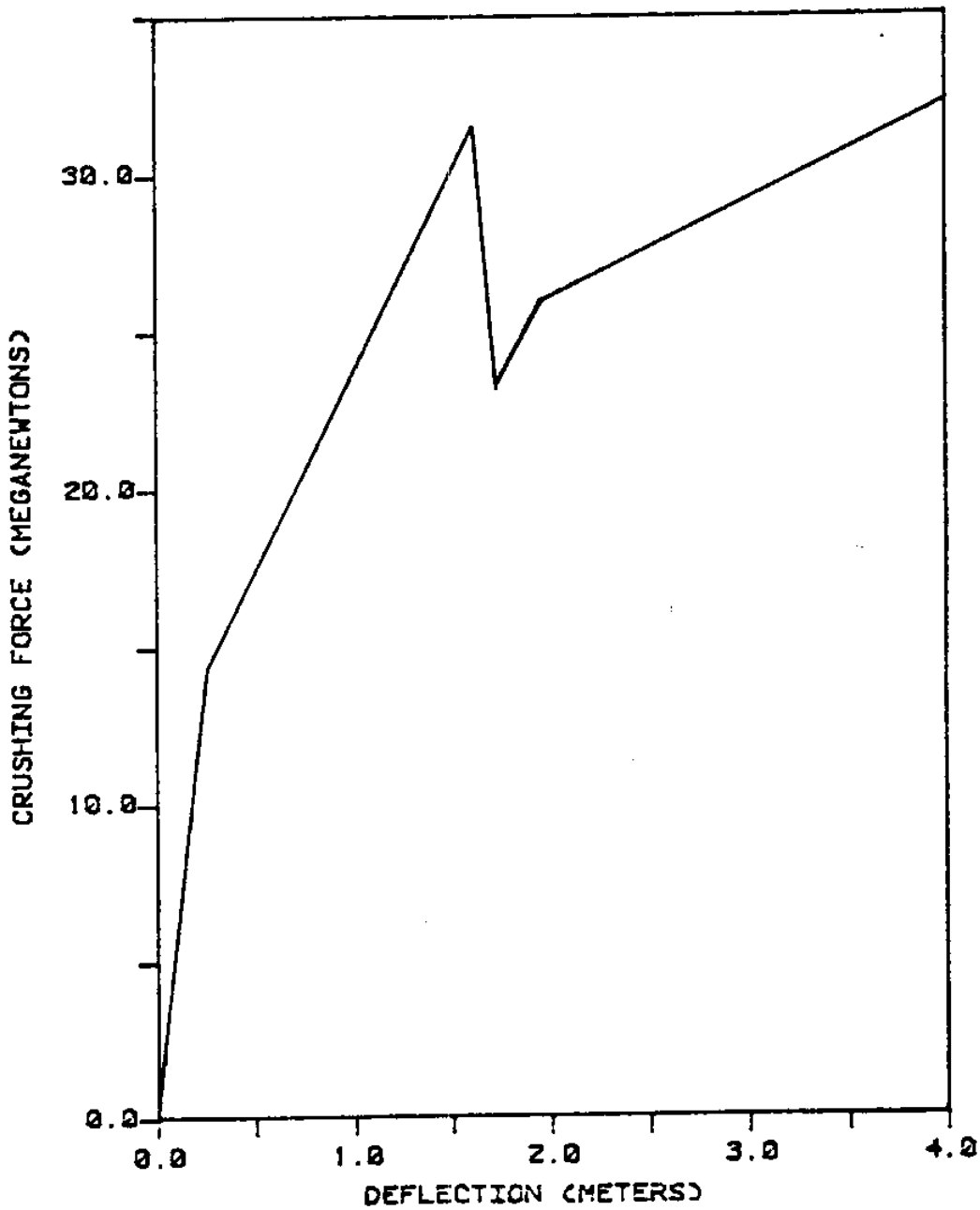

TYPICAL LOAD-DEFORMATION CURVE
FOR A SUPPLY VESSEL'S STERN

FIGURE 3.7

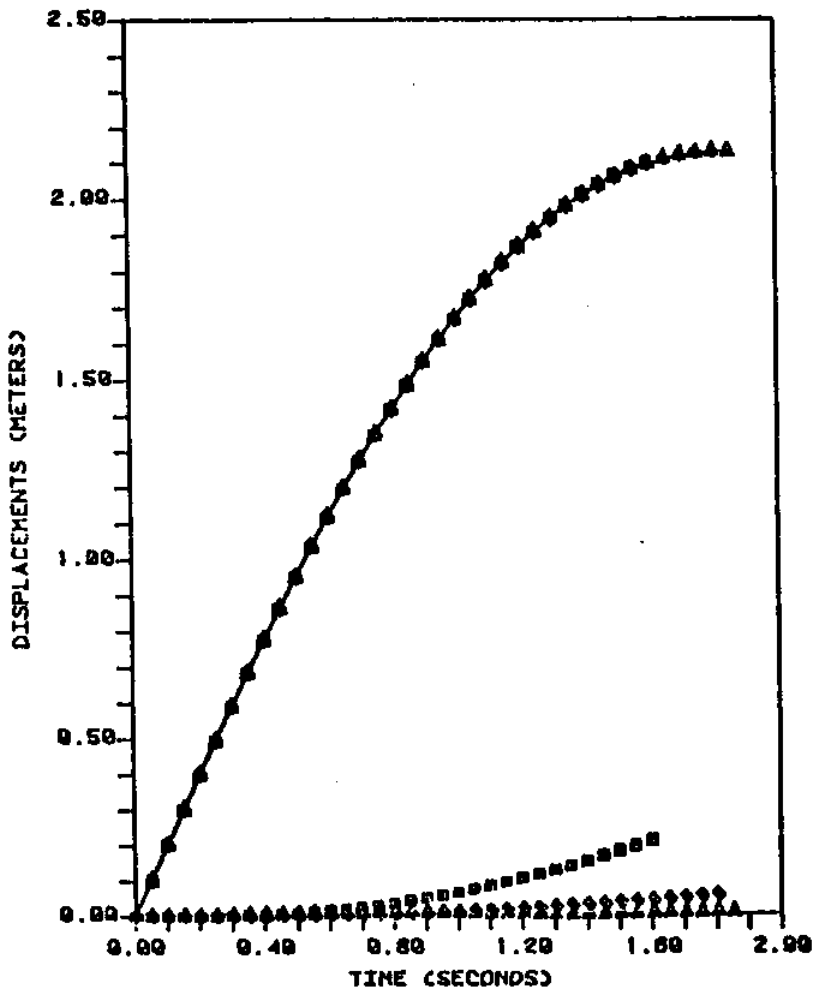

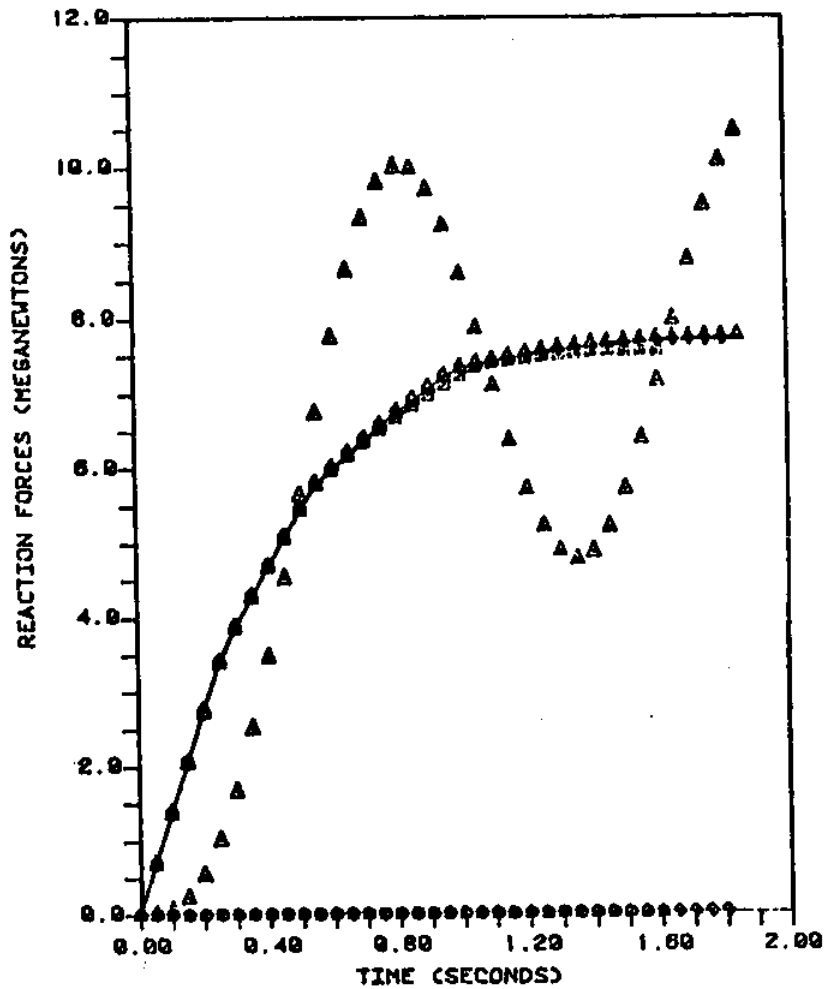

COLLISION SCENARIO (I)

LEGENT	Force: / Displ:	Contact Ship	Foundat. Platf.
Semisubmersible			
Fixed Jacket			
Tension Leg Pltf.			

FIGURE 3.8

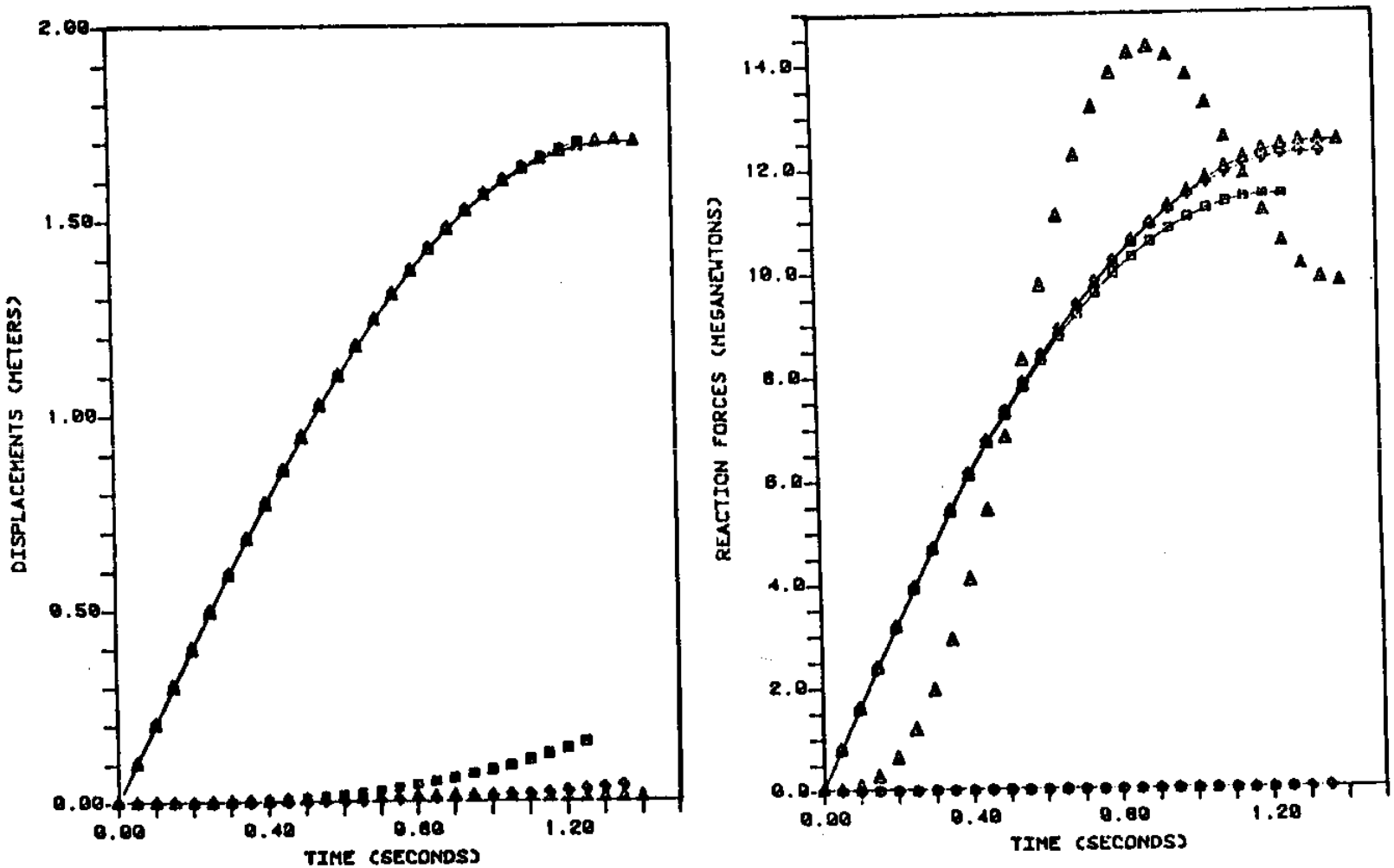

COLLISION SCENARIO (II)

FIGURE 3.9

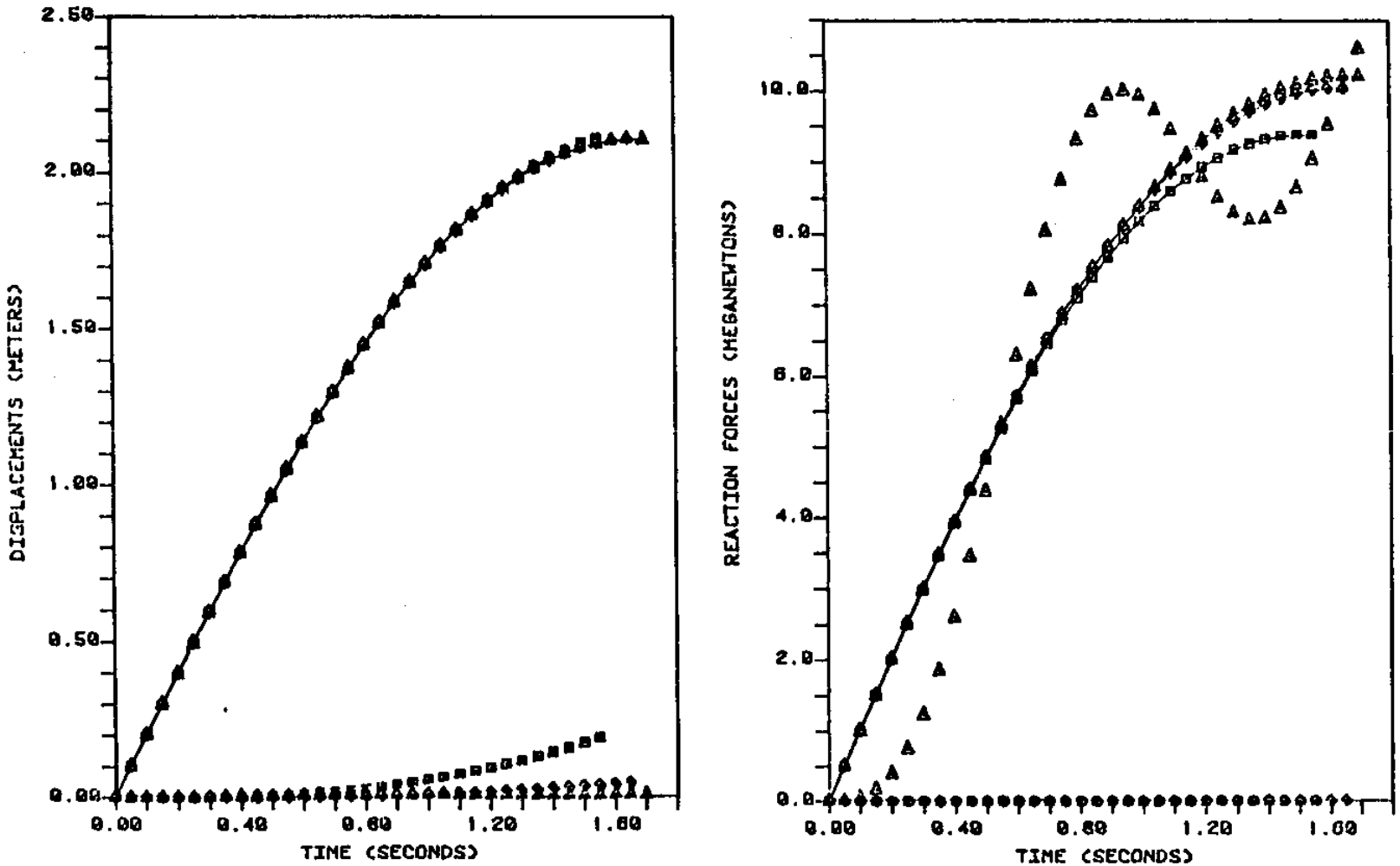

COLLISION SCENARIO (III)

FIGURE 3.10

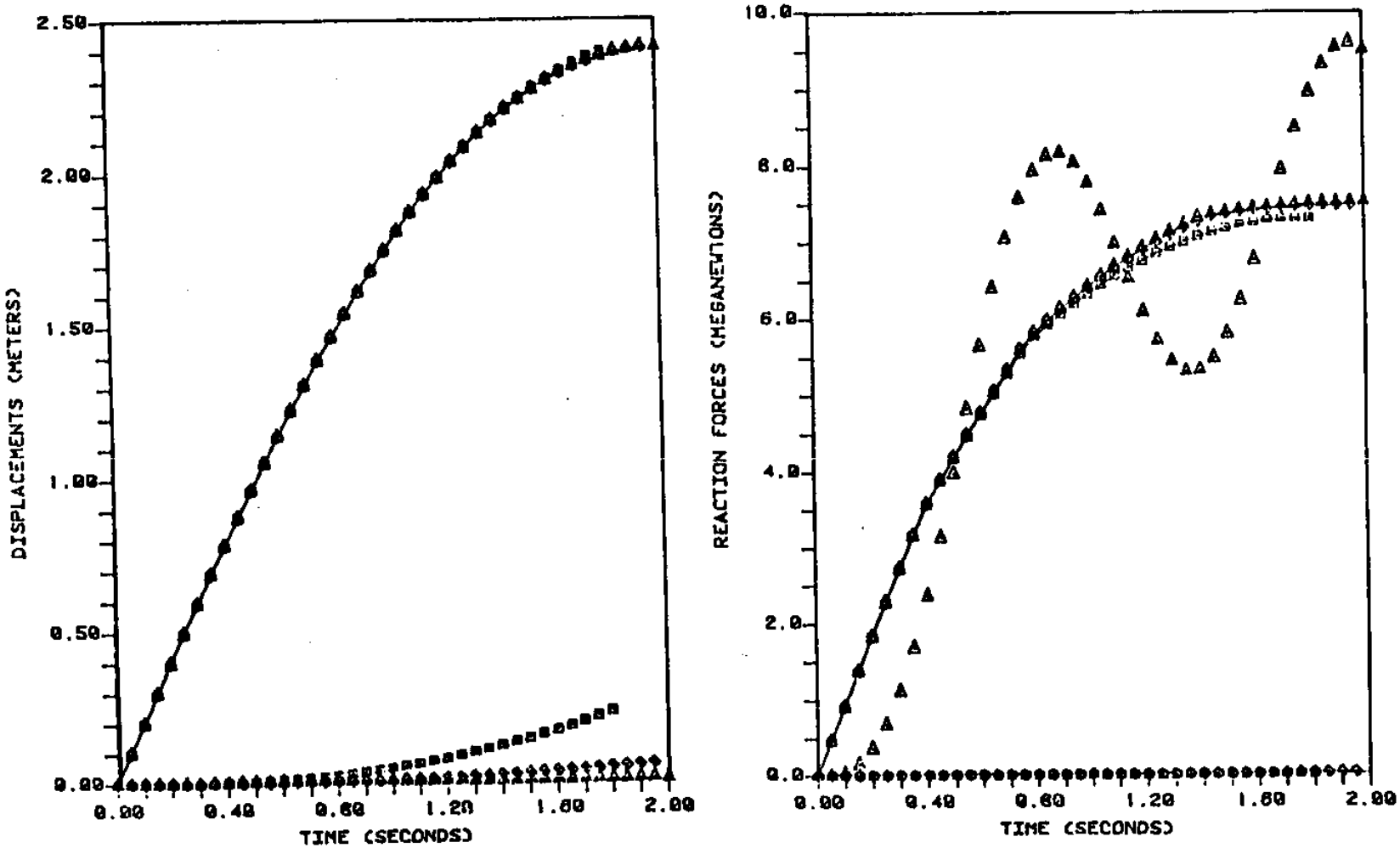

COLLISION SCENARIO (IV)

FIGURE 3.11

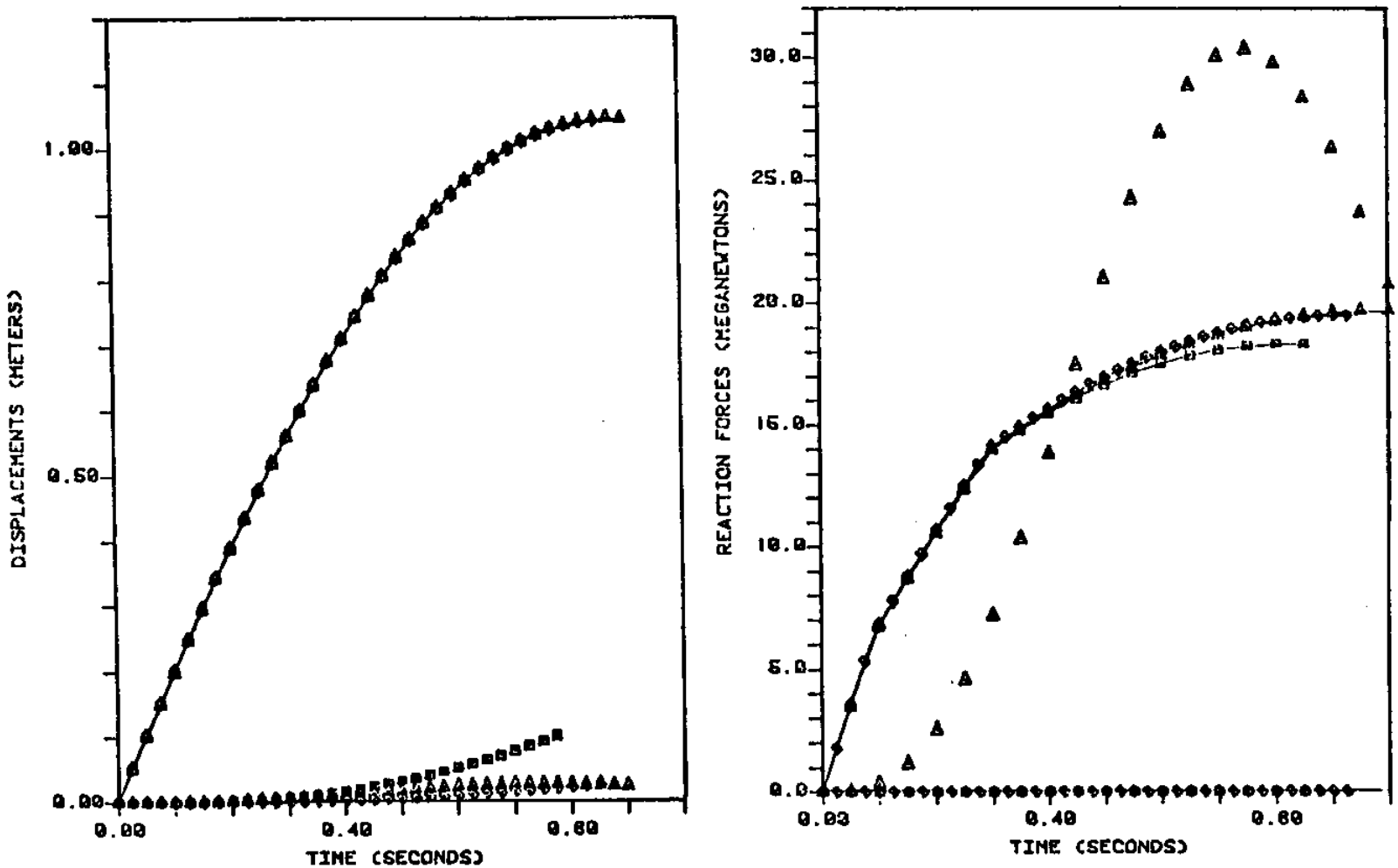

COLLISION SCENARIO (V)

FIGURE 3.12

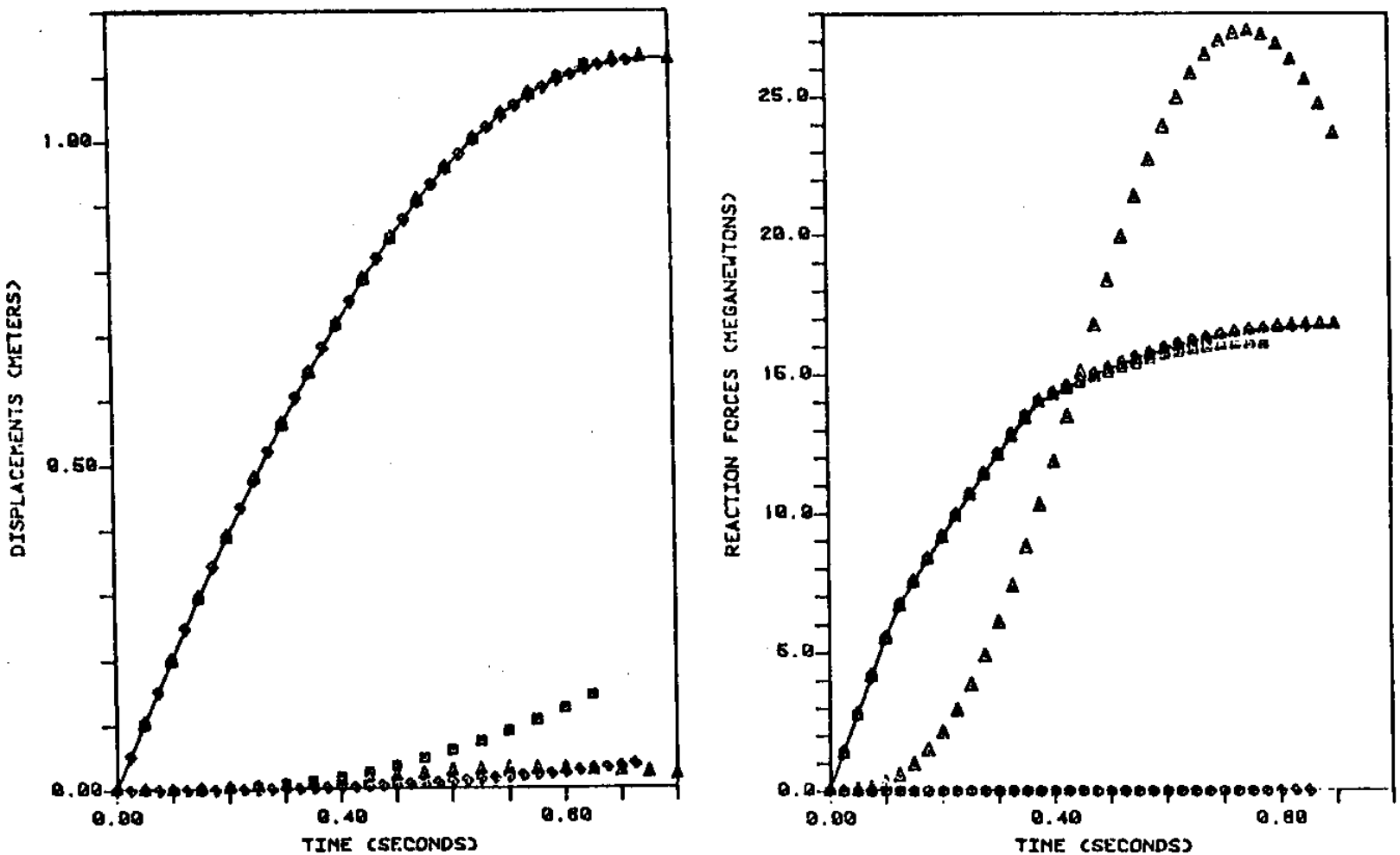

COLLISION SCENARIO (VI)

FIGURE 3.13

reaction while the deflection of the tension leg platform is kept small by means of its inertia only (due to its large mass) since its foundation reaction is virtually zero.

Fig. 3.14 shows the variation of the contact force level for the various collision scenarios studied and as an extension with the structural stiffness of the ship and the platform. We note that the effect of the "soft" bow (vs. the "stiff" bow) in reducing the maximum contact force is non-existent when the stiffness of the platform (its brace in this case) is lower than the stiffness of the bow itself. On the contrary, when the stiffness of the platform is higher than the stiffness of the bow, the effect of a "soft" bow can be very significant. Noting that the contact force for a stern collision with a leg is relatively high and recalling that, due to operational procedures, a supply vessel is more likely to impact on a platform by the stern*, we conclude that a specially designed "soft" stern can be very helpful in reducing the maximum contact force. In that way the damage to the paltform due to a collision can be reduced together with the risk of further structural failures and consequent total loss. Of course, a low-reaction force, high energy capacity fender placed at the stern of the ship or on the leg of the platform would give the same result as a "soft" stern. The problem with such a fender is that it would be bulky and most probably impractical to use but then, it may be much more economically attractive.

* In most installations the supply vessel anchors or is moored at a buoy by the bow and backs-up towards the platform with the stern. A line that gives-in at that point or a miscalculation will result in a collision by the stern.

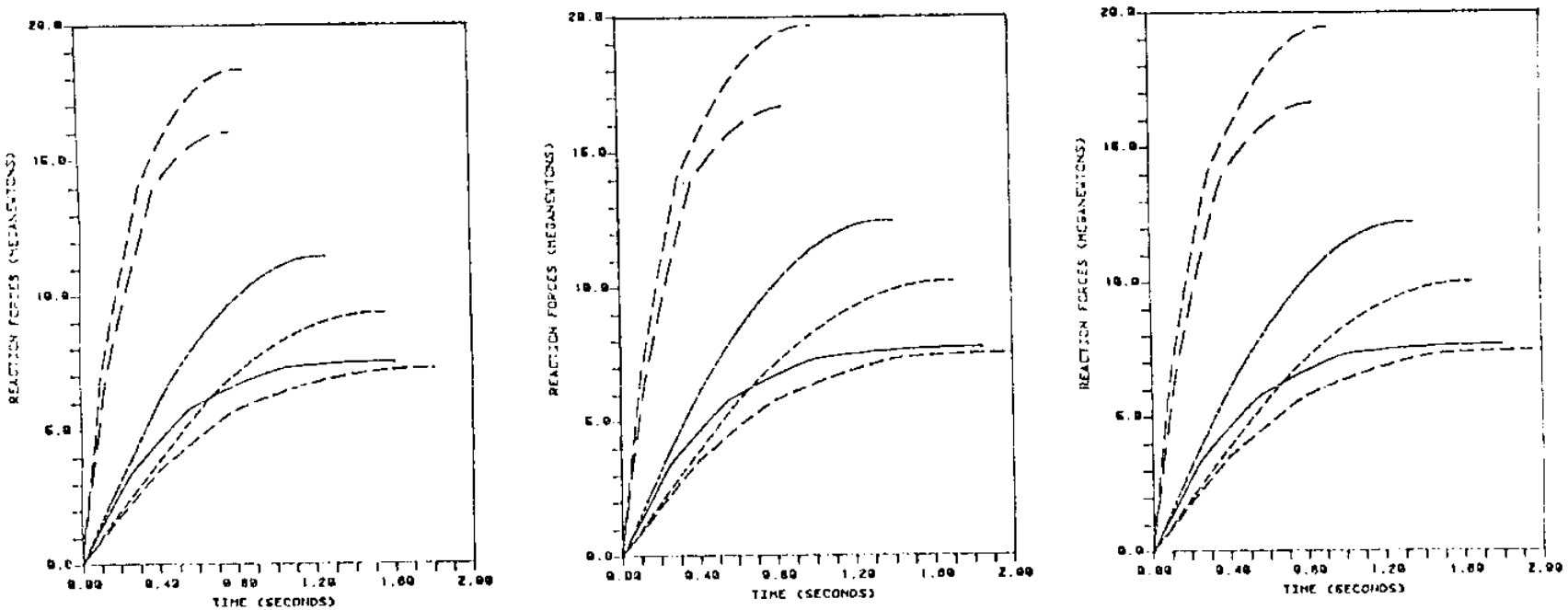

Collision with a Semisubmersible

Collision with a Fixed Jacket

Collision with a Tension Leg Platf.

VARIATION OF CONTACT FORCE FOR SEVERAL COLLISION SCENARIOS

FIGURE 3.14

Scenario (i) ———
(ii) - - - - - -
(iii) — - — - —
(iv) — - - - - -
(v) - - - - - -
(vi) — - - — - —

CHAPTER 4
COST BENEFIT ANALYSIS FOR MINOR COLLISIONS

4.1 Introduction

A collision with an offshore platform can be characterized, based on the extent of the damages to the structure, as major or minor. A minor collision will result in only repairable local damage of the structure and most probably will not call for cease of operations. A major collision on the other hand will, in addition, damage the platform globally and will certainly force an indefinite cease of operations at least from the damaged platform. Table IV.1 summarizes the risk of collision of several types of vessels with a platform together with the consequences of such a collision.

Designing a platform to withstand a major collision and remain operational can, even if it is proved to be technically feasible, be extremely uneconomical. Instead, several precautionary measures are taken so that the risk of such a major collision can be decreased. According to the 1964 Continental Shelf Convention, offshore installations must be sited off recognized shipping lanes. Further, the Convention established the right of the costal states to declare safety zones, of 500 meters radius, around each of the installations. These zones, which for permanent platforms are marked on navigational charts are prohibited to all marine traffic not requiring access to the installation for approved operational purposes. The installations themselves are required to have lights flashing the Morse letter "U" during the night and other means of identification during the day. Since all these platforms are large structures they tend to give good radar return to vessels using such equipment (hopefully all large ships under conditions of poor visibility).

Table IV.1

Type of Ship	Probability of Collision	Damage Extent
Supply vessel	$P > 10^{-2}$	local
Crane Vessel		local or global
Rigs and Buoy Fenders		local
Tanker for Loading	$P > 10^{-3}$	global
Stand-by Vessel		local
Fishing Vessel		local
Pleasure Craft		local
Commercial Traffic	$P > 10^{-6}$	global
Supply Vessels servicing another installation		local or global
Fishing Vessel		local

Adopted from Ref. [32]

In addition to the above safety measures, in the North Sea (where there is relatively high concentration of platforms), each group of installations in a certain vicinity is required to have a stand-by safety boat in permanent attendance.

As it turns out, the above safety measures and specifically the 500 meters safety zone have very positive results in limiting the collisions to mostly the ones with the servicing vessels which have to berth alongside the platform. From Table IV.2 we can see that 37 out of 43 collisions involving offshore installations in the North Sea in the 1974-1976 period are collisions with supply vessels. Still, although most of these collisions are minor ones, it can be seen from Table I.3 that they occupy the third place in platform accident frequency and so they are responsible as a total for considerable capital losses. Thus, designing the structure in a way that it can withstand a minor collision with very little damage could be very attractive economically.

In this chapter, ways of estimating the risk of a minor collision are discussed (with particular emphasis to supply boats) and a method is outlined for a cost benefit analysis of a collision damage vs strengthening of the platform. Ref [27] presents a similar. very brief, simplified cost-benefit method which though is restricted by the fact that it investigates only various fender investment alternatives, so it examines the problem from the point of view of an already constructed structure rather than from the initial design stage. In the following formulation, the total cost of the structure (including both the initial fabrication cost and the expected damage losses due to collision) is minimized and the optimum local strength characteristics (around the waterline) of the platform are defined. The cost of repairing the damage

TABLE IV.4

INCIDENTS INVOLVING UK OFFSHORE INSTALLATIONS IN THE NORTH SEA IN 1974/6

	Safety zone infringements		Collisions	
Southern Basin				
Service craft	6		2	
Fishing Vessels	69		1	
Unknown & others	35		1	
Total		110		4
Northern Basin				
Service craft	0		17	
Fishing vessels	6		0	
Unknown & others	3		0	
Total		9		17
East Shetland Basin				
Service Craft	0		18	
Fishing vessles	0		2	
Unknown & others	0		2	
Total		0		22
		---		--
Total, all areas		119		43

From Ref. [28]

due to a minor collision together with the initial construction cost vs. strength are considered. In addition, the platform's damage calculation method, presented in the first three chapters, combined with probabilistic data on the risk of such a collision as well as the impacting ship's displacement and impact velocity are used. In the next section methods of estimating these probabilistic data are presented.

4.2 Risk Analysis of Offshore Collisions

In broad terms, risk is defined as the product of the probability of occurrence and the expected consequences. As far as the risk of collision is concerned the marine traffic around a platform may be divided in three general groups:

1) Vessels having business with the platform and which will approach very close to or even berth alongside it:
   - (i) Supply Vessels
   - (ii) Crane Vessels
   - (iii) Tugs and Buoy Tenders
2) Vessels wishing to go close to the installation but not normally expected to enter the 500 meter safety zone:
   - (i) Tankers for loading at a nearby SPM
   - (ii) Stand-by boat
   - (iii) Fishing vessels
   - (iv) Pleasure crafts
3) Vessels on passage through the area:
   - (i) Ordinary commercial traffic
   - (ii) Fishing Vessels
   - (iii) Supply vessels visiting another installation.

As it can be seen from Table 4.1 collision of one of the vessels of the first group with a platform has the highest probability of occurence while collision of one of the vessels of the third group is the least probable. Besides the probability of occurence there are two more major parameters that influence the extent of collision damages and consequently risk. These are the displacement and impact velocity of the colliding ship. Thus, to correctly assess the risk of collision we need three pieces of probabilistic information:

(i) probability of collision, P_n

(ii) probability density function of impact velocity, pdf_{V_c}

(iii) probability density function of impacting vessel's mass, pdf_{M_s}.

All the above functions depend on which group, of the ones described earlier, the impacting vessel belongs to. As it has been shown in the introduction of the chapter, the majority of the collisions are minor ones and with vessels belonging to the first group. Thus, the following analysis will be for simplicity confined to these vessels and more specifically to the supply vessels servicing the platforms*. A risk assessment can be based entirely on past experience or simulation techniques. Both methods have advantages and disadvantages.

4.2.1 Collision Probability Based on Past Experience

If the analysis is based on past collision statistics several limitations arise. Due to the nature of the events, the sample size is very

* As it has already been discussed, it is infeasible or uneconomical to design a platform to withstand a major collision (like one with a passing cargo ship) and so, a case like this is irrelevant to the following cost-benefit analysis.

small, creating considerable uncertainty for the calculated probability. In addition to that, whether the basic assumption of independence of events holds is questionable. That is so, because after one or several accidents have occurred, changes will be introduced to the system (i.e. changes in the codes). Those changes will almost certainly influence the probability of consequent collisions. On the other hand, if the sample size is large enough (as in the case of North Sea) and most occurred collisions are minor ones not involving many fatalities and excessive damage (so that the codes might not be changed), probabilities derived based on past statistics can be very realistic.

Their main advantage is that they incorporate uncertain factors, like the relative movement of a mobile rig due to waves, which the simplified analytical methods have to neglect. Their major disadvantage, however, is that they can been used with confidence only for platforms in the region where the statistics were compiled. This is so, because both the environmental and the operating conditions are locked in the past statistics and there is no way to differentiate for different ones in another region.

4.2.2 Collision Probability Based on Simulation Techniques

In the case that we need to estimate the probability of collision of a vessel with a platform in a region where there are not enough past collision statistics we can create them using a simulation method. The input to the calculations is the probability density functions of the wind, wave, and current intensity and direction. In such a way, this method lends itself handy in almost any region where platforms are or will be located since the above required data are readily available for these sites.

The shortcoming of this method is, of course, that it gives results as good as the analytical model which is used for the simulation. Still, considering that it can be used for every location where weather data are available, and past collision statistics are not, makes it better than nothing. Another limitation of this method is that it calculates a conditional probability given that a certain ith critical failure has occurred on the approaching vessel (loss of power, loss of steering, etc.). Then, this conditional probability is combined with the probability that the ith critical failure will occur to yield the probability of collision due to the ith critical failure:

$$P_i \text{ (collision)} = P(\text{collision/failure } i) \cdot P(\text{failure } i)$$

To obtain the total collision probability, given that the i critical failures are independent of each other, we have to sum all the P_i (collision). So,

$$P_n \text{ (collision)} = \sum_{i}^{m} [P(\text{collision/failure } i) \cdot P_n(\text{failure } i)] \qquad (4.1)$$

where m: number of possible critical failures

n: operating lifetime of the installation (years)

It is easily seen that, if there exist many critical failures with non-negligible probability of occurrence, i.e. P_n(failure i), the above method tends to be costly and time consuming. In our case of the supply boat where the only probable critical failure during the berthing approach are: (i) loss of power, (ii) loss of steering, and (iii) loss of mooring line(s) the above outlined simulation method is relatively easy to employ.

4.3 Cost - Benefit Analysis

Usually, when the structural analysis for a platform has been performed the only objective is to design the most economic (in terms of initial cost and sometimes maintenance) structure that complies with the pertaining codes and that can withstand the extreme environmental loads which might be imposed on it during its operating life. The resulting structure is then checked for several accidental loading conditions, usually specified by the codes. If it is not found adequate, it is strengthened until it is. In that process, no economic considerations are given to the structural-strength vs. accidental-load-damage aspect of the problem even if the accident has a relatively high probability of occurrence. In the case of an offshore collision, the above probabilty has been calculated to be (for a North Sea Installation) about 0.35/yr. for a mobile rig and 0.1/yr. for a fixed platform (Ref. [28]). Although the usual damages resulting for most of the expected collisions are small, it is easy to see that a significant collision damage cost can be accumulated using the 30-year operating life of the installation. The expected economic loss from collisions during the platform's lifetime can be written as:

$$c_c = c_d\,(D_p) \cdot P_n \tag{4.2}$$

where c_c = Expected cost of collisions

c_d = Cost of collision as a function of the collision damage

D_p = Platform's damage due to collision

P_n = Probability of collisions during the n years of the platform's operating lifetime

As discussed in Chapter 3, the platform's damage due to a collision is a function of several variables and can be written as:

$$D_p = D_p\ (V_c,\ M_s,\ M_p,\ S_s,\ S_p) \tag{4.3}$$

where V_c: Ship's impact velocity

M_s: Impacting ship's mass plus hydrodynamic added mass

M_p: Platform's mass plus hydrodynamic added mass

S_s: Ship's loaded vs. plastic deformation characteristics

S_p: Platform's local load vs. plastic deformation characteristics (i.e. of a brace)

In addition, it is logical to assume that S_s is a function of M_s for similar types of vessels (like the supply vessels of our case). V_c is a continuous variable and has a certain probability density function. Although M_s can take several distinct values at each site at a certain time (based on the displacements of the existing supply vessel fleet servicing that site at that time), in the long run it can be thought of as a continuous variable with an associated probability density function (See Fig. 4.1). Then, the total expected economic loss from collision during the platform's lifetime can be written as:

$$C_c = \int_{V_c}\int_{M_s} c_d[D_p(V_c, M_s,\ M_p,\ S_s(M_s), S_p)]\cdot P_n \cdot pdf_{V_c} \cdot pdf_{M_s} \cdot dV_c \cdot dM_s$$

where pdf_{V_c}: probability density function of V_c

pdf_{M_s}: probability density fucntion of M_s

At this point we should note that if we wanted to be vigorous we should write the $(P_n \cdot pdf_{V_c} \cdot pdf_{M_s})$ term as a joint pdf, which would be a function of V_c and M_s. This pdf would be almost impossible to determine and so a simplification was introduced by breaking it into three terms, all relatively easy to obtain. Both P_n and pdf_{V_c} can be obtained either from past collision records or using the simulation method like [28]

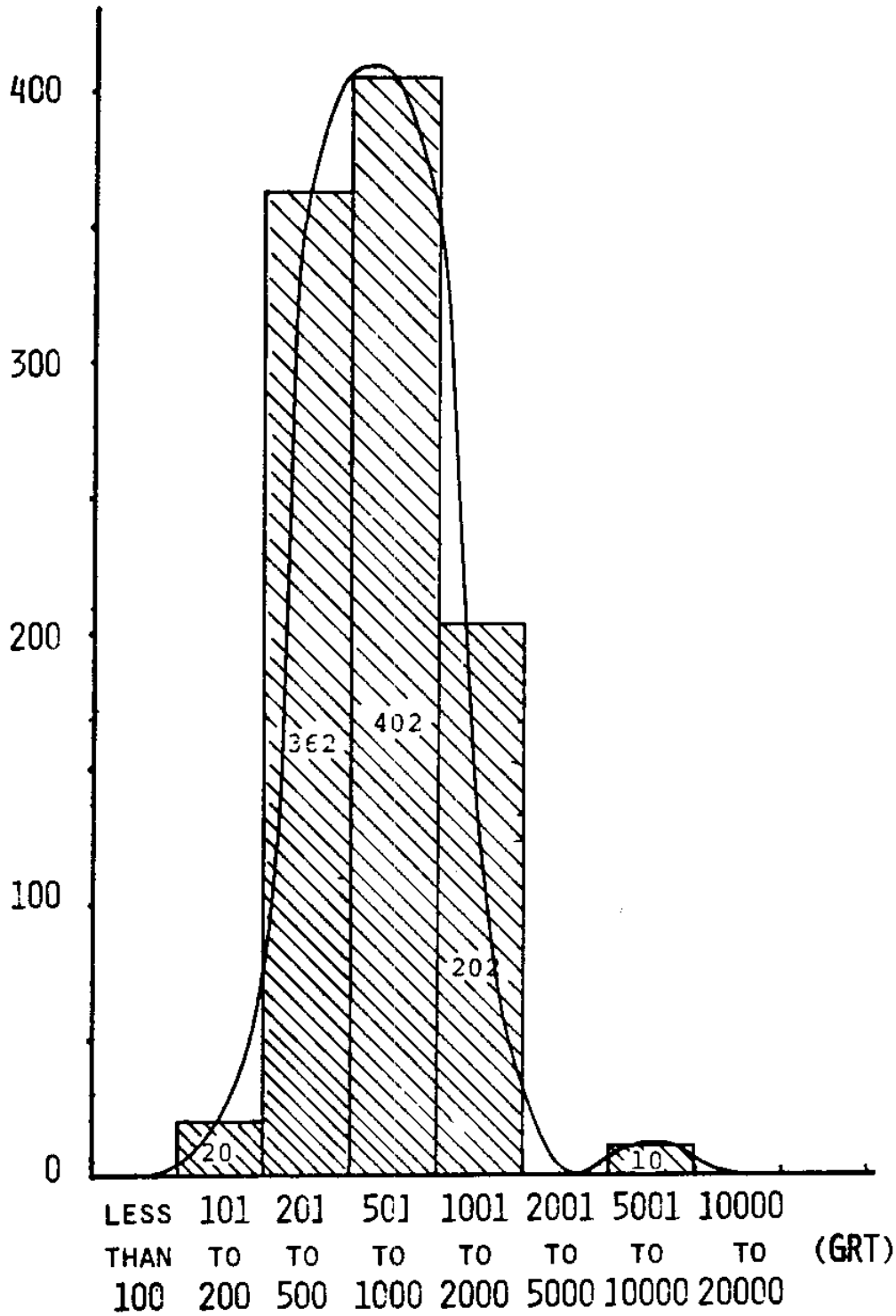

DISTRIBUTION OF MOVEMENTS OF SUPPLY VESSELS TO AND FROM SCOTTISH EAST COAST PORTS IN JULY 1975

FIGURE 4.1

and [29], while M_s can be obtained from histograms of supply vessels involved in offshore collisions, similar to the one of Fig. 4.2. The cost of the structure C_s and cost of damage C_d are related and can be taken from past experience of the yard most likely to handle the job or from compiled statistics like [30] and [31]. Although they both refer to ship construction costs, they are applicable in the offshore contruction also since both the cost of steel and labor and the labor intensity and overheads are the same for the offshore jacket construction as they are for shipbuilding.

Now that the cost of collision is determined we can write the total cost of the structure as:

$$C_t = C_s + C_c \tag{4.5}$$

where C_s is the initial fabrication cost and can be determined from the same sources as C_d

Noting that C_s is a function of the platform's strength characteristics S_p and substituting 4.4 in 4.5 we arrive at the final expression for the total cost of the structure in terms of its strength characteristics S_p

$$C_t = C_s(S_p) + \int_{V_c}\int_{M_s} C_d\,[D_p(V_c, M_s, M_p, S_s(M_s), S_p)]\; P_n \cdot pdf_{V_c} \cdot pdf_{M_s} \cdot dV_c \cdot dM_s \tag{4.6}$$

To obtain the economically optimum platform's strength, S_p, the above expression can be minimized with S_p taken as the minimization variable. S_p is subject to the constraint:

$$S_p \geq S_d$$

where S_d is the design strength for analysis based only on environmental loads.

DISTRIBUTION OF THE TONNAGE OF SUPPLY VESSELS INVOLVED IN COLLISIONS IN 1974-76 IN THE NORTHERN NORTH SEA (Ref[28])

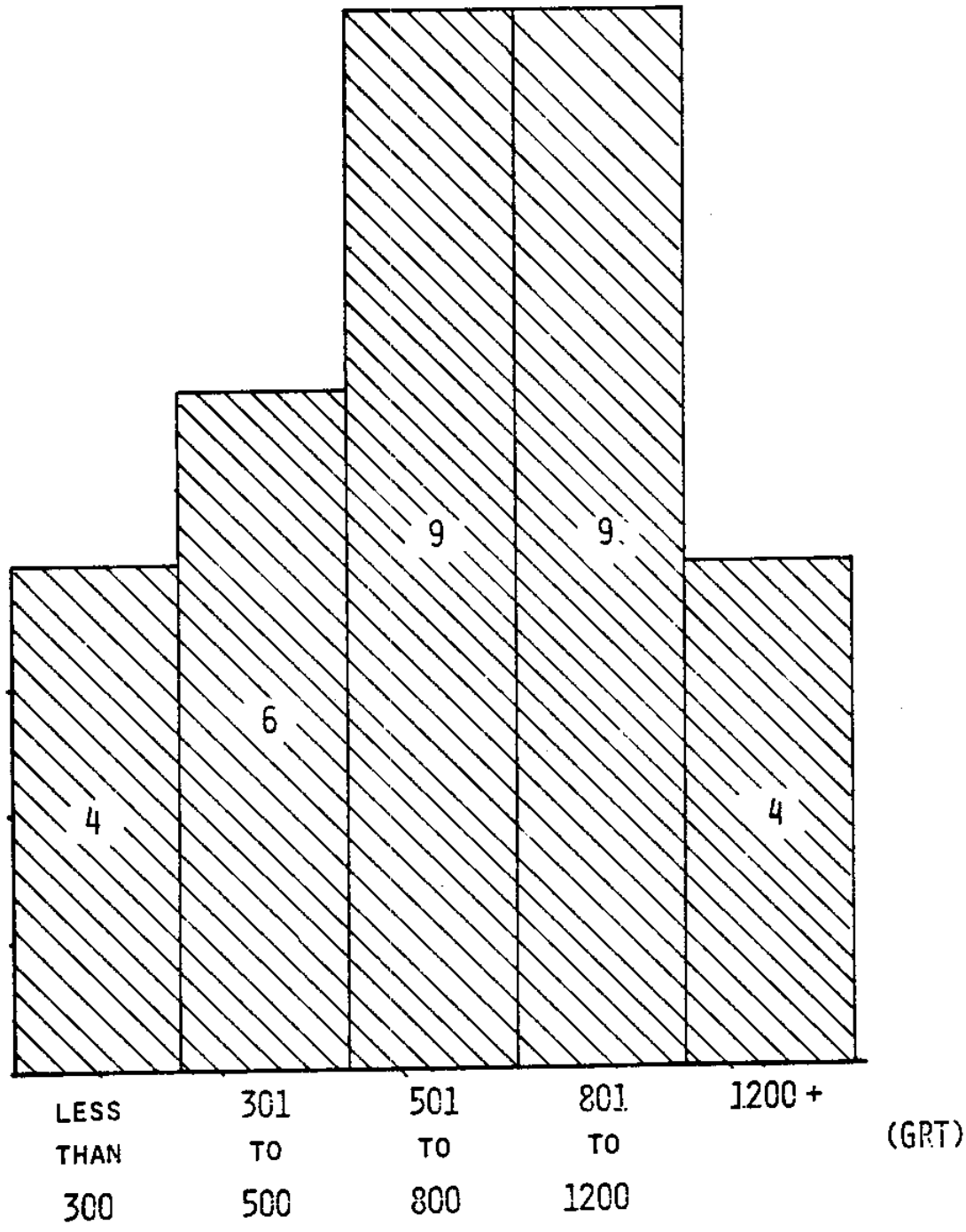

FIGURE 4.2

During the minimization process, the effective mass of the platform, M_p, is treated as an input variable and can be assumed constant for small changes in the local strength of the structure, S_p, around the waterline. Also, the strength of the impacting ship, S_s, is considered as input variable function and the strength characteristics of a typical supply vessel can be used.

4.4 Conclusions

As discussed earlier, this is just an outline of a method rather than a detailed analysis.Much of the required input is described in very general terms and some more refinements will be required to define the exact set of data required before applying it. However, these details were not included because they depend on the particular characteristics of a location and installation and they should be adjusted accordingly every time. Thus, although the formulation was presented in a rather general way, care was taken to link each set of required data to realistic and existing sources or to feasible and practical methods of gathering them. When the presented method is used with the help of a computer, the extent of damages can be calculated easily and repeatedly (as demonstrated in Chapter 3). It can thus be proved to be of very good help in economically optimizing structures such as mobile rigs which have (in the North Sea) a probability of minor collisions of 0.35, i.e. more than one every three years in their 15 year life.

In concluding, we should add that the above formulation is general enough so that it can also be used to analyze the economic feasibility of any fender system, either energy dissipating (one use only) or not. To

perform such an analysis, the fender's load vs. deformation characteristics have to be combined with the platforms's local strength characteristics to obtain S_p, and the fender's cost has to be included in the structure's cost, C_s.

REFERENCES

1. Johnson, W., Soden, P.D. and Al-Hassani, S.T.S., Inextensional Collapse of Thin-Walled Tubes under Axial Compression, J. Strain Analysis, 12, 1977, pp. 317-330.

2. Al-Hassani, S.T.S., Johnson, W. and Lowe, W.T., Characteristics of Inverting Tubes Under Axial Loading, J. Mechanical Engineering Sciences, 14, 1972, pp. 370-381.

3. Updike, D.P., On the Large Deformation of a Rigid Plastic Spherical Shell Compressed by a Rigid Plate, J. Engineering for Industry, 1972, pp. 949-955.

4. Kitching, R., Houlston, R. and Johnson, W., A Theoretical and Experimental Study of Hemispherical Shells Subject to Axial Loads Between Flat Plates, Int. J. Mechanical Sciences, 17, 1975, pp. 693-703.

5. Morris, A.J. and Calladine, C.R., The Local Strength of a Thin Spherical Shell Loaded Radially Through a Rigid Boss, Proc. 1st Int. Conf. on Pressure Vessel Technology, ASEM, 1969.

6. Duszek, M., Plastic Analysis of Shallow Spherical Shells at Moderately Large Deflection, Theory of Thin Shells, IUTAM Symposium, Copenhagen, 1967, pp. 374-388.

7. Oliveira, J.G. de, Wierzbicki, T., Crushing Analysis of Rotationally Symmetric Plastic Shells, Report 81-8, Dept. of Ocean Engineering, M.I.T. June 1981.

8. Thomas, S.G., Reid, S.R., Johnson, W., Large Deformation of Thin-Walled Circular Tubes Under Transverse Loading - I, Int. J. Mechanical Sciences, Vol. 18, 1976, pp. 325-333.

9. Watson, A.R., Reid, S.R., Johnson, W. and Thomas S.G., Large Deformation of Thin-Walled Circular Tubes Under Transverse Load - II, Int. J. Mechanical Sciences, Vol. 18, 1976, pp. 387-397.

10. Watson, A.R., Reid, S.R. and Johnson, W., Large Deformation of Thin-Walled Circular Tubes Under Transverse Loading - III, Int. J. Mechanical Sciences, Vol. 18, 1976, pp. 501-509.

11. Morris, A.J., Experimental Investigation into the Effects of Indenting a Cylindrical Shell by a Load Applied Through a Rigid Boss, J. Mechanical Engineering Sciences, Vol. 13, 1971, pp. 36-46.

12. Amdahl, J., Impact Capacity of Steel Platforms and Tests on Large Deformations of Tubes under Transverse Loading, Impacts and Collisions Offshore, Progress Report No. 10, Det norske Veritas, January 1980.

13. Morris, A.J., Calladine, C.R., Simple Upper Bound Calculations for the Indentation of Cylindrical Shells, Int. J. of Mechanical Sciences, 1971, Vol. 13, pp. 331-343.

14. Pogorielov, A.V., Geometrical Methods in Nonlinear Theory of Elastic Shells, Izd. Nauka, Moscow, 1967.

15. Symmonds P.S., Plastic Shear Deformations in Dynamic Load Problems, Engineering Plasticity (Ed. J. Heyman and F.A. Leckie), Cambridge University Press, 1968.

16. Calladine, C.R., Simple Ideas in the Large-Deflection Plastic Theory of Plates and Slabs, Engineering Plasticity (Ed. J. Heyman and F.A. Leckie), Cambridge University Press, 1968.

17. Pettersen, E. Johnsen, K.R., New Non-Linear Methods for Estimation of Collision Resistance of Mobile Offshore Units, OTC 4135, 13th, May 1981.

18. Hodge, P.G., Post-Yield Behavior of a Beam with Partial End Fixity, Int. J. Mechanical Sciences, 1974, Vol. 16, pp. 385-388.

19. Oliveira, J.G. de, Simple Methods of Estimating the Energy Absorption Capability of Steel Tubular Members Used in Offshore Structures, Report SK/r50, Division of Marine Structures, NTU.

20. Sørensen, A.K., Behavior of Reinforced and Prestress Concrete Tubes Under Static and Impact Loading, BOSS '76, pp. 798-813.

21. Bathe, K.J., Wilson, E.L., Numerical Methods in Finite Element Analysis, Prentice Hall, 1976.

22. Thorensen, C.A., Torset, O.P., Fenders for Offshore Structures, D.I.A.N.C. 24th International Navigation Congress, Leningrad, 1977.

23. Kjeoy, H., Amdahl, J., Ship Impact Forces in Collision with Platform Legs, Impacts and Collisions Offshore, Progress Report No. 8, Det norske Veritas, October 1979.

24. Searle, J.W., A Feasibility Study on the Establishment of Force/Time Curve for the Structural Deformation of an Ocean-Going Tug in Collision with a Rigid Structure, The British Ship Research Association, Report No. W.260, August 1975.

25. McDermott, J.F. et al., Tanker Structural Analysis of Minor Collisions, Trans. SNAME, 1974.

26. DnV, Impact Loads from Boats, Technical Note, Fixed Offshore Installations, Det norske Veritas, May 1982.

27. Larsen, C.M. Engseth, A.G., Ship Collision and Fendering of Offshore Concrete Structures, European Offshore Petroleum Conference and Exhibition, 1978, pp. 145-154.

28. NMI, The Risk of Ship/Platform Encounters in UK Waters, National Maritime Institute, R39, May 1978.

29. Amdahl, J., Andersen, E., Computer Simulation Analysis of the Collision Probability Offshore, Impacts and Collisions Offshore, Progress Report No. 5, Det norske Veritas, October 1978.

30. Drewry, H.P., (Shipping Consultants) Ltd., The Cost of Ships, Shipping Study No. 9, London, England

31. Drewry, H.P., (Shipping Consultants) Ltd., The Rising Cost of Ships, Shipping Study No. 29, London, England

32. Borse, E., Design Basis Accidents and Accident Analysis With Particular Reference to Offshore Platforms, J. of Occupational Accidents, 2 (1979) pp. 227-243

33. Holand, I., Moan, T., Risk Assessment of Offshore Structures: Experience and Principles, PCAC'81, Ottawa, July 1981

APPENDIX A

A.1 Calculation of Angular Rotation $\dot{\omega}'$

We define: (fig. A1 and Fig 1.4)

$\vec{\dot{w}}$ as the vector of the downward velocity of the inner hinge (negative Y direction).

$\dot{w}$ as the downward velocity of the external load

$\vec{m}$ as the vector along the Y' axis

$\vec{\dot{w}}_{\omega}$ as the vector of the component of the velocity of the inner hinge which is parallel to the negative Y' axis (fig.1.4)

$\dot{\omega}'$ as the rate of angular rotation of the plasticized zone section as deformation progresses

ℓ' as the width of the plasticized zone (fig.1.4)

To calculate $\vec{\dot{w}}$ we need to consider the following factors:

- The cross-section between the inner and outer hinges (plasticized zone) rotates as a rigid body about the instantaneous center (taken as the outer hinge).
- The average downwards (parallel to the negative Y axis) velocity of the above cross section is the velocity at which the external load moves.
- The region inside the inner hinge has been assumed to move as a rigid body downwards and so does the inner hinge.

We can now write $\dot{\vec{w}}$ as:

$$\dot{\vec{w}} = 2\dot{w}\hat{j}$$

$$\vec{m} = -\hat{i} + \frac{1}{\tan\alpha}\ \hat{j}$$

The component of $\dot{\vec{w}}$ along $\vec{m}$ is $\dot{\vec{w}}_\omega$. It is given by:

$$\dot{\vec{w}}_\omega = \frac{\dot{\vec{w}}\cdot\vec{m}}{|\vec{m}|}\left[\frac{\vec{m}}{|\vec{m}|}\right]$$

$$= 2\dot{w}\cos\alpha\ [\sin\alpha\hat{i} - \cos\alpha\ \hat{j}] \qquad \text{(A1)}$$

The rate of angular rotation is then

$$\dot{\omega}' = \frac{|\dot{\vec{w}}_\omega|}{\ell'} \qquad \text{(A2)}$$

with $$\ell' = \frac{\eta_o}{\cos\alpha}\ \sin\gamma' \qquad \text{(A3)}$$

From (A1), (A2), and (A3) we obtain

$$\dot{\omega}' = \frac{2\ \dot{w}\ \cos^2\alpha}{\eta_o\ \sin\gamma'} \qquad \text{(A4)}$$

<u>A.2 Evaluation of the Equation Describing the Parabolic Approximation of the Cross-Section of the Plasticized Zone</u>

We define: $\vec{p}$ as a vector along the λ' axis

(Fig A1) $\vec{n}$ as a vector along the outward normal to the parabolic expansion of the cylinder's surface at a general point A on the outer hinge

$\vec{v}$ as a vector along the x' axis

$\vec{t}$ as a vector tangent to the parabolic expansion to the cylinder's surface at A and perpendicular to p

σ' as the angle between $\vec{v}$ and $\vec{t}$

β as the angle between $\vec{n}$ and Y-axis

γ as the projection on the X-Y plane of the angle between the outer hinge and the X' axis

Let us write the equation describing the cross-section of the plasticized zone between the outer and the inner hinge as

$$y'(x') = ax'^2 + bx' + c$$

We evaluate the three constants by fitting this curve at the points A and B and at the slope ($\tan\sigma'$) at the outer hinge A. We obtain:

$$a = -\frac{\tan\sigma'}{\ell'}$$

$$b = \tan\sigma'$$

$$c = 0$$

This gives:

$$y'(x') = \tan\sigma' \left[-\frac{1}{\ell'} x'^2 + x'\right] \tag{A5}$$

Before being able to evaluate $\tan\sigma'$ we need to calculate $\vec{t}$ and $\vec{v}$. We have that:

$$\vec{p} = \hat{i} + \tan\alpha \cdot \hat{j} - \tan\gamma \cdot \hat{k}$$

$$\vec{n} = \cot\beta \cdot \hat{j} + \hat{k} \tag{A6}$$

From(1.2) we have:

$$\tan\beta = -\frac{dY}{dZ} = \frac{Z}{R} \tag{A7}$$

Angle γ is equal to the angle between the λ-axis and the X-axis. So, we can write:

$$\frac{dX}{dZ} = -\frac{Z}{R\tan\alpha} = \frac{1}{\tan(-\gamma)} = -\cot\gamma \tag{A(B)}$$

Combining the above and (A7) we obtain:

$$\tan\beta = \tan\alpha \cdot \cot\gamma$$

Substituting back in (A6) we come to:

$$\vec{n} = \left(\frac{\tan\gamma}{\tan\alpha}\right)\hat{j} + \hat{k}$$

By definition we have:

$$\vec{t} = \vec{n} \times \vec{p}$$

$$= \frac{1}{\tan\alpha}\left[-(\tan^2\gamma + \tan^2\alpha)\hat{i} + \tan\alpha\cdot\hat{j} - \tan\gamma\cdot\hat{k}\right] \quad \text{(A9)}$$

also,

$$\vec{v} = \vec{m} \times \vec{p}$$

$$= \frac{1}{\tan\alpha}\left[\tan\gamma \cdot\hat{i} + \tan\gamma\cdot\tan\alpha\cdot\hat{j} + \frac{1}{\cos^2\alpha}\cdot\hat{k}\right] \quad \text{(A10)}$$

The angle σ' can then be calculated from:

$$\cos\sigma' = \frac{\vec{t}\cdot\vec{v}}{|\vec{t}|\,|\vec{v}|}$$

and after some pages of tedious algebra we obtain:

$$\cos\sigma' = \frac{\cos\alpha}{\sqrt{1 + \cos^2\gamma\cdot\tan^2\alpha}}$$

and

$$\tan\sigma' = \frac{\tan\alpha}{\cos\alpha}\sqrt{\cos^2\alpha + \cot^2\gamma} \quad \text{(A11)}$$

Substituting (A3) and (A11) in (A5) we obtain:

$$y'(x') = \frac{\tan\alpha}{\sin\gamma'}\left[-\left(\frac{\cos\alpha}{\eta_0\sin\gamma'}\right)x'^2 + x'\right] \quad \text{(A12)}$$

A.3 Evaluation of the First Moment of Area of the Cross-Section Between the Inner and Outer Hinge

The equation of the cross section of the plasticized zone is given by (A5) as:

$$y'(x') = \tan\sigma' \left[\frac{1}{\ell'} x'^2 + x' \right]; \quad 0 \le x' \le \ell'$$

The first moment of area (about the x' axis) of an arc of thickness h and given by the above equation is approximately given by:

$$M' = h \int_0^{\ell'} y' \, dx'$$

$$= \frac{h}{6} \tan\sigma' \cdot \ell'^2 \qquad \text{(A13)}$$

Substituting (A3) and (A11) in (A13) we obtain:

$$\left(\frac{M'}{\ell'}\right) = \frac{\eta_0}{6} \frac{\tan\alpha}{\cos\alpha} \qquad \text{(A14)}$$

A.4 Relation Between θ' and w_L

We define: θ' as γ' at $X'=0$

θ as the projection on the X-Y plane of θ'

From (A8) we can write:

$$\cot\theta = \frac{Z(X=0)}{R\tan\alpha} \qquad \text{(A15)}$$

From (3) we have:

$$Z(X=0) = \sqrt{2Rw_L} \qquad \text{(A16)}$$

Combining (A15) and (A16) we obtain:

$$\cot\theta = \frac{\sqrt{2 \frac{w_L}{R}}}{\tan\alpha} \qquad \text{(A17)}$$

We now need to find the relation between γ' and γ. γ' is the angle between the λ' axis and the X' axis. From geometry it can be shown to be equal to the angle between the Y axis and the vector $\vec{v}$. Then from analytic geometry we have:

$$\cos\gamma' = \frac{(-\hat{k})\cdot\vec{v}}{|\vec{v}|}$$

$$= \frac{1}{\sqrt{1 + \tan^2\gamma \cdot \cos^2\alpha}}$$

We also have the trigonometric identity:

$$\cos\gamma' = \frac{1}{\sqrt{1 + \tan^2\gamma'}}$$

Combining the above two relations we conclude that:

$$\tan\gamma' = \tan\gamma \cdot \cos\alpha$$

or,

$$\cot\theta' = \frac{\cot\theta}{\cos\alpha} \tag{A18}$$

Combining (A17) with (A18) we obtain:

$$\cot\theta' = \frac{\sqrt{2\frac{w_L}{R}}}{\sin\alpha} \tag{A19}$$

A.5 Relation Between λ' and γ'

We have that

$$d\lambda' = \frac{dX'}{\cos\gamma'} \tag{A20}$$

From(1.4)we obtain:

$$dX' = -\frac{Z'}{R\sin\alpha}\, dZ'$$

$$\frac{dX'}{dZ'} = -\frac{Z'}{R\sin\alpha} = -\cot\gamma'$$

From the above, differentiating with respect to γ' we obtain:

$$dZ' = -\frac{R\sin\alpha}{\sin^2\gamma'}\, d\gamma'$$

Combining the above two expressions we get:

$$dX' = \cos\gamma' \; \frac{R\sin\alpha}{\sin^3\gamma'}\, d\gamma'$$

Substituting the above in (A20) we obtain:

$$d\lambda' = \frac{R\sin\alpha}{\sin^3\gamma'}\, d\gamma' \tag{A21}$$

A.6 Calculation of the Rate of Membrane Extension

We define: $\dot{w}_p$ as the rate of downward (parallel to the negative Y-axis) motion of the inner hinge.

$\dot{\omega}_p$ as the rate of rotation of the longitudinal section of the plasticized zone.

Figure A2 shows two subsequent (during deformation) cuts of the cylinder by a plane parallel to the X-Y plane. Lines AEG and BFH are the intersection of the hinge planes with the cutting plane. CE and DIF represent the cut of the deformed rigid region (inside the inner hinge) by the cutting plane. $\overline{EI}$ is the vertical displacement of the point E for a deflection increment (of the load) of Δw. We have:

$$\overline{EF} = \overline{GH} = \frac{\Delta w}{\tan\alpha}$$

$$\overline{EI} = \overline{EF} = \tan 2\alpha$$

From the above we get:

$$\overline{EI} = \frac{\Delta w}{\tan\alpha} \tan 2\alpha$$

By taking the limit as $\Delta w \to 0$ and rates instead of displacement we obtain:

$$\dot{w}_p = \dot{w} \frac{\tan 2\alpha}{\tan \alpha} \tag{A22}$$

and

$$\dot{\omega}_p = \frac{\dot{w}_p}{\eta_o} = \frac{\dot{w}}{\eta_o} \frac{\tan 2\alpha}{\tan\alpha}$$

The rate of membrane extension of the material along the longitudinal direction (X-axis) can be given by:

$$\dot{W}_e = \dot{\omega}_p \cdot \eta_o \tan\alpha$$

Combining the above two expressions we arrive at:

$$\dot{W}_e = \dot{w} \tan 2\alpha \qquad \text{(A23)}$$

A.7 Complete Numerical Results

Symbol Equivalence:

THICKNESS RATIO ..... $\frac{R}{h}$

LOADING BEAM WIDTH ..... $\frac{B}{R}$

WL ..... $\frac{W_L}{R}$

PO ..... $\left(\frac{P_B}{M_O}\right)_{min}$

ALPHAMIN ..... α_{min}

C1M ..... Load Due to Hoop and Bending

C2M .... Load Due to Membrane Extension

FILE: CA 1 A1 VM/SP CONVERSATIONAL MONITOR SYSTEM

THICKNESS RATIO= 10.000 LOADING BEAM WIDTH= 0.0

WL	PO	ALPHAMIN	POD	C1M	C2M
0.0500	27.0081	4.5000	6.0392	18.9607	8.0475
0.1000	42.6070	5.0000	9.5272	29.8825	12.7245
0.1500	55.7440	5.5000	12.4647	38.4889	17.2551
0.2000	67.5409	6.0000	15.1026	45.6561	21.8848
0.2500	78.4659	6.0000	17.5455	53.8864	24.5795
0.3000	88.7138	6.5000	19.8370	59.3327	29.3811
0.3500	98.4503	6.5000	22.0142	66.5643	31.8861
0.4000	107.8082	6.5000	24.1066	73.5550	34.2532
0.4500	116.8333	7.0000	26.1247	77.4024	39.4309
0.5000	125.5320	7.0000	28.0698	83.7568	41.7752
0.5500	134.0040	7.0000	29.9642	89.9615	44.0424
0.6000	142.2795	7.0000	31.8147	96.0330	46.2465
0.6500	150.3829	7.0000	33.6266	101.9844	48.3985
0.7000	158.3348	7.0000	35.4047	107.8269	50.5079
0.7500	166.1527	7.0000	37.1529	113.5698	52.5828
0.8000	173.8103	7.5000	38.8652	115.1001	58.7103
0.8500	181.3572	7.5000	40.5527	120.4695	60.8877
0.9000	188.8119	7.5000	42.2196	125.7634	63.0485
0.9500	196.1851	7.5000	43.8683	130.9868	65.1983
1.0000	203.4873	7.5000	45.5011	136.1444	67.3428

THICKNESS RATIO= 10.000 LOADING BEAM WIDTH= 0.465

WL	PO	ALPHAMIN	POD	C1M	C2M
0.0500	34.3219	4.0000	7.6746	27.1811	7.1408

FILE: CA 1 A1 VM/SP CONVERSATIONAL MONITOR SYSTEM

0.1000	49.9016	5.0000	11.1583	37.1772	12.7245
0.1500	62.9593	5.5000	14.0781	45.7042	17.2551
0.2000	74.6228	5.5000	16.6862	54.6094	20.0134
0.2500	85.4306	6.0000	19.1028	60.8511	24.5795
0.3000	95.5677	6.0000	21.3696	68.5170	27.0507
0.3500	105.2550	6.0000	23.5357	75.8981	29.3570
0.4000	114.4776	6.5000	25.5980	80.2244	34.2532
0.4500	123.3899	6.5000	27.5908	86.8784	36.5115
0.5000	132.0486	6.5000	29.5269	93.3663	38.6823
0.5500	140.4894	6.5000	31.4144	99.7078	40.7816
0.6000	148.6749	7.0000	33.2447	102.4284	46.2465
0.6500	156.6841	7.0000	35.0356	108.2857	48.3985
0.7000	164.5484	7.0000	36.7941	114.0405	50.5079
0.7500	172.2843	7.0000	38.5239	119.7015	52.5828
0.8000	179.9065	7.0000	40.2283	125.2763	54.6302
0.8500	187.4272	7.0000	41.9100	130.7709	56.6563
0.9000	194.8581	7.0000	43.5716	136.1912	58.6669
0.9500	202.2092	7.0000	45.2153	141.5418	60.6674
1.0000	209.4517	7.5000	46.8348	142.1089	67.3428

THICKNESS RATIO= 10.000 LOADING BEAM WIDTH= 1.000

WL	PO	ALPHAMIN	POD	C1M	C2M
0.0500	40.7514	4.0000	9.1123	33.6106	7.1408
0.1000	56.7401	4.5000	12.6875	45.3104	11.4297
0.1500	69.9225	5.0000	15.6352	54.2701	15.6525
0.2000	81.6772	5.5000	18.2636	61.6638	20.0134
0.2500	92.4641	5.5000	20.6756	69.9865	22.4776
0.3000	102.6197	6.0000	22.9465	75.5690	27.0507

FILE: CA 1 A1 VM/SP CONVERSATIONAL MONITOR SYSTEM

0.3500	112.2155	6.0000	25.0921	82.8586	29.3570
0.4000	121.4477	6.0000	27.1565	89.9114	31.5364
0.4500	130.3497	6.5000	29.1471	93.8382	36.5115
0.5000	138.9249	6.5000	31.0645	100.2426	38.6823
0.5500	147.2848	6.5000	32.9339	106.5032	40.7816
0.6000	155.4588	6.5000	34.7616	112.6364	42.8224
0.6500	163.4701	6.5000	36.5530	118.6550	44.8151
0.7000	171.3026	7.0000	38.3044	120.7947	50.5079
0.7500	178.9716	7.0000	40.0193	126.3887	52.5828
0.8000	186.5294	7.0000	41.7092	131.8992	54.6302
0.8500	193.9884	7.0000	43.3771	137.3321	56.6563
0.9000	201.3600	7.0000	45.0255	142.6931	58.6669
0.9500	208.6541	7.0000	46.6565	147.9867	60.6674
1.0000	215.8804	7.0000	48.2723	153.2175	62.6628

THICKNESS RATIO= 10.000 LOADING BEAM WIDTH= 2.000

WL	PO	ALPHAMIN	POD	C1M	C2M
0.0500	50.2714	4.0000	11.2410	43.1306	7.1408
0.1000	67.2811	4.5000	15.0445	55.8514	11.4297
0.1500	80.9317	4.5000	18.0969	66.8720	14.0597
0.2000	92.9105	5.0000	20.7754	74.7558	18.1546
0.2500	103.9094	5.5000	23.2348	81.4318	22.4776
0.3000	114.0982	5.5000	25.5131	89.3607	24.7375
0.3500	123.7957	5.5000	27.6816	96.9491	26.8466
0.4000	133.0463	6.0000	29.7500	101.5099	31.5364
0.4500	141.9167	6.0000	31.7335	108.3011	33.6156
0.5000	150.5259	6.0000	33.6586	114.9118	35.6141

FILE: CA 1 A1 VM/SP CONVERSATIONAL MONITOR SYSTEM

0.5500	158.9142	6.0000	35.5343	121.3672	37.5470
0.6000	167.0445	6.5000	37.3523	124.2221	42.8224
0.6500	174.9806	6.5000	39.1268	130.1655	44.8151
0.7000	182.7721	6.5000	40.8691	136.0037	46.7684
0.7500	190.4365	6.5000	42.5829	141.7468	48.6897
0.8000	197.9886	6.5000	44.2716	147.4032	50.5855
0.8500	205.4410	6.5000	45.9380	152.9794	52.4616
0.9000	212.7792	7.0000	47.5789	154.1123	58.6669
0.9500	220.0030	7.0000	49.1942	159.3357	60.6674
1.0000	227.1602	7.0000	50.7946	164.4974	62.6628

THICKNESS RATIO= 17.650 LOADING BEAM WIDTH= 0.0

WL	PO	ALPHAMIN	POD	C1M	C2M
0.0500	39.1441	4.0000	6.5884	26.5406	12.6035
0.1000	61.9047	4.5000	10.4192	41.7313	20.1734
0.1500	81.1717	5.0000	13.6621	53.5450	27.6266
0.2000	98.3773	5.0000	16.5580	66.3344	32.0429
0.2500	114.3716	5.0000	19.2500	78.3832	35.9883
0.3000	129.3259	5.5000	21.7670	85.6642	43.6617
0.3500	143.5446	5.5000	24.1601	96.1604	47.3842
0.4000	157.2051	5.5000	26.4594	106.3032	50.9019
0.4500	170.4036	5.5000	28.6808	116.1457	54.2579
0.5000	183.1522	6.0000	30.8265	120.2933	62.8589
0.5500	195.5023	6.0000	32.9052	129.2320	66.2704
0.6000	207.5638	6.0000	34.9353	137.9771	69.5868
0.6500	219.3727	6.0000	36.9229	146.5478	72.8249
0.7000	230.9594	6.0000	38.8730	154.9604	75.9990
0.7500	242.3498	6.0000	40.7901	163.2287	79.1211

FILE: CA 1 A1 VM/SP CONVERSATIONAL MONITOR SYSTEM

0.8000	253.5664	6.0000	42.6780	171.3647	82.2017
0.8500	264.6279	6.0000	44.5398	179.3777	85.2504
0.9000	275.5527	6.0000	46.3786	187.2772	88.2758
0.9500	286.3560	6.0000	48.1969	195.0702	91.2858
1.0000	297.0322	6.5000	49.9938	194.6212	102.4113

THICKNESS RATIO= 17.650 LOADING BEAM WIDTH= 0.465

WL	PO	ALPHAMIN	POD	C1M	C2M
0.0500	48.5327	3.5000	8.1686	37.5215	11.0112
0.1000	71.1778	4.0000	11.9800	53.2772	17.9006
0.1500	90.1990	4.5000	15.1815	65.3835	24.8154
0.2000	107.3278	4.5000	18.0645	78.5455	28.7823
0.2500	123.0415	5.0000	20.7092	87.0532	35.9883
0.3000	137.8872	5.0000	23.2079	98.2807	39.6066
0.3500	152.0455	5.5000	25.5909	104.6613	47.3842
0.4000	165.5080	5.5000	27.8568	114.6061	50.9019
0.4500	178.5291	5.5000	30.0484	124.2712	54.2579
0.5000	191.1770	5.5000	32.1772	133.6933	57.4837
0.5500	203.5046	5.5000	34.2521	142.9012	60.6034
0.6000	215.5385	6.0000	36.2775	145.9517	69.5868
0.6500	227.2233	6.0000	38.2442	154.3984	72.8249
0.7000	238.6951	6.0000	40.1750	162.6961	75.9990
0.7500	249.9785	6.0000	42.0741	170.8574	79.1211
0.8000	261.0950	6.0000	43.9452	178.8934	82.2017
0.8500	272.0630	6.0000	45.7912	186.8127	85.2504
0.9000	282.8997	6.0000	47.6151	194.6240	88.2758
0.9500	293.6196	6.0000	49.4194	202.3340	91.2858

FILE: CA 1 A1 VM/SP CONVERSATIONAL MONITOR SYSTEM

1.0000	304.2378	6.0000	51.2066	209.9495	94.2884

THICKNESS RATIO= 17.650 LOADING BEAM WIDTH= 1.000

WL	PO	ALPHAMIN	POD	C1M	C2M
0.0500	56.9588	3.5000	9.5868	45.9476	11.0112
0.1000	80.0218	4.0000	13.4685	62.1211	17.9006
0.1500	99.1932	4.0000	16.6953	77.1735	22.0197
0.2000	116.2158	4.5000	19.5604	87.4334	28.7823
0.2500	132.0287	4.5000	22.2219	99.7025	32.3262
0.3000	146.7516	5.0000	24.6999	107.1450	39.6066
0.3500	160.7909	5.0000	27.0629	117.8076	42.9833
0.4000	174.3031	5.0000	29.3371	128.1287	46.1743
0.4500	187.2651	5.5000	31.5188	133.0072	54.2579
0.5000	199.7909	5.5000	33.6270	142.3072	57.4837
0.5500	212.0026	5.5000	35.6824	151.3992	60.6034
0.6000	223.9424	5.5000	37.6920	160.3062	63.6362
0.6500	235.6439	5.5000	39.6615	169.0465	66.5974
0.7000	247.1357	5.5000	41.5957	177.6356	69.5001
0.7500	258.3542	6.0000	43.4839	179.2333	79.1211
0.8000	269.3828	6.0000	45.3401	187.1812	82.2017
0.8500	280.2668	6.0000	47.1720	195.0166	85.2504
0.9000	291.0234	6.0000	48.9825	202.7478	88.2758
0.9500	301.6670	6.0000	50.7739	210.3812	91.2858
1.0000	312.2117	6.0000	52.5487	217.9234	94.2884

THICKNESS RATIO= 17.650 LOADING BEAM WIDTH= 2.000

WL	PO	ALPHAMIN	POD	C1M	C2M
0.0500	69.4460	3.0000	11.6885	60.0204	9.4256

FILE: CA 1 A1 VM/SP CONVERSATIONAL MONITOR SYSTEM

0.1000	93.6881	3.5000	15.7687	78.0491	15.6390
0.1500	113.3345	4.0000	19.0754	91.3148	22.0197
0.2000	130.7408	4.0000	22.0051	105.2011	25.5397
0.2500	146.5672	4.5000	24.6689	114.2410	32.3262
0.3000	161.4445	4.5000	27.1729	125.8682	35.5763
0.3500	175.5571	5.0000	29.5482	132.5738	42.9833
0.4000	188.9587	5.0000	31.8038	142.7843	46.1743
0.4500	201.9131	5.0000	33.9842	152.6945	49.2186
0.5000	214.4948	5.0000	36.1019	162.3501	52.1448
0.5500	226.7250	5.5000	38.1603	166.1216	60.6034
0.6000	238.5458	5.5000	40.1499	174.9096	63.6362
0.6500	250.1283	5.5000	42.0994	183.5309	66.5974
0.7000	261.5022	5.5000	44.0137	192.0023	69.5001
0.7500	272.6924	5.5000	45.8971	200.3373	72.3552
0.8000	283.7200	5.5000	47.7532	208.5477	75.1724
0.8500	294.6030	5.5000	49.5849	216.6426	77.9604
0.9000	305.3579	5.5000	51.3951	224.6308	80.7271
0.9500	315.9368	6.0000	53.1756	224.6511	91.2858
1.0000	326.3828	6.0000	54.9338	232.0946	94.2884

THICKNESS RATIO= 25.000 LOADING BEAM WIDTH= 0.0

WL	PO	ALPHAMIN	POD	C1M	C2M
0.0500	49.1865	3.5000	6.9560	33.5899	15.5966
0.1000	77.9292	4.0000	11.0209	52.5742	25.3550
0.1500	102.2531	4.5000	14.4608	67.1037	35.1493
0.2000	123.9689	4.5000	17.5318	83.2007	40.7682
0.2500	144.1469	4.5000	20.3854	98.3590	45.7879

FILE: CA 1 A1 VM/SP CONVERSATIONAL MONITOR SYSTEM

0.3000	163.0562	5.0000	23.0596	106.9562	56.1000
0.3500	180.9717	5.0000	25.5932	120.0888	60.8829
0.4000	198.1797	5.0000	28.0268	132.7769	65.4027
0.4500	214.8022	5.0000	30.3776	145.0875	69.7148
0.5000	230.9308	5.0000	32.6585	157.0713	73.8595
0.5500	246.6065	5.5000	34.8754	160.7659	85.8406
0.6000	261.7920	5.5000	37.0230	171.6558	90.1363
0.6500	276.6584	5.5000	39.1254	182.3278	94.3307
0.7000	291.2441	5.5000	41.1881	192.8022	98.4421
0.7500	305.5823	5.5000	43.2159	203.0963	102.4862
0.8000	319.7014	5.5000	45.2126	213.2251	106.4766
0.8500	333.6257	5.5000	47.1818	223.2004	110.4256
0.9000	347.3779	5.5000	49.1266	233.0338	114.3443
0.9500	360.9775	5.5000	51.0499	242.7343	118.2433
1.0000	374.4438	5.5000	52.9543	252.3114	122.1325

THICKNESS RATIO= 25.000 LOADING BEAM WIDTH= 0.465

WL	PO	ALPHAMIN	POD	C1M	C2M
0.0500	60.1382	3.0000	8.5048	46.7874	13.3508
0.1000	88.6723	3.5000	12.5402	66.5207	22.1516
0.1500	112.6165	4.0000	15.9264	81.4271	31.1894
0.2000	134.2481	4.5000	18.9855	93.4800	40.7682
0.2500	154.0612	4.5000	21.7875	108.2734	45.7879
0.3000	172.7988	4.5000	24.4374	122.4073	50.3914
0.3500	190.7009	4.5000	26.9692	136.0132	54.6877
0.4000	207.6869	5.0000	29.3714	142.2841	65.4027
0.4500	224.0989	5.0000	31.6924	154.3841	69.7148
0.5000	240.0382	5.0000	33.9465	166.1787	73.8595

FILE: CA 1 A1 VM/SP CONVERSATIONAL MONITOR SYSTEM

0.5500	255.5716	5.0000	36.1433	177.7036	77.8680
0.6000	270.7527	5.0000	38.2902	188.9881	81.7647
0.6500	285.6250	5.0000	40.3935	200.0556	85.5696
0.7000	300.1108	5.5000	42.4421	201.6690	98.4421
0.7500	314.3237	5.5000	44.4521	211.8377	102.4862
0.8000	328.3259	5.5000	46.4323	221.8494	106.4766
0.8500	342.1406	5.5000	48.3860	231.7152	110.4256
0.9000	355.7900	5.5000	50.3163	241.4458	114.3443
0.9500	369.2925	5.5000	52.2258	251.0494	118.2433
1.0000	382.6672	5.5000	54.1173	260.5349	122.1325

THICKNESS RATIO= 25.000 LOADING BEAM WIDTH= 1.000

WL	PO	ALPHAMIN	POD	C1M	C2M
0.0500	69.9594	3.0000	9.8937	56.6086	13.3508
0.1000	98.8982	3.5000	13.9863	76.7465	22.1516
0.1500	123.0365	4.0000	17.4000	91.8472	31.1894
0.2000	144.4974	4.0000	20.4350	108.3222	36.1752
0.2500	164.4477	4.5000	23.2564	118.6598	45.7879
0.3000	182.9903	4.5000	25.8787	132.5989	50.3914
0.3500	200.7047	4.5000	28.3839	146.0170	54.6877
0.4000	217.7546	4.5000	30.7951	159.0070	58.7476
0.4500	234.1461	5.0000	33.1133	164.4313	69.7148
0.5000	249.9348	5.0000	35.3461	176.0753	73.8595
0.5500	265.3264	5.0000	37.5228	187.4585	77.8680
0.6000	280.3743	5.0000	39.6509	198.6097	81.7647
0.6500	295.1211	5.0000	41.7364	209.5517	85.5696
0.7000	309.6028	5.0000	43.7844	220.3038	89.2991

FILE: CA 1 A1 VM/SP CONVERSATIONAL MONITOR SYSTEM

0.7500	323.8494	5.0000	45.7992	230.8820	92.9676
0.8000	337.8511	5.5000	47.7793	231.3747	106.4766
0.8500	351.5657	5.5000	49.7189	241.1402	110.4256
0.9000	365.1194	5.5000	51.6357	250.7753	114.3443
0.9500	378.5310	5.5000	53.5324	260.2878	118.2433
1.0000	391.8188	5.5000	55.4115	269.6865	122.1325

THICKNESS RATIO= 25.000 LOADING BEAM WIDTH= 2.000

WL	PO	ALPHAMIN	POD	C1M	C2M
0.0500	84.7833	3.0000	11.9902	71.4326	13.3508
0.1000	115.0083	3.0000	16.2646	96.0464	18.9619
0.1500	139.5363	3.5000	19.7334	112.2875	27.2489
0.2000	161.3791	4.0000	22.8224	125.2039	36.1752
0.2500	181.2784	4.0000	25.6366	140.6490	40.6294
0.3000	200.0488	4.0000	28.2912	155.3345	44.7143
0.3500	217.7659	4.5000	30.7967	163.0782	54.6877
0.4000	234.6561	4.5000	33.1854	175.9086	58.7476
0.4500	250.9889	4.5000	35.4952	188.3681	62.6208
0.5000	266.8555	4.5000	37.7391	200.5118	66.3438
0.5500	282.3154	5.0000	39.9254	204.4477	77.8680
0.6000	297.2095	5.0000	42.0318	215.4448	81.7647
0.6500	311.8044	5.0000	44.0958	226.2350	85.5696
0.7000	326.1377	5.0000	46.1228	236.8387	89.2991
0.7500	340.2397	5.0000	48.1172	247.2722	92.9676
0.8000	354.1372	5.0000	50.0826	257.5500	96.5874
0.8500	367.8530	5.0000	52.0223	267.6836	100.1696
0.9000	381.4082	5.0000	53.9393	277.6838	103.7244
0.9500	394.8201	5.0000	55.8360	287.5588	107.2612
1.0000	408.1064	5.0000	57.7150	297.3174	110.7893

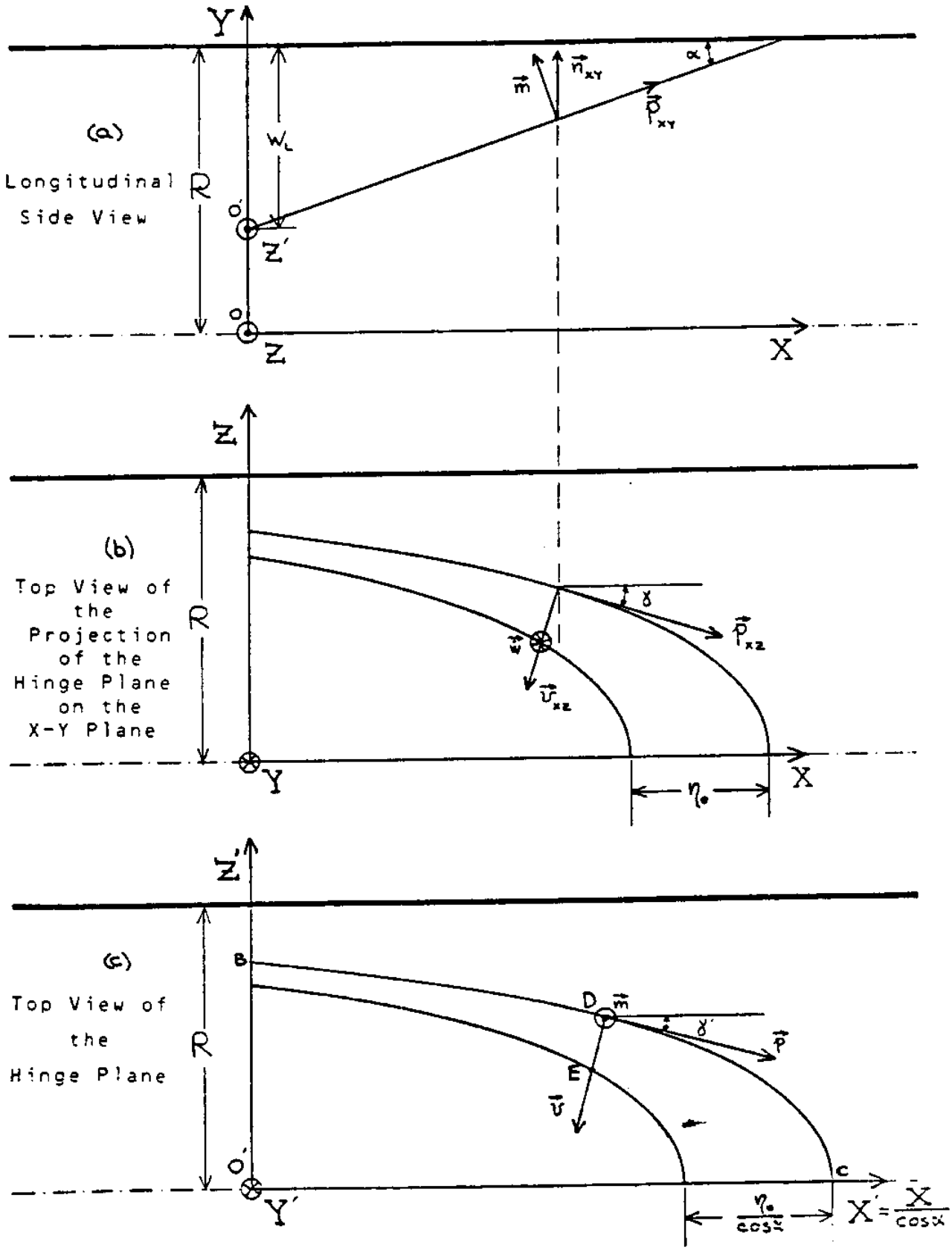

FIGURE A1a,b,c

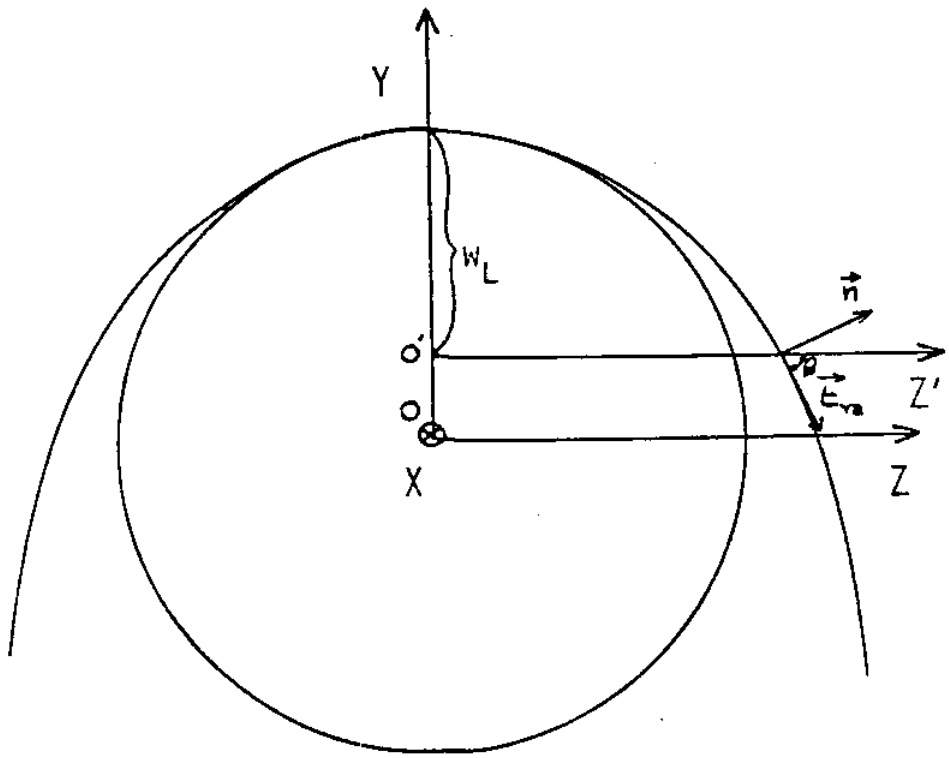

TRANSVERSE CYLINDER'S SECTION

FIGURE A1d

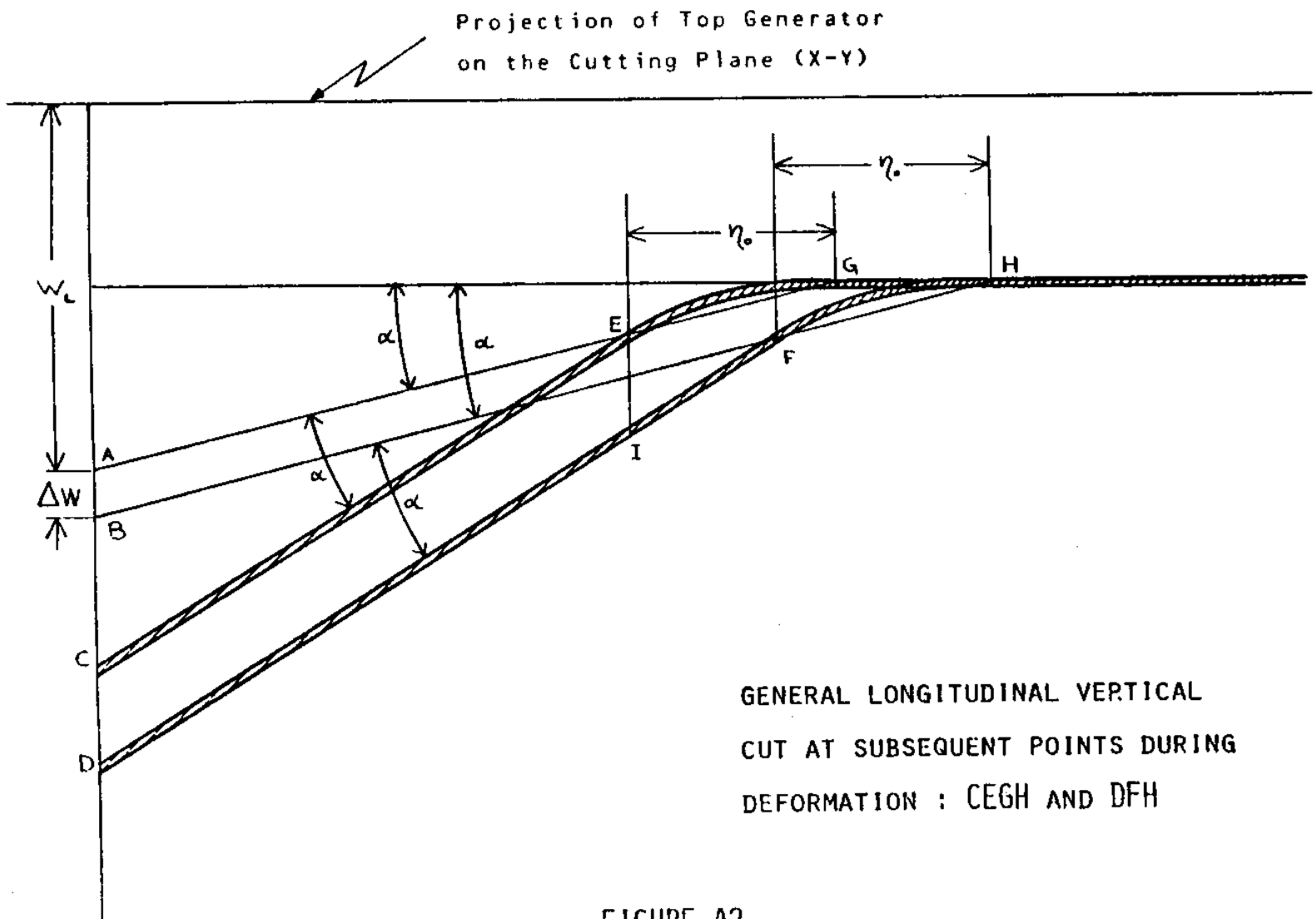

GENERAL LONGITUDINAL VERTICAL CUT AT SUBSEQUENT POINTS DURING DEFORMATION : CEGH AND DFH

FIGURE A2

Appendix B

B.1 Calculation of the Location of the Plastic Neutral Axis for an Indented Section Subject to Both Global Bending and Local Extension

We define: ξ as the distance of the plastic neutral axis from the center of the cylindrical section when the cylinder undergoes both local and global deformation. See Fig. B1.

ξ_{bend} as the distance of the plastic neutral axis from the center of the cylindrical section when the cylinder undergoes only global bending. See Fig. B1.

$\dot{w}_L$ as the local deflection rate. See Fig. 4a.

$\dot{w}_G$ as the global deflection rate. See Fig. 4b.

$\dot{\psi}$ as the rate of angular rotation of the cross-section. See Fig. 4b.

L as the length of the cylinder

ρ as the angle spanning the deformed arc of the indented cross-section. See Fig. B1.

ω See Fig. B1

ϕ See Fib. B1

From Fig. B2 we can write:

- Based on geometry:

$$\cos\omega = 2\cos\beta + \frac{\xi_{bend}}{R} \tag{B1}$$

- Based on pure bending (equating areas on both sides of the simple bending neutral axis):

$$\sin\omega = \frac{\xi_{bend}}{R} \tag{B2}$$

Combining (B1) and (B2) and substituting (1.24) for β we obtain:

$$\cos\omega - \sin\omega = w(1 - \tilde{w}_L) \quad \text{For } \tilde{w}_L > 0.5$$
$$\omega = 0 \quad \text{for } w_L \leq 0.5 \tag{B3}$$

Solving (B3) for ω in terms of w_L we get:

$$\omega = \cos^{-1}\left[(1 - \tilde{w}_L) \pm \sqrt{\tilde{w}_L(2 - \tilde{w}_L) - \frac{1}{2}}\right] \quad \text{for } \tilde{w}_L \geq 0.5$$
$$\omega = 0 \quad \text{for } \tilde{w}_L \leq 0.5 \tag{B4}$$

Let us now assume that some extension prevails in the global bending compression region of the section and its measure given by $\phi + \omega$ (see Fig. B1). By equating the areas under tension with the areas under compression and simplifying we obtain a relationship between $\phi + \omega$ and

$$(\phi + \omega) = \sin^{-1}\left(\frac{\xi}{R}\right) \tag{B5}$$

The rate of compression (due to global bending) at any arbitrary point of the deformed arc of the indented section is given by:

$$\text{rate of compression} = \dot{\psi}[\xi + 2R\cos\beta - R\cos(\phi + \omega)] \tag{B6}$$

Where $\dot{\psi}$ is given by:

$$= \frac{2\dot{w}_G}{L} \tag{B7}$$

The rate of extension due to local deformation is given by $\dot{w}_e$. From A23 we have:

$$\text{rate of extension} = \dot{w}_L \tan 2\alpha \tag{B8}$$

Equating (B6) and (B8) and substituting in (B5), (B6), and (1.24) we obtain the relation between ϕ, $\dot{w}_L$, and $\dot{w}_G$ in terms of $\tilde{w}_L$, $\frac{L}{R}$, and α:

$$\dot{w}_G[2(1 - \tilde{w}_L) + \sin(\phi + \omega) - \cos(\phi + \omega)] - \dot{w}_L\left[\left(\frac{L}{R}\right)\frac{\tan 2\alpha}{2}\right] = 0 \tag{B9}$$

We define: $$\xi = \frac{\dot{w}_L}{\dot{w}} \tag{B10}$$

$$(1 - \xi) = \frac{\dot{w}_G}{\dot{w}} \tag{B11}$$

By dividing (B9) by $\dot{w}$ and substituting (B10) and B(11) we obtain:

$$(1 - \xi)[2(1 - \tilde{w}_L) + \sin(\phi + \omega) - \cos(\phi + \omega)] - \xi[\left(\frac{L}{R}\right) \frac{\tan 2\alpha}{2}] = 0 \tag{B12}$$

B.2 Evaluation of the Integrals Over the Sectional Areas That are Under Tension and Under Compression

From (2.1), (2.2a,b,c), and (2.4) we have:

$$\dot{D}_H = 4h\sigma_o \int [\dot{\psi} d_I + \dot{\psi} d_{II} + \left|\dot{\psi} d_{III} - \dot{W}_e\right|] ds$$

By substituting (2.3a,b,c), (A23), and (B7) in the above expression we obtain:

$$\dot{D}_H = 16M_o \left(\frac{R}{h}\right) \left\{ \frac{2\dot{w}_G}{L} \left[\int_0^{\frac{\pi}{2} - \sin^{-1}\frac{\xi}{R}} [\cos t - \frac{\xi}{R}] R dt + \int_{-\sin^{-1}\left(\frac{\xi}{R}\right)}^{\frac{\pi}{2} - \beta} [\frac{\xi}{R} - \cos t] R dt \right] + \left| \int_0^{\beta} \frac{2\dot{w}_G}{L} \left[\left(\frac{\xi}{R}\right) + 2\cos\beta - \cos t - \dot{w}_L \tan 2\alpha \right] R dt \right| \right\}$$

Evaluating the integrals and substituting for $\sin^{-1} \frac{\xi}{R}$ and β from (B5) and (1.24) and for ζ from (B10) and (B11) we obtain:

$$\dot{D}_H = 16M_o\dot{w}\left(\frac{R}{h}\right) \left\{ 2 \frac{(1-\zeta)}{\frac{L}{R}} \left[2[\cos(\phi + \omega) + (\phi + \omega) \sin(\phi + \omega)] - \sin[\cos^{-1} (1 - \tilde{w}_L)] - \cos^{-1} (1 - \tilde{w}_L) \sin(\phi + \omega) \right] + \left| 2 \frac{(1-\zeta)}{\frac{L}{R}} \left[\left[2(1 - \tilde{w}_L) + \sin(\phi + \omega) \right] \cos^{-1} (1 - \tilde{w}_L) - \sin[\cos^{-1} (1 - \tilde{w}_L)] \right] - \zeta[\tan 2\alpha \cdot \cos^{-1} (1 - \tilde{w}_L)] \right| \right\} \tag{B.13}$$

B.3 Maximum Load That an Indented Section can Sustain Under Pure Global Bending

If an indented section undergoes only global bending we can calculate the crumpled load that it can sustain by putting the local deflection rate $\dot{w}_L$ equal to zero in (B13). This results to ϕ being equal to zero also. Thus, we can obtain the following expression for the rate of energy dissipation:

$$\dot{D}^G = 32M_o\dot{w}_G \frac{\left(\frac{L}{R}\right)}{\left(\frac{L}{R}\right)} \Big[2[\cos\omega + \omega \sin\omega] - \sin[\cos^{-1}(1 - \tilde{w}_L)]$$

$$- \cos^{-1}(1 - \tilde{w}_L) \sin\omega + [2(1 - \tilde{w}_L) + \sin\omega] \cos^{-1}(1 - \tilde{w}_L)$$

$$- \sin[\cos^{-1}(1 - \tilde{w}_L)] \Big]$$

The external rate of work

$$\dot{D}^G_{ext} = P_G \cdot \dot{w}_G$$

Equating the above two expressions we obtain the maximum load an indented section can sustain under global bending vs. the indentation:

$$P_G = 64M_o \frac{\left(\frac{R}{R}\right)}{\left(\frac{L}{R}\right)} \Big[(1 - \tilde{w}_L) \cos^{-1}(1 - \tilde{w}_L) - \sin[\cos^{-1}(1 - \tilde{w}_L)] + \cos\omega + \omega \sin\omega \Big] \tag{B14}$$

where ω is given by (B4)

B.4 Listing of the Program Used for the Calculation and Minimization of the Global Load

Symbol Equivalence :

LTR	$\frac{L}{R}$
THR	$\frac{R}{h}$
WLO	$\dot{w}$
WL	$\frac{\dot{w}_L}{R}$
W	$\frac{w}{R}$
PMIN	$\left(\frac{P_B}{H_0}\right)_{min}$
ZMIN	ζ_{min}
ALDMIN	α_{min}
PHIDMI	ϕ_{min}

```
      REAL LTR
   10 WRITE(6,210)
  210 FORMAT(' ENTER THICKNESS RATIO, LENGTH RATIO, LOADING WIDTH')
      READ(5,*)THR,LTR,WLO
      WRITE(7,215)THR,LTR,WLO
  215 FORMAT(///5X,'R/H=',F7.3,10X,'L/R=',F6.3,10X,'B/R=',F6.3//)
      WRITE(7,214)
  214 FORMAT(5X,'W',9X,'WL',7X,'PMIN',4X,'ZETAMIN',3X,'ALPHAMIN',4X,
     +'PHIMIN'/)
      DO 1 I=1,20
      WL=FLOAT(I)*.05
      CALL MINIM(W,WL,THR,LTR,WLO,ZMIN,ALDMIN,PMIN,PHIDMI,IND,IND2)
      WRITE(7,211)W,WL,PMIN,ZMIN,ALDMIN,PHIDMI
      IF(W.EQ.0)GO TO 2
  211 FORMAT(6F10.4)
      IF(IND.NE.0)WRITE(7,212)IND
  212 FORMAT('+',I5)
      IF(IND2.NE.0)WRITE(7,213)IND2
  213 FORMAT('+',I5)
    1 CONTINUE
    2 WRITE(6,216)
  216 FORMAT(' ENTER 1 FOR NEW GEOMETRIC PARAMETERS'/7X,'0 TO STOP')
      READ(5,*)IST
      IF(IST.EQ.1)GO TO 10
      STOP
      END
      SUBROUTINE MINIM(W,WL,THR,LTR,WLO,ZMIN,ALDMIN,PMIN,PHIDMI,INDMI,
     +IND2MI)
      REAL LTR
      DIMENSION P(80,11)
      PI=3.141592654
      DO 1 I=1,80
      ALD=FLOAT(I)*.5+1.5
      AL=ALD*PI/180.
      SWL=SQRT(2.*WL)
      G2=16.*TAN(AL)*SQRT(THR*2./3.*ATAN(SWL/SIN(AL))+(COS(AL)**2*SWL/
     +TAN(AL)+(SWL/TAN(AL))**3/3.+WLO*SWL/TAN(AL)**2))
      DO 2 J=1,11
      Z=1.-FLOAT(J-1)*.1
      WLD=1.-WL
      PHI=0.
      OMG=0.
      IF(WL.LT..5)GO TO 12
      CALL NEWT2(WLD,OMG,IND)
   12 ANG=OMG+PHI
      IND=0
      A1=2.*WLD+SIN(OMG)-COS(OMG)
      B=TAN(2.*AL)/2.*LTR
      A2=WLD+SIN(ACOS(WLD))
      Z1=A1/(B+A1)
      Z2=A2/(B+A2)
      IF(Z.LE.Z1)GO TO 10
      IF(Z.GE.Z2)GO TO 11
      CALL NEWTON(Z,ANG,WLD,AL,LTR,IND)
      GO TO 10
```

```
   11 ANG=ACOS(WLD)
   10 CONTINUE
      ZD=1.-Z
      G3=8.*THR*(2.*ZD/LTR*(2.*(COS(ANG)+ANG*SIN(ANG))-SIN(ACOS(WLD))-
     +ACOS(WLD)*SIN(ANG))+ABS(2.*ZD/LTR*((2.*WLD+SIN(ANG))*ACOS(WLD)-
     +SIN(ACOS(WLD))))-Z*TAN(2.*AL)*ATAN(SWL)))
      P(I,J)=Z*G2+2.*G3
      IF(I.EQ.1.AND.J.EQ.1)GO TO 20
      PTST=P(I,J)
      IF(PTST.GE.PMIN)GO TO 2
      IMIN=1
      ALDMIN=ALD
      ZMIN=Z
      PHIDMI=(ANG-OMG)*180./PI
      OMGDMI=OMG*180./PI
      PMIN=P(I,J)
      INDMI=IND
      IND2MI=IND2
      GO TO 2
   20 PMIN=P(1,1)
      INDMI=IND
      IND2MI=IND2
      ALDMIN=ALD
      ZMIN=Z
      PHIDMI=(PHI-OMG)*180./PI
      OMGDMI=OMG*180./PI
    2 CONTINUE
      IF(IMIN.NE.1)GO TO 32
    1 CONTINUE
      IF(ZMIN.EQ.0)GO TO 31
   32 W=W+.05/ZMIN
      GO TO 30
   31 W=0.
   30 CONTINUE
      RETURN
      END
      SUBROUTINE NEWTON(Z,A,WLD,AL,LTR,IND)
      REAL LTR
      DO 1 I=1,500
      A1=A
      A=A-((2.*WLD-COS(A)+SIN(A))*(1.-Z)-Z*TAN(2.*AL)/2.*LTR)/(1.-Z)/
     +(SIN(A)+COS(A))
      IF(A1.EQ.0.AND.A.EQ.0.)GO TO 10
      IF(A1.EQ.0.)GO TO 1
      T=(A-A1)/A1
      IF(T.LT..01)GO TO 10
    1 CONTINUE
      IND=1
   10 CONTINUE
      RETURN
      END
      SUBROUTINE NEWT2(WLD,A,IND)
      DO 1 I=1,500
      A1=A
      A=A-(2.*WLD-COS(A)+SIN(A))/(SIN(A)+COS(A))
      IF(A1.EQ.0.AND.A.EQ.0.)GO TO 10
      IF(A1.EQ.0.)GO TO 1
      T=(A-A1)/A1
      IF(T.LT..01)GO TO 10
    1 CONTINUE
      IND=2
   10 CONTINUE
      RETURN
      END
```

B.5 Complete Numerical Results

FILE: LO 1 A1 VM/SP CONVERSATIONAL MONITOR SYSTEM

R/H= 10.000 L/R=10.000 B/R= 0.0

W	WL	PMIN	ZETAMIN	ALPHAMIN	PHIMIN
0.0500	0.0500	31.3567	1.0000	2.0000	0.0
0.1500	0.1000	37.6121	0.5000	7.5000	25.8419
0.2750	0.1500	39.3469	0.4000	11.5000	31.7883
0.4417	0.2000	39.9561	0.3000	17.0000	36.8699
0.6083	0.2500	40.0162	0.3000	17.0000	41.4096
0.8583	0.3000	39.2438	0.2000	25.0000	45.5730
1.3583	0.3500	38.0833	0.1000	34.5000	49.4584
1.6583	0.4000	36.5522	0.1000	34.5000	53.1301
2.3583	0.4500	35.4670	0.1000	34.0000	55.1467
2.8583	0.5000	33.9445	0.1000	33.5000	56.3687
3.3583	0.5500	32.7542	0.1000	33.5000	55.6727
3.8583	0.6000	31.4462	0.1000	33.0000	52.6241
4.3583	0.6500	29.9691	0.1000	32.5000	49.8629
4.8583	0.7000	28.6286	0.1000	31.5000	45.3155
5.3583	0.7500	27.2035	0.1000	30.5000	41.4415
5.8583	0.8000	25.9283	0.1000	29.0000	36.5945
0.0	0.8500	24.0086	0.0	2.0000	0.0

R/H= 10.000 L/R=15.000 B/R= 0.0

W	WL	PMIN	ZETAMIN	ALPHAMIN	PHIMIN
0.0500	0.0500	26.7222	1.0000	4.5000	18.1949
0.2167	0.1000	29.7566	0.3000	11.5000	25.8419
0.4667	0.1500	29.8648	0.2000	18.5000	31.7883
0.9667	0.2000	29.1554	0.1000	26.5000	24.6028
1.4667	0.2500	28.3053	0.1000	26.0000	27.2169
1.9667	0.3000	27.5503	0.1000	26.0000	31.4295
2.4667	0.3500	26.7191	0.1000	30.0000	49.4584
2.9667	0.4000	25.7557	0.1000	30.0000	53.1301
3.4667	0.4500	25.2255	0.1000	29.0000	53.6317
3.9667	0.5000	24.2122	0.1000	29.0000	57.2593
4.4667	0.5500	23.5278	0.1000	29.0000	56.6589
4.9667	0.6000	22.8876	0.1000	28.0000	52.1113
5.4667	0.6500	22.0079	0.1000	27.5000	49.8087
0.0	0.7000	20.6749	0.0	2.0000	0.0

R/H= 10.000 L/R=20.000 B/R= 0.0

W	WL	PMIN	ZETAMIN	ALPHAMIN	PHIMIN

FILE: LO 1 A1 VM/SP CONVERSATIONAL MONITOR SYSTEM

0.1250	0.0500	23.2346	0.4000	5.5000	18.1949
0.3750	0.1000	24.0258	0.2000	12.5000	18.3517
0.8750	0.1500	23.2774	0.1000	22.5000	20.4273
1.3750	0.2000	22.6378	0.1000	22.5000	24.8502
1.8750	0.2500	22.0443	0.1000	26.5000	41.4096
2.3750	0.3000	21.4487	0.1000	26.5000	45.5730
2.8750	0.3500	21.0121	0.1000	26.5000	49.4584
3.3750	0.4000	20.6860	0.1000	26.0000	53.1301
3.8750	0.4500	20.0400	0.1000	26.0000	56.6330
4.3750	0.5000	19.5392	0.1000	25.0000	56.9211
4.8750	0.5500	19.1209	0.1000	25.0000	56.2833
0.0	0.6000	18.0486	0.0	2.0000	0.0

R/H= 17.650 L/R=10.000 B/R= 0.0

W	WL	PMIN	ZETAMIN	ALPHAMIN	PHIMIN
0.0500	0.0500	38.6963	1.0000	4.0000	18.1949
0.1333	0.1000	58.9662	0.6000	5.5000	25.8419
0.2333	0.1500	63.1815	0.5000	8.0000	31.7883
0.3583	0.2000	65.5050	0.4000	12.0000	36.3699
0.4833	0.2500	65.8420	0.4000	12.0000	41.4096
0.6500	0.3000	65.5636	0.3000	17.0000	45.5730
0.9000	0.3500	64.7619	0.2000	24.5000	49.4584
1.1500	0.4000	62.6892	0.2000	24.5000	53.1301
1.6500	0.4500	60.8938	0.1000	34.0000	55.1467
2.1500	0.5000	58.0840	0.1000	33.5000	56.3587
2.6500	0.5500	55.8729	0.1000	33.5000	55.6727
3.1500	0.6000	53.4438	0.1000	33.0000	52.0241
3.6500	0.6500	50.7152	0.1000	32.5000	49.8529
4.1500	0.7000	48.2137	0.1000	31.5000	45.3155
4.6500	0.7500	45.5581	0.1000	30.5000	41.4415
5.1500	0.8000	43.1427	0.1000	29.0000	36.5945
5.6500	0.8500	40.5370	0.1000	27.5000	32.6064
0.0	0.9000	38.2269	0.0	2.0000	0.0

R/H= 17.650 L/R=15.000 B/R= 0.0

W	WL	PMIN	ZETAMIN	ALPHAMIN	PHIMIN
0.0500	0.0500	38.6963	1.0000	4.0000	18.1949
0.1750	0.1000	48.7455	0.4000	7.5000	25.8419
0.3417	0.1500	49.8429	0.3000	12.0000	31.7883
0.5917	0.2000	49.6840	0.2000	19.0000	36.8899
0.8417	0.2500	48.4544	0.2000	19.0000	41.4096
1.3417	0.3000	47.1818	0.1000	29.0000	31.4095
1.8417	0.3500	45.0251	0.1000	30.0000	49.4584
2.3417	0.4000	43.7971	0.1000	30.0000	53.1301
2.8417	0.4500	42.7147	0.1000	29.0000	53.6317

FILE: LO 1 A1 VM/SP CONVERSATIONAL MONITOR SYSTEM

3.3417	0.5000	40.8044	0.1000	29.0000	57.2593
3.8417	0.5500	39.6509	0.1000	29.0000	56.6589
4.3417	0.6000	38.1954	0.1000	28.0000	52.1113
4.8417	0.6500	36.5072	0.1000	27.5000	49.8087
5.3417	0.7000	34.9502	0.1000	26.5000	45.9859
5.8417	0.7500	33.5955	0.1000	25.0000	41.0470
0.0	0.8000	30.9727	0.0	2.0000	0.0

R/H= 17.650 L/R=20.000 B/R= 0.0

W	WL	PMIN	ZETAMIN	ALPHAMIN	PHIMIN
0.1000	0.0500	37.6566	0.5000	4.0000	18.1949
0.2667	0.1000	40.3594	0.3000	9.0000	25.8419
0.7667	0.1500	40.0756	0.1000	22.5000	30.4278
1.2667	0.2000	38.7615	0.1000	22.5000	24.8302
1.7667	0.2500	37.6044	0.1000	26.5000	41.4096
2.2667	0.3000	36.4033	0.1000	26.5000	45.5730
2.7667	0.3500	35.4894	0.1000	26.5000	49.4584
3.2667	0.4000	34.7643	0.1000	26.0000	53.1301
3.7667	0.4500	33.4887	0.1000	26.0000	56.5330
4.2667	0.5000	32.4422	0.1000	25.0000	55.9211
4.7667	0.5500	31.5722	0.1000	25.0000	55.2833
5.2667	0.6000	30.7617	0.1000	24.0000	52.0510
0.0	0.6500	29.5456	0.0	2.0000	0.0

R/H= 25.000 L/R=10.000 B/R= 0.0

W	WL	PMIN	ZETAMIN	ALPHAMIN	PHIMIN
0.0500	0.0500	48.6323	1.0000	3.5000	18.1949
0.1000	0.1000	70.2151	1.0000	4.0000	25.8419
0.1833	0.1500	84.1035	0.6000	5.5000	31.7883
0.2833	0.2000	87.2363	0.5000	8.0000	35.8699
0.4083	0.2500	88.5552	0.4000	12.0000	41.4096
0.5333	0.3000	88.8371	0.4000	12.0000	45.5730
0.7000	0.3500	87.9454	0.3000	17.0000	49.4584
0.8667	0.4000	86.2313	0.3000	17.0000	53.1301
1.1167	0.4500	84.4123	0.2000	23.5000	53.8832
1.6167	0.5000	81.0128	0.1000	33.5000	56.2587
2.1167	0.5500	77.8030	0.1000	33.5000	55.6727
2.6167	0.6000	74.2814	0.1000	33.0000	52.6241
3.1167	0.6500	70.0350	0.1000	32.5000	49.8629
3.6167	0.7000	66.0053	0.1000	31.5000	45.3155
4.1167	0.7500	62.8371	0.1000	30.5000	41.4415
4.6167	0.8000	59.3035	0.1000	29.0000	36.5245
5.1167	0.8500	55.4035	0.1000	27.5000	32.6064
5.6167	0.9000	52.3345	0.1000	25.0000	27.1748
0.0	0.9500	48.1516	0.0	2.0000	0.0523

FILE: LO 1 A1 VM/SP CONVERSATIONAL MONITOR SYSTEM

R/H= 25.000 L/R=15.000 B/R= 0.0

W	WL	PMIN	ZETAMIN	ALPHAMIN	PHIMIN
0.0500	0.0500	48.6323	1.0000	3.5000	18.1949
0.1500	0.1000	65.3035	0.5000	5.5000	25.8419
0.2750	0.1500	67.6979	0.4000	8.0000	31.7883
0.4417	0.2000	67.9705	0.3000	12.0000	36.8699
0.6917	0.2500	66.6484	0.2000	19.0000	41.4096
0.9417	0.3000	65.3223	0.2000	19.0000	45.5730
1.4417	0.3500	63.5703	0.1000	30.0000	49.4584
1.9417	0.4000	60.8911	0.1000	30.0000	53.1301
2.4417	0.4500	59.2568	0.1000	29.0000	53.6317
2.9417	0.5000	56.4661	0.1000	29.0000	57.2593
3.4417	0.5500	54.7492	0.1000	29.0000	56.6569
3.9417	0.6000	52.5850	0.1000	28.0000	52.1113
4.4417	0.6500	50.1004	0.1000	27.5000	49.8087
4.9417	0.7000	47.7871	0.1000	26.5000	45.9859
5.4417	0.7500	45.7404	0.1000	25.0000	41.0470
5.9417	0.8000	43.5941	0.1000	23.5000	36.7917
0.0	0.8500	40.0143	0.0	2.0000	0.0

R/H= 25.000 L/R=20.000 B/R= 0.0

W	WL	PMIN	ZETAMIN	ALPHAMIN	PHIMIN
0.0500	0.0500	48.6323	1.0000	3.5000	18.1949
0.2167	0.1000	55.1090	0.3000	9.0000	25.8419
0.4667	0.1500	55.2639	0.2000	12.5000	22.8515
0.9667	0.2000	54.0806	0.1000	22.5000	24.8302
1.4667	0.2500	52.3660	0.1000	26.5000	41.4096
1.9667	0.3000	50.5616	0.1000	26.5000	45.5730
2.4667	0.3500	49.1684	0.1000	26.5000	49.4584
2.9667	0.4000	48.0381	0.1000	26.0000	53.1301
3.4667	0.4500	46.1381	0.1000	26.0000	56.6330
3.9667	0.5000	44.5440	0.1000	25.0000	56.9211
4.4667	0.5500	43.2209	0.1000	25.0000	56.2333
4.9667	0.6000	41.9570	0.1000	24.0000	52.0510
5.4667	0.6500	40.2639	0.1000	23.5000	49.8684
0.0	0.7000	38.7655	0.0	2.0000	0.0

R/H= 17.650 L/R= 6.110 B/R= 0.465

W	WL	PMIN	ZETAMIN	ALPHAMIN	PHIMIN

FILE: LO 1 A1 VM/SP CONVERSATIONAL MONITOR SYSTEM

0.0500	0.0500	48.1414	1.0000	3.5000	18.1949
0.1000	0.1000	69.9630	1.0000	4.5000	25.8419
0.1714	0.1500	83.2612	0.7000	6.0000	31.7883
0.2548	0.2000	88.6253	0.6000	9.0000	36.8699
0.3381	0.2500	90.9107	0.6000	9.0000	41.4096
0.4381	0.3000	92.7598	0.5000	13.0000	45.5730
0.5381	0.3500	93.5743	0.5000	13.0000	49.4584
0.6631	0.4000	93.4010	0.4000	17.5000	53.1301
0.7881	0.4500	92.1173	0.4000	17.5000	56.6330
0.9548	0.5000	89.3903	0.3000	23.0000	58.0509
1.2048	0.5500	87.3691	0.2000	30.0000	56.2310
1.7048	0.6000	84.2170	0.1000	37.5000	53.4179
2.2048	0.6500	79.7633	0.1000	37.0000	49.5376
2.7048	0.7000	75.2582	0.1000	36.5000	46.1763
3.2048	0.7500	70.8180	0.1000	35.5000	40.7316
3.7048	0.8000	66.2765	0.1000	34.5000	35.3877
4.2048	0.8500	61.5696	0.1000	33.5000	32.8775
4.7048	0.9000	57.2651	0.1000	31.5000	27.3512
5.2048	0.9500	53.1166	0.1000	29.0000	22.3714
0.0	1.0000	48.5240	0.0	2.0000	0.1923

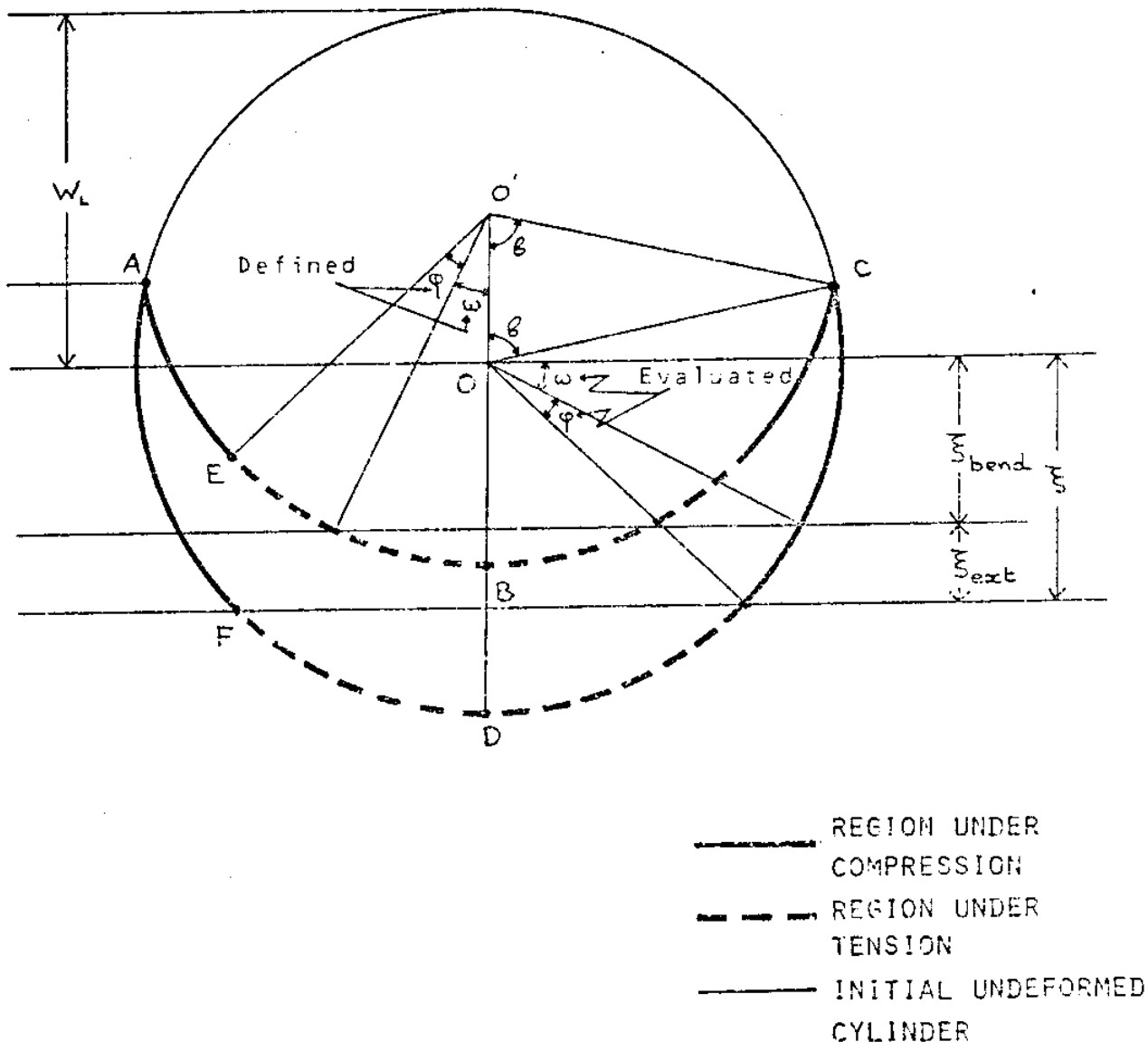
W_L
O'
A
C
Defined
φ
ω
β
β
O
ω
Evaluated
φ
E
ξ_{bend}
ξ
ξ_{ext}
B
F
D
REGION UNDER COMPRESSION
REGION UNDER TENSION
INITIAL UNDEFORMED CYLINDER

FIGURE B1

APPENDIX C

C.1 Method for Combining in Series two Non-Linear Springs which are Given by Force-Deflection Curves Consisting of Linear Segments

The basic idea used is that for each force level, the combined deflection of the springs is given by the sum of the deflection of each individual spring under that force level. Fig. C1 shows parts of the piecewise linear characteristics of the two springs (1 and 2) to be combined. Then, we have the following general expression of combined deflection vs. force:

$$\delta_c = F_c \left[\frac{({}_i\delta_1 - {}_{i-1}\delta_1)}{({}_iF_1 - {}_{i-1}F_1)} + \frac{({}_j\delta_2 - {}_{j-1}\delta_2)}{({}_jF_2 - {}_{j-1}F_2)} \right] + {}_{i-1}\delta_1 + {}_{j-1}\delta_2 \qquad \text{(C1)}$$

for ${}_{i-1}F_1 \leq F_c \leq {}_iF_1$ (C2a)

${}_{j-1}F_2 \leq F_c \leq {}_jF_2$ (C2b)

${}_iF_1 - {}_{i-1}F_1 > 0$ (C2c)

${}_jF_1 - {}_{j-1}F_1 > 0$

The expression for δ_c changes only at points of slope discontinuity of either curve (i.e. at A, B, C, and D in Fig. C1). Thus, we calculate δ_c only at these points, and the combined force-deflection curve consists of linear segments in between these calculated points (see Fig. C2).

In the case where the slope of one or more of the linear segments is negative the above procedure is slightly altered. Since it would be easier to explain we will use an example. In Fig. C3, A is a local peak on the spring load-deflection curve (I). The combined spring's reaction has also a local peak at point A where the combined deflection is $(\delta_c)_A = \delta_A + \delta_p$. Since we have plastic

deformation, when the load level drops (past A) the deformation of the spring (II) remains constant, δ_p. Thus, at point B we have for a force level F_B a combined deflection $(\delta_c)_B = \delta_B + \delta_p$. The deformation of spring (II) starts increasing again at point A' where $(\delta_c)_{A'} = \delta_{A'} + \delta_p$ After we have reached again a force level equal to the local maximum at A (i.e. ptA') we can proceed as discussed in the previous paragraph using equation (C1).

C.2 Calculation of the Initial Critical Time Step

To calculate the initial critical time step we need to have the natural periods of the dynamic system. Since the system is non-linear we cannot really talk about natural periods for that system. Instead, we should calculate the natural periods of the linearized sytem. We define the linearized stiffnesses as follows:

$$k_1 = \left.\frac{dF_1}{d\delta_1}\right|_{\delta_1=\pm 0} \tag{C.3a}$$

$$k_2 = \left.\frac{dF_2}{d\delta_2}\right|_{\delta_2=\pm 0} \tag{C.3b}$$

$$k = \left.\frac{dF_R}{dx}\right|_{x=\pm 0}$$

For two linear springs in series we have:

$$K = \frac{k_1 k_2}{k_1 + k_2} \tag{C.4}$$

The linearized system can be written as follows:

$$m_1\ddot{x}_1 + K\cdot(x_1 - x) = 0$$

$$m_2\ddot{x} - K\cdot(x_1 - x) + kx = 0$$

Or, in a matrix form:

$$\begin{bmatrix} m_1 & \\ & m_2 \end{bmatrix} \begin{bmatrix} x_1 \\ x \end{bmatrix} + \begin{bmatrix} K & -K \\ -K & k+K \end{bmatrix} \begin{bmatrix} x_1 \\ x \end{bmatrix} = \begin{bmatrix} 0 \\ 0 \end{bmatrix} \qquad \text{(C.5a,b)}$$

The natural frequencies are the roots of the quadratic equation:

$$(-m_1\omega^2 + K)(-m_2\omega^2 + k + K) - K^2 = 0$$

$$\text{or } (m_1 m_2)\omega^4 - [m_1(k + K) + m_2 K]\omega^2 + Kk = 0$$

After solving for ω and simplifying we obtain:

$$\omega = \sqrt{\frac{1}{2}\left\{\left(\frac{K}{m_1}\right) + \left(\frac{k+K}{m_2}\right) \pm \sqrt{\left(\frac{K}{m_1}\right)^2 + \left(\frac{k+K}{m_2}\right)^2 + 2\left(\frac{K}{m_1}\right)\left(\frac{k+K}{m_2}\right) - 4\left[\left(\frac{K}{m_1}\right)\left(\frac{k+K}{m_2}\right) - \frac{K^2}{m_1 m_2}\right]}\right\}} \qquad \text{(C.6)}$$

Since $T_{cr} = \frac{T_{min}}{\pi}$ we obtain the following expression for the initial critical time step.

$$\Delta t_{cr} = \frac{2\sqrt{2}}{\sqrt{\left(\frac{K}{m_1}\right) + \left(\frac{k+K}{m_2}\right) \pm \sqrt{\left(\frac{K}{m_1}\right)^2 + \left(\frac{k+K}{m_2}\right) + 2\left(\frac{K}{m_1}\right)\left(\frac{K-k}{m_2}\right)}}} \qquad \text{(C.7)}$$

C.3 Calculation of the Equivalent Mass and Added Mass of a Bottom-Supported Structure

Let the structure have a moment of inertia about its bottom support point of I and a hydrodynamic added inertia about the same point of I_A. Also, let the depth of water where the platform is installed be H_w (see Fig. C4).

Then, the equivalent mass of the structure can be taken as a lumped mass at the waterline level. So we have:

$$M_E = \frac{I+I_A}{H_w^{\ 2}}$$

If we know separately the mass of the jacket and the mass of the deck (usually a significant percentage of the total mass) as well as the deck level from the waterline we can estimate I. We need to assume that the distribution of mass of the jacket is uniform over its length. Then, we obtain for the equivalent mass:

$$M_E = \frac{(H_D+H_w)^2(M_D+\frac{1}{3}M_J)+I_A}{H_w^{\ 2}} \qquad (C.8)$$

where H_D: distance of the deck from the waterline

H_w: water depth

M_D: mass of the deck

M_J: mass of the jacket

I_A: jacket's added moment of inertia

C.4 Listing of the Program Used for the Solution of the Differential Equations of Motion Characterizing the Collision

Symbol Explanation :

FA(1,I),D(1,I) ..... Ship's Load-Deflection Characteristics

FA(2,I),D(2,I) ...Platform's Load-Deflection Characteristics

FR(I),XR(I) ... Foundation's Load-Deflection Characteristics

F(J),XC(J)...Combined Ship's and Platform's Load-Deflection Characteristics

DTCR ..... Critical Timestep

X1 ..... Deflection of the Ship's Center of Gravity

X2 ..... Deflection of the Platform's Center of gravity

M1 ..... Ship's Mass

M2 ..... Platform's Mass

```
      IMPLICIT REAL*8(A-H,O-Z)
      REAL*8 M1,M2,KM1,KM2,KS,KS2
      DIMENSION FA(2,50),D(2,50),FR(50),XR(50),F(100),XC(100),X(36000),
     +X2(36000),INDI(100),INDJ(100)
C READ FORCE-DEFLECTION DATA: SHIP,PLATFORM LOCAL,PLATFORM GLOBAL
      READ(2,100)N1,N2,N3
  100 FORMAT(3I5)
      N=N1
      IF(N2.GT.N)N=N2
      IF(N3.GT.N)N=N3
      WRITE(5,222)
  222 FORMAT(' ENTER 1 FOR SEPARATE PLASTIC STIFFNESSES' INPUT'/7X,
     +'0 OTHERWISE')
      READ(5,*)IRD
      IF(IRD.EQ.1)GO TO 25
      READ(2,223)((XC(I),F(I),XR(I),FR(I)),I=1,N)
  223 FORMAT(2(F10.4,F10.3,5X))
      GO TO 8
   25 DO 1 I=1,N
      READ(2,101)D(1,I),FA(1,I),D(2,I),FA(2,I),XR(I),FR(I)
  101 FORMAT(3(F10.4,F10.3,5X))
    1 CONTINUE
      WRITE(6,221)
  221 FORMAT(//'INPUT SPRING DATA')
      WRITE(6,220)N1,N2,N3,((FA(1,I),D(1,I),FA(2,I),D(2,I),FR(I),XR(I)),
     +I=1,N)
  220 FORMAT(/3I5/(3(F10.3,F10.4,5X)))
C CALCULATE FORCE-DEFLECTION PAIRS FOR COMBINED LOCAL
C SHIP-PLATFORM SPRING
      CALL SORT(FA,D,N1,N2,F,XC,INDI,INDJ)
      NT=N1+N2
      CALL COMBIN(F,XC,INDI,INDJ,FA,D,N1,N2,NPT)
      CALL OUT1(F,XC,INDI,INDJ,NPT)
    8 WRITE(5,200)
  200 FORMAT(/' ENTER MASSES: SHIP, PLATFORM')
      READ(5,*)M1,M2
      IF(IPER.EQ.1)GO TO 10
      XI=XC(2)
      IF(XR(2).LT.XI)XI=XR(2)
      XIH=XI/2.
      CALL INTERP(F,XC,NPT,XIH,FI,KS)
      CALL INTERP(FR,XR,N3,XIH,F2I,KS2)
      KM1=KS/M1
      KM2=(KS+KS2)/M2
      A1=DSQRT(KM1**2+KM2**2+2.*KM1*(KS-KS2)/M2)
      PI=3.141592654
      T1=2.8284271*PI/DSQRT(KM1+KM2+A1)
      T2=2.8284271*PI/DSQRT(KM1+KM2-A1)
      WRITE(5,205)T1,T2
  205 FORMAT(//'NATURAL PERIODS :',5X,'T1 =',F10.5,5X,'T2 =',F10.5//
     +'ENTER 1 FOR A NEW PLATFORM MASS, 0 TO CONTINUE')
      WRITE(6,209)T1,T2
  209 FORMAT(//'NATURAL PERIODS :  T1=',F10.5,'  T2=',F10.5)
      READ(5,*)IPER
      IF(IPER.EQ.1)GO TO 8
```

```
      WRITE(6,231)M1,M2
  231 FORMAT(//'M1=',F10.4,5X,'M2=',F10.4)
    7 WRITE(5,201)
  201 FORMAT(' ENTER SHIP'S INITIAL CONDITIONS: VELOCITY, ACCELERATION')
      READ(5,*)VO,AO
      WRITE(6,232)VO,AO
  232 FORMAT(//'INITIAL VELOCITY=',F10.4,5X,'INITIAL ACCELERATION=',F10
     +.4)
    6 WRITE(5,202)
  202 FORMAT(' ENTER TIME INTERVAL, PRINT INTERVAL, AND XMAX')
      READ(5,*)DT,NI2,XMAX
      WRITE(6,230)DT
  230 FORMAT(//'DT=',F10.7)
      WRITE(6,204)
  204 FORMAT(///8X,'TIME',10X,'X(SHIP)',10X,'X(PLATF)',7X,
     +'CONTACT FORCE',4X,'FOUNDATION REACTION',9X,'DTCR',9X,'T2'/)
      WRITE(5,204)
C INITIALISE X(-DT),X2(-DT)
      X(2)=0.
      V2=VO
      A2 =AO
      X2(2)=0.
      X(1)=X(2)-DT*V2+DT**2/2.*A2
      X2(1)=0.
C ITERATE FOR X(T+DT), X2(T+DT)
      IP=0
      DO 2 J=2,36000
      IF(X(J).GT.XMAX.OR.X2(J).GT.XMAX)GO TO 20
      XI=X(J)
      X2I=X2(J)
      CALL INTERP(FR,XR,N3,X2I,F2I,KS2)
      CALL INTERP(F,XC,NFT,XI,FI,KS)
      IF(KS.GT.0.01.AND.KS2.GT.0.01)GO TO 15
      DTCR=0.0
      T2=0.0
      GO TO 16
   15 KM1=KS/M1
      KM2=(KS+KS2)/M2
      A1=DSQRT(KM1**2+KM2**2+2.*KM1*(KS-KS2)/M2)
      DTCR=2.8284271/DSQRT(KM1+KM2+A1)
      T2=2.8284271*PI/DSQRT(KM1+KM2-A1)
   16 X2(J+1)=DT**2/M2*(FI-F2I)+2.*X2(J)-X2(J-1)
      X(J+1)=DT**2/M2*F2I-(1./M1+1./M2)*DT**2*FI+2.*X(J)-X(J-1)
      T=DFLOAT(J-2)*DT
      X1=X2(J+1)+X(J+1)
      X2J=X2(J+1)
      IF(X(J+1).LT.X(J))ISTOP=1
      IF(IP NE.NI2)GO TO 5
      IP=0
      WRITE(6,203)T,X1,X2J,FI,F2I,DTCR,T2
  203 FORMAT(5X,F10.7,5X,2(F10.3,5X),5X,2(F10.3,10X),F10.4,5X,F10.4)
      WRITE(5,203)T,X1,X2J,FI,F2I,DTCR
      IF(ISTOP.EQ.1)GO TO 12
    5 IP=IP+1
    2 CONTINUE
```

```
      IF(J.EQ.36000)GO TO 11
   12 WRITE(5,210)
  210 FORMAT(///'NEGATIVE D(X1-X2) REACHED')
      WRITE(6,210)
   11 WRITE(5,206)
  206 FORMAT(/'ENTER : 1 FOR NEW TIMESTEP'/8X,'2 FOR NEW INITIAL CONDITI
     +ONS'/8X,'3 FOR NEW MASSES'/8X,'0 TO STOP')
      READ(5,*)NO
      ISTOP=0
      IF(NO.EQ.0)STOP
      IF(NO.EQ.1)GO TO 6
      IF(NO.EQ.2)GO TO 7
      IF(NO.EQ.3)GO TO 8
   20 WRITE(5,207)
  207 FORMAT(///'XMAX HAS BEEN REACHED. ENTER 1 FOR A NEW XMAX, 0 TO STOP
     +')
      READ(5,*)IMAX
      IF(IMAX.EQ.1)GO TO 6
      STOP
      END
      SUBROUTINE SORT(FA,D,N1,N2,F,X,INDI,INDJ)
      IMPLICIT REAL*8(A-H,O-Z)
      DIMENSION FA(2,50),D(2,50),F(100),X(100),INDI(100),INDJ(100)
C COMBINE FA(I,J) IN A SINGLE ARRAY F(IC)
      IC=2
      N=N1
      DO 3 I=1,2
      IF(I.EQ.2)N=N2
      DO 3 J=2,N
      IC=IC+1
      F(IC)=FA(I,J)
      INDI(IC)=I
      INDJ(IC)=J
      X(IC)=D(I,J)
    3 CONTINUE
C SORT F(IC) IN AN ASCENDING ORDER
      N=N1+N2
      NM1=N-1
      DO 4 I=3,NM1
      IP1=I+1
      DO 4 J=IP1,N
      IF(F(I).LE.F(J))GO TO 5
    6 FSV=F(I)
      XSV=X(I)
      ISV=INDI(I)
      JSV=INDJ(I)
      F(I)=F(J)
      X(I)=X(J)
      INDI(I)=INDI(J)
      INDJ(I)=INDJ(J)
      F(J)=FSV
      X(J)=XSV
      INDI(J)=ISV
      INDJ(J)=JSV
      GO TO 4
```

```
    5 IF(F(I).EQ.F(J).AND.X(I).GT.X(J))GO TO 6
    4 CONTINUE
      F(1)=0.
      X(1)=0.
      INDI(1)=1
      INDJ(1)=1
      F(2)=0.
      X(2)=0.
      INDI(2)=2
      INDJ(2)=1
      RETURN
      END
      SUBROUTINE COMBIN(F,X,I,J,FA,D,N1,N2,NPT)
      IMPLICIT REAL*8(A-H,O-Z)
      DIMENSION F(100),X(100),I(100),J(100),FA(2,50),D(2,50)
      NPT=0
      NS=N1+N2
      DO 1 M=3,NS
      MM1=M-1
      IF(I(M).EQ.1.AND.J(M).EQ.N1.OR.I(M).EQ.2.AND.J(M).EQ.N2)NPT=MM1
      IND=M
    3 IND=IND+1
      IF(I(IND).EQ.(3-I(M)))GO TO 2
      GO TO 3
    2 CONTINUE
      SL=(D(I(IND),J(IND))-D(I(IND),(J(IND)-1)))/
     +(FA(I(IND),J(IND))-FA(I(IND),(J(IND)-1)))
      X(MM1)=X(M)+D(I(IND),(J(IND)-1))+(F(M)-FA(I(IND),(J(IND)-1)))*SL
      F(MM1)=F(M)
      IF(NPT.EQ.MM1)GO TO 4
      A=FA(I(IND),(J(IND)+1))-FA(I(IND),J(IND))
      B=FA(I(M),(J(M)+1))-FA(I(M),J(M))
      IF(B.EQ.0..OR.F(M).EQ.F(IND).AND.A.EQ.0.)GO TO 4
      GO TO 1
    4 X(M)=D(1,N1)+D(2,N2)
      F(M)=F(M+1)
      GO TO 10
    1 CONTINUE
   10 X(1)=0.
      IF(NPT.NE.MM1)NPT=M
      RETURN
      END
      SUBROUTINE INTERP(F,X,N,XI,FI,KS)
      IMPLICIT REAL*8(A-H,O-Z)
      REAL*8 KS
      DIMENSION F(100),X(100)
      DO 1 I=2,N
      IF(X(I).GT.XI)GO TO 2
    1 CONTINUE
    2 KS=(F(I)-F(I-1))/(X(I)-X(I-1))
      FI=F(I-1)+KS*(XI-X(I-1))
      RETURN
      END
      SUBROUTINE OUT1(F,X,I,J,N)
      IMPLICIT REAL*8(A-H,O-Z)
      DIMENSION F(100),X(100),I(100),J(100)
      WRITE(6,211)
  211 FORMAT(///'CONTACT FORCE'S FORCE-DEFLECTION CHARACTERISTICS'
     +/' CONTACT FORCE',7X,'PLASTIC DEFORM.',8X,'I',8X,'J'/)
      WRITE(6,212)((F(K),X(K),I(K+1),J(K+1)),K=1,N)
  212 FORMAT(2X,F10.3,10X,F10.3,8X,I2,8X,I2)
      RETURN
      END
```

C.5 Complete Numerical Results

Semisubmersible: Collision Scenario (i)

NATURAL PERIODS : T1= 5.12429 T2= 159.91882

M1= 5.5000 M2= 28.0000

INITIAL VELOCITY= 2.0000 INITIAL ACCELERATION= 0.0

DT= 0.0010000

TIME	X(SHIP)	X(PLATF)	CONTACT FORCE	FOUNDATION REACTION
0.0500000	0.102	0.000	0.691	0.000
0.1000000	0.202	0.000	1.379	0.000
0.1500000	0.301	0.000	2.061	0.000
0.2000000	0.399	0.001	2.736	0.000
0.2500000	0.495	0.001	3.401	0.000
0.3000000	0.591	0.002	3.872	0.000
0.3500000	0.684	0.004	4.280	0.000
0.4000000	0.776	0.005	4.677	0.000
0.4500000	0.865	0.007	5.063	0.000
0.5000000	0.952	0.010	5.437	0.001
0.5500000	1.037	0.013	5.777	0.001
0.6000000	1.119	0.016	5.974	0.001
0.6500000	1.198	0.020	6.163	0.001
0.7000000	1.275	0.025	6.343	0.001
0.7500000	1.348	0.030	6.514	0.002
0.8000000	1.419	0.036	6.677	0.002
0.8500000	1.487	0.042	6.831	0.002
0.9000000	1.551	0.049	6.975	0.003
0.9500000	1.612	0.057	7.110	0.003
1.0000000	1.671	0.065	7.235	0.003
1.0500000	1.725	0.074	7.337	0.004
1.1000000	1.777	0.084	7.373	0.004
1.1500000	1.825	0.094	7.405	0.005
1.2000000	1.870	0.105	7.434	0.005
1.2500000	1.911	0.116	7.460	0.006
1.3000000	1.949	0.128	7.482	0.007
1.3500000	1.984	0.141	7.500	0.007
1.4000000	2.015	0.155	7.516	0.008
1.4500000	2.043	0.169	7.527	0.009
1.5000000	2.067	0.184	7.535	0.009
1.5500000	2.085	0.199	7.540	0.010
1.6000000	2.105	0.215	7.541	0.011

Semisubmersible: Collision Scenario (ii)

NATURAL PERIODS : T1= 4.76792 T2= 159.91665

M1= 5.5000 M2= 28.0000

INITIAL VELOCITY= 2.0000 INITIAL ACCELERATION= 0.0

DT= 0.0010000

TIME	X(SHIP)	X(PLATF)	CONTACT FORCE	FOUNDATION REACTION
0.0500000	0.102	0.000	0.798	0.000
0.1000000	0.202	0.000	1.592	0.000
0.1500000	0.300	0.000	2.379	0.000
0.2000000	0.398	0.001	3.156	0.000
0.2500000	0.494	0.001	3.919	0.000
0.3000000	0.589	0.003	4.665	0.000
0.3500000	0.681	0.004	5.391	0.000
0.4000000	0.771	0.006	6.094	0.000
0.4500000	0.858	0.009	6.717	0.000
0.5000000	0.943	0.012	7.271	0.001
0.5500000	1.023	0.015	7.798	0.001
0.6000000	1.101	0.020	8.297	0.001
0.6500000	1.174	0.025	8.764	0.001
0.7000000	1.244	0.031	9.199	0.002
0.7500000	1.309	0.038	9.599	0.002
0.8000000	1.370	0.046	9.964	0.002
0.8500000	1.426	0.054	10.292	0.003
0.9000000	1.478	0.064	10.582	0.003
0.9500000	1.525	0.074	10.832	0.004
1.0000000	1.567	0.085	11.042	0.004
1.0500000	1.604	0.098	11.211	0.005
1.1000000	1.636	0.111	11.339	0.006
1.1500000	1.662	0.126	11.424	0.006
1.2000000	1.684	0.141	11.466	0.007
1.2500000	1.700	0.157	11.467	0.008

Semisubmersible: Collision Scenario (iii)

NATURAL PERIODS : T1= 5.98747 T2= 159.92472

M1= 5.5000 M2= 28.0000

INITIAL VELOCITY= 2.0000 INITIAL ACCELERATION= 0.0

DT= 0.0050000

TIME	X(SHIP)	X(PLATF)	CONTACT FORCE	FOUNDATION REACTION
0.0500000	0.110	0.000	0.506	0.000
0.1000000	0.210	0.000	1.010	0.000
0.1500000	0.309	0.000	1.512	0.000
0.2000000	0.407	0.001	2.010	0.000
0.2500000	0.505	0.001	2.502	0.000
0.3000000	0.601	0.002	2.987	0.000
0.3500000	0.696	0.003	3.464	0.000
0.4000000	0.790	0.004	3.931	0.000
0.4500000	0.881	0.006	4.387	0.000
0.5000000	0.971	0.008	4.832	0.000
0.5500000	1.058	0.010	5.263	0.001
0.6000000	1.143	0.013	5.680	0.001
0.6500000	1.226	0.017	6.081	0.001
0.7000000	1.305	0.021	6.459	0.001
0.7500000	1.382	0.025	6.790	0.001
0.8000000	1.456	0.030	7.105	0.002
0.8500000	1.526	0.036	7.402	0.002
0.9000000	1.593	0.043	7.600	0.002
0.9500000	1.656	0.050	7.939	0.003
1.0000000	1.716	0.058	8.179	0.003
1.0500000	1.772	0.066	8.398	0.003
1.1000000	1.824	0.076	8.597	0.004
1.1500000	1.873	0.086	8.774	0.004
1.2000000	1.917	0.097	8.929	0.005
1.2500000	1.957	0.109	9.062	0.006
1.3000000	1.994	0.121	9.172	0.006
1.3500000	2.026	0.134	9.260	0.007
1.4000000	2.053	0.149	9.324	0.008
1.4500000	2.077	0.164	9.365	0.009
1.5000000	2.096	0.179	9.383	0.009
1.5500000	2.111	0.196	9.378	0.010

Semisubmersible: Collision Scenario (iv)

NATURAL PERIODS : T1= 6.27490 T2= 159.92690

M1= 5.5000 M2= 28.0000

INITIAL VELOCITY= 2.0000 INITIAL ACCELERATION= 0.0

DT= 0.0500000

TIME	X(SHIP)	X(PLATF)	CONTACT FORCE	FOUNDATION REACTION
0.0500000	0.200	0.000	0.461	0.0
0.1000000	0.299	0.000	0.920	0.000
0.1500000	0.398	0.000	1.378	0.000
0.2000000	0.496	0.001	1.832	0.000
0.2500000	0.593	0.001	2.281	0.000
0.3000000	0.688	0.002	2.724	0.000
0.3500000	0.783	0.003	3.161	0.000
0.4000000	0.875	0.005	3.579	0.000
0.4500000	0.966	0.007	3.884	0.000
0.5000000	1.055	0.009	4.182	0.000
0.5500000	1.142	0.011	4.473	0.000
0.6000000	1.226	0.014	4.755	0.001
0.6500000	1.309	0.018	5.029	0.001
0.7000000	1.389	0.022	5.293	0.001
0.7500000	1.466	0.026	5.546	0.001
0.8000000	1.541	0.031	5.777	0.001
0.8500000	1.613	0.037	5.925	0.002
0.9000000	1.683	0.043	6.067	0.002
0.9500000	1.749	0.049	6.201	0.002
1.0000000	1.813	0.056	6.329	0.003
1.0500000	1.874	0.064	6.449	0.003
1.1000000	1.932	0.072	6.561	0.003
1.1500000	1.987	0.081	6.660	0.004
1.2000000	2.038	0.091	6.764	0.004
1.2500000	2.087	0.101	6.853	0.005
1.3000000	2.132	0.111	6.935	0.005
1.3500000	2.175	0.123	7.003	0.006
1.4000000	2.214	0.135	7.074	0.006
1.4500000	2.249	0.147	7.132	0.007
1.5000000	2.282	0.161	7.181	0.008
1.5500000	2.311	0.175	7.222	0.008
1.6000000	2.337	0.189	7.254	0.009
1.6500000	2.360	0.204	7.278	0.010
1.7000000	2.379	0.220	7.294	0.011
1.7500000	2.395	0.237	7.302	0.011

Semisubmersible: Collision Scenario (v)

NATURAL PERIODS : T1= 2.49349 T2= 163.44814

M1= 7.0000 M2= 28.0000

INITIAL VELOCITY= 2.0000 INITIAL ACCELERATION= 0.0

DT= 0.0005000

TIME	X(SHIP)	X(PLATF)	CONTACT FORCE	FOUNDATION REACTION
0.0500000	0.101	0.000	3.546	0.000
0.1000000	0.199	0.000	6.767	0.000
0.1500000	0.295	0.001	8.723	0.000
0.2000000	0.388	0.003	10.598	0.000
0.2500000	0.478	0.006	12.377	0.000
0.3000000	0.562	0.010	14.021	0.000
0.3500000	0.642	0.015	14.786	0.001
0.4000000	0.717	0.021	15.484	0.001
0.4500000	0.786	0.029	16.111	0.001
0.5000000	0.849	0.038	16.664	0.002
0.5500000	0.906	0.049	17.142	0.003
0.6000000	0.958	0.061	17.541	0.003
0.6500000	1.003	0.075	17.861	0.004
0.7000000	1.041	0.090	18.099	0.005
0.7500000	1.073	0.107	18.254	0.006
0.8000000	1.099	0.126	18.326	0.006
0.8500000	1.118	0.146	18.315	0.008

Semisubmersible: Collision Scenario (vi)

NATURAL PERIODS : T1= 2.55377 T2= 159.90668

M1= 5.5000 M2= 28.0000

INITIAL VELOCITY= 2.0000 INITIAL ACCELERATION= 0.0

DT= 0.0005000

TIME	X(SHIP)	X(PLATF)	CONTACT FORCE	FOUNDATION REACTION
0.0500000	0.101	0.000	2.776	0.000
0.1000000	0.199	0.000	5.509	0.000
0.1500000	0.295	0.001	7.518	0.000
0.2000000	0.388	0.003	9.130	0.000
0.2500000	0.476	0.005	10.654	0.000
0.3000000	0.560	0.008	12.076	0.000
0.3500000	0.638	0.012	13.382	0.001
0.4000000	0.710	0.018	14.239	0.001
0.4500000	0.776	0.025	14.683	0.001
0.5000000	0.835	0.033	15.067	0.002
0.5500000	0.887	0.042	15.339	0.002
0.6000000	0.932	0.053	15.648	0.003
0.6500000	0.970	0.065	15.843	0.003
0.7000000	1.000	0.079	15.973	0.004
0.7500000	1.024	0.094	16.037	0.005
0.8000000	1.040	0.110	16.036	0.006

Fixed Jacket: Collision Scenario (i)

NATURAL PERIODS : T1= 1.11995 T2= 5.62572

M1= 5.5000 M2= 32.0000

INITIAL VELOCITY= 2.0000 INITIAL ACCELERATION= 0.0

DT= 0.0010000

TIME	X(SHIP)	X(PLATF)	CONTACT FORCE	FOUNDATION REACTION
0.0500000	0.102	0.000	0.691	0.009
0.1000000	0.202	0.000	1.379	0.071
0.1500000	0.301	0.000	2.062	0.234
0.2000000	0.399	0.001	2.737	0.539
0.2500000	0.495	0.001	3.403	1.015
0.3000000	0.591	0.002	3.874	1.674
0.3500000	0.684	0.003	4.284	2.505
0.4000000	0.776	0.003	4.684	3.473
0.4500000	0.865	0.005	5.075	4.535
0.5000000	0.952	0.006	5.455	5.639
0.5500000	1.037	0.007	5.792	6.729
0.6000000	1.119	0.008	5.995	7.745
0.6500000	1.198	0.009	6.192	8.625
0.7000000	1.275	0.009	6.332	9.316
0.7500000	1.348	0.010	6.565	9.779
0.8000000	1.419	0.010	6.741	9.993
0.8500000	1.486	0.010	6.910	9.954
0.9000000	1.550	0.010	7.072	9.680
0.9500000	1.612	0.009	7.227	9.202
1.0000000	1.669	0.009	7.345	8.571
1.0500000	1.724	0.008	7.392	7.845
1.1000000	1.775	0.007	7.436	7.084
1.1500000	1.823	0.006	7.478	6.349
1.2000000	1.867	0.006	7.516	5.703
1.2500000	1.908	0.005	7.552	5.197
1.3000000	1.946	0.005	7.584	4.874
1.3500000	1.980	0.005	7.613	4.761
1.4000000	2.010	0.005	7.639	4.869
1.4500000	2.038	0.005	7.662	5.193
1.5000000	2.061	0.006	7.682	5.708
1.5500000	2.081	0.006	7.699	6.377
1.6000000	2.098	0.007	7.712	7.147
1.6500000	2.111	0.008	7.723	7.962
1.7000000	2.121	0.009	7.730	8.758
1.7500000	2.127	0.009	7.735	9.475
1.8000000	2.130	0.010	7.737	10.056
1.8500000	2.129	0.010	7.736	10.457

Fixed Jacket: Collision Scenario (ii)

NATURAL PERIODS : T1= 1.11930 T2= 5.23745

M1= 5.5000 M2= 32.0000

INITIAL VELOCITY= 2.0000 INITIAL ACCELERATION= 0.0

DT= 0.0010000

TIME	X(SHIP)	X(PLATF)	CONTACT FORCE	FOUNDATION REACTION
0.0500000	0.102	0.000	0.798	0.010
0.1000000	0.202	0.000	1.592	0.082
0.1500000	0.300	0.000	2.379	0.270
0.2000000	0.398	0.001	3.157	0.623
0.2500000	0.494	0.001	3.922	1.171
0.3000000	0.589	0.002	4.670	1.934
0.3500000	0.681	0.003	5.400	2.908
0.4000000	0.771	0.004	6.109	4.076
0.4500000	0.858	0.005	6.738	5.401
0.5000000	0.942	0.007	7.304	6.830
0.5500000	1.023	0.008	7.846	8.295
0.6000000	1.100	0.010	8.365	9.726
0.6500000	1.174	0.011	8.858	11.050
0.7000000	1.243	0.012	9.325	12.204
0.7500000	1.308	0.013	9.764	13.135
0.8000000	1.369	0.014	10.175	13.804
0.8500000	1.425	0.014	10.556	14.190
0.9000000	1.476	0.014	10.906	14.295
0.9500000	1.522	0.014	11.225	14.136
1.0000000	1.564	0.014	11.510	13.752
1.0500000	1.600	0.013	11.760	13.192
1.1000000	1.630	0.013	11.974	12.523
1.1500000	1.655	0.012	12.152	11.809
1.2000000	1.675	0.011	12.292	11.122
1.2500000	1.689	0.011	12.395	10.526
1.3000000	1.697	0.010	12.454	10.074
1.3500000	1.700	0.010	12.475	9.807
1.4000000	1.697	0.010	12.457	9.746

Fixed Jacket: Collision Scenario (iii)

NATURAL PERIODS : T1= 1.12105 T2= 6.56714

M1= 5.5000 M2= 32.0000

INITIAL VELOCITY= 2.0000 INITIAL ACCELERATION= 0.0

DT= 0.0010000

TIME	X(SHIP)	X(PLATF)	CONTACT FORCE	FOUNDATION REACTION
0.0500000	0.102	0.000	0.506	0.007
0.1000000	0.202	0.000	1.010	0.052
0.1500000	0.301	0.000	1.512	0.172
0.2000000	0.400	0.000	2.010	0.395
0.2500000	0.497	0.001	2.503	0.744
0.3000000	0.594	0.001	2.989	1.230
0.3500000	0.689	0.002	3.467	1.852
0.4000000	0.782	0.003	3.937	2.599
0.4500000	0.874	0.003	4.397	3.450
0.5000000	0.964	0.004	4.847	4.374
0.5500000	1.051	0.005	5.286	5.336
0.6000000	1.137	0.006	5.712	6.293
0.6500000	1.219	0.007	6.126	7.205
0.7000000	1.299	0.008	6.513	8.033
0.7500000	1.376	0.009	6.862	8.743
0.8000000	1.449	0.009	7.197	9.307
0.8500000	1.520	0.010	7.517	9.707
0.9000000	1.587	0.010	7.823	9.937
0.9500000	1.650	0.010	8.113	10.003
1.0000000	1.710	0.010	8.388	9.922
1.0500000	1.766	0.010	8.645	9.722
1.1000000	1.818	0.009	8.884	9.438
1.1500000	1.866	0.009	9.106	9.111
1.2000000	1.910	0.009	9.308	8.783
1.2500000	1.949	0.008	9.491	8.497
1.3000000	1.985	0.008	9.654	8.287
1.3500000	2.016	0.008	9.796	8.183
1.4000000	2.042	0.008	9.917	8.204
1.4500000	2.064	0.008	10.017	8.358
1.5000000	2.081	0.009	10.096	8.641
1.5500000	2.094	0.009	10.153	9.036
1.6000000	2.102	0.010	10.188	9.518
1.6500000	2.106	0.010	10.202	10.052
1.7000000	2.105	0.011	10.195	10.597

Fixed Jacket: Collision Scenario (iv)

NATURAL PERIODS : T1= 1.12132 T2= 6.88085

M1= 5.5000 M2= 32.0000

INITIAL VELOCITY= 2.0000 INITIAL ACCELERATION= 0.0

DT= 0.0010000

TIME	X(SHIP)	X(PLATF)	CONTACT FORCE	FOUNDATION REACTION
0.0500000	0.102	0.000	0.461	0.006
0.1000000	0.202	0.000	0.920	0.047
0.1500000	0.301	0.000	1.377	0.156
0.2000000	0.400	0.000	1.831	0.360
0.2500000	0.498	0.001	2.281	0.678
0.3000000	0.594	0.001	2.725	1.120
0.3500000	0.690	0.002	3.163	1.687
0.4000000	0.784	0.002	3.592	2.368
0.4500000	0.877	0.003	3.889	3.143
0.5000000	0.967	0.004	4.190	3.975
0.5500000	1.056	0.005	4.485	4.824
0.6000000	1.143	0.006	4.773	5.646
0.6500000	1.228	0.006	5.054	6.401
0.7000000	1.310	0.007	5.328	7.051
0.7500000	1.390	0.008	5.594	7.563
0.8000000	1.467	0.008	5.915	7.931
0.8500000	1.542	0.008	5.973	8.129
0.9000000	1.614	0.008	6.125	8.160
0.9500000	1.683	0.008	6.270	8.033
1.0000000	1.749	0.008	6.414	7.770
1.0500000	1.813	0.007	6.549	7.401
1.1000000	1.873	0.007	6.679	6.966
1.1500000	1.931	0.006	6.802	6.508
1.2000000	1.985	0.006	6.918	6.074
1.2500000	2.036	0.006	7.027	5.705
1.3000000	2.084	0.005	7.130	5.438
1.3500000	2.129	0.005	7.225	5.303
1.4000000	2.171	0.005	7.313	5.317
1.4500000	2.209	0.005	7.394	5.485
1.5000000	2.243	0.006	7.382	5.799
1.5500000	2.275	0.006	7.407	6.235
1.6000000	2.303	0.007	7.429	6.762
1.6500000	2.328	0.007	7.449	7.341
1.7000000	2.349	0.008	7.465	7.929
1.7500000	2.367	0.009	7.479	8.480
1.8000000	2.381	0.009	7.491	8.954
1.8500000	2.393	0.009	7.499	9.314
1.9000000	2.400	0.010	7.505	9.533
1.9500000	2.405	0.010	7.509	9.595
2.0000000	2.408	0.009	7.510	9.485

Fixed Jacket: Collision Scenario (v)

NATURAL PERIODS : T1= 1.10102 T2= 2.84600

M1= 7.0000 M2= 32.0000

INITIAL VELOCITY= 2.0000 INITIAL ACCELERATION= 0.0

DT= 0.0005000

TIME	X(SHIP)	X(PLATF)	CONTACT FORCE	FOUNDATION REACTION
0.0500000	0.101	0.000	3.546	0.046
0.1000000	0.199	0.000	6.769	0.369
0.1500000	0.295	0.001	8.727	1.167
0.2000000	0.388	0.003	10.610	2.557
0.2500000	0.478	0.005	12.402	4.572
0.3000000	0.562	0.007	14.045	7.193
0.3500000	0.642	0.010	14.829	10.337
0.4000000	0.717	0.014	15.556	13.829
0.4500000	0.786	0.017	16.224	17.455
0.5000000	0.849	0.021	16.834	20.985
0.5500000	0.906	0.024	17.386	24.192
0.6000000	0.957	0.027	17.830	26.871
0.6500000	1.001	0.029	18.316	28.851
0.7000000	1.039	0.030	18.693	30.014
0.7500000	1.071	0.030	19.011	30.297
0.8000000	1.095	0.030	19.269	29.704
0.8500000	1.113	0.028	19.464	28.300
0.9000000	1.124	0.026	19.596	26.211
0.9500000	1.127	0.024	19.661	23.607
1.0000000	1.124	0.021	19.658	20.697

Fixed Jacket: Collision Scenario (vi)

NATURAL PERIODS : T1= 1.10587 T2= 2.83913

M1= 5.5000 M2= 32.0000

INITIAL VELOCITY= 2.0000 INITIAL ACCELERATION= 0.0

DT= 0.0005000

TIME	X(SHIP)	X(PLATF)	CONTACT FORCE	FOUNDATION REACTION
0.0500000	0.101	0.000	2.776	0.036
0.1000000	0.199	0.000	5.511	0.255
0.1500000	0.295	0.001	7.521	0.934
0.2000000	0.388	0.002	9.138	2.094
0.2500000	0.476	0.004	10.672	3.801
0.3000000	0.560	0.006	12.110	6.040
0.3500000	0.638	0.009	13.444	8.749
0.4000000	0.710	0.012	14.283	11.821
0.4500000	0.775	0.015	14.753	15.082
0.5000000	0.834	0.018	15.172	18.318
0.5500000	0.886	0.021	15.542	21.309
0.6000000	0.931	0.024	15.861	23.852
0.6500000	0.969	0.026	16.131	25.775
0.7000000	0.999	0.027	16.351	26.948
0.7500000	1.022	0.027	16.521	27.299
0.8000000	1.037	0.027	16.641	26.813
0.8500000	1.045	0.026	16.710	25.537
0.9000000	1.045	0.024	16.727	23.576

TLP: Collision Scenario (i)

NATURAL PERIODS : T1= 5.49412 T2= 97.34153

M1= 5.5000 M2= 134.6500

INITIAL VELOCITY= 2.0000 INITIAL ACCELERATION= 0.0

DT= 0.0010000

TIME	X(SHIP)	X(PLATF)	CONTACT FORCE	FOUNDATION REACTION
0.0500000	0.102	0.000	0.691	0.000
0.1000000	0.202	0.000	1.379	0.000
0.1500000	0.301	0.000	2.063	0.000
0.2000000	0.399	0.000	2.740	0.000
0.2500000	0.495	0.000	3.408	0.000
0.3000000	0.591	0.000	3.880	0.000
0.3500000	0.684	0.001	4.292	0.000
0.4000000	0.776	0.001	4.695	0.001
0.4500000	0.866	0.002	5.088	0.001
0.5000000	0.952	0.002	5.471	0.001
0.5500000	1.037	0.003	5.802	0.002
0.6000000	1.119	0.003	6.006	0.002
0.6500000	1.198	0.004	6.202	0.002
0.7000000	1.274	0.005	6.391	0.003
0.7500000	1.348	0.006	6.573	0.004
0.8000000	1.418	0.008	6.747	0.004
0.8500000	1.486	0.009	6.912	0.005
0.9000000	1.550	0.010	7.070	0.006
0.9500000	1.611	0.012	7.219	0.007
1.0000000	1.669	0.014	7.340	0.008
1.0500000	1.723	0.015	7.385	0.009
1.1000000	1.774	0.017	7.427	0.010
1.1500000	1.822	0.020	7.466	0.011
1.2000000	1.867	0.022	7.502	0.013
1.2500000	1.907	0.024	7.535	0.014
1.3000000	1.945	0.027	7.565	0.016
1.3500000	1.979	0.030	7.591	0.017
1.4000000	2.010	0.032	7.615	0.019
1.4500000	2.037	0.035	7.636	0.021
1.5000000	2.060	0.038	7.653	0.022
1.5500000	2.081	0.042	7.668	0.024
1.6000000	2.097	0.045	7.679	0.026
1.6500000	2.111	0.049	7.688	0.026
1.7000000	2.120	0.052	7.690	0.031
1.7500000	2.127	0.056	7.695	0.033
1.8000000	2.129	0.060	7.694	0.035

TLP: Collision Scenario (ii)

NATURAL PERIODS : T1= 5.11202 T2= 97.34073

M1= 5.5000 M2= 134.6500

INITIAL VELOCITY= 2.0000 INITIAL ACCELERATION= 0.0

DT= 0.0005000

TIME	X(SHIP)	X(PLATF)	CONTACT FORCE	FOUNDATION REACTION
0.0500000	0.101	0.000	0.798	0.000
0.1000000	0.201	0.000	1.592	0.000
0.1500000	0.299	0.000	2.381	0.000
0.2000000	0.397	0.000	3.161	0.000
0.2500000	0.493	0.000	3.928	0.000
0.3000000	0.588	0.001	4.681	0.000
0.3500000	0.680	0.001	5.417	0.000
0.4000000	0.770	0.001	6.131	0.001
0.4500000	0.857	0.002	6.762	0.001
0.5000000	0.942	0.002	7.333	0.001
0.5500000	1.022	0.003	7.880	0.002
0.6000000	1.099	0.004	8.401	0.002
0.6500000	1.173	0.005	8.896	0.003
0.7000000	1.242	0.006	9.361	0.004
0.7500000	1.307	0.008	9.796	0.005
0.8000000	1.368	0.010	10.200	0.006
0.8500000	1.424	0.011	10.570	0.007
0.9000000	1.475	0.013	10.907	0.008
0.9500000	1.521	0.016	11.208	0.009
1.0000000	1.562	0.018	11.473	0.010
1.0500[illegible]	1.598	0.021	11.700	0.012
1.100[illegible]	1.628	0.023	11.890	0.014
1.150[illegible]	1.654	0.026	12.042	0.015
1.200[illegible]	1.673	0.030	12.154	0.017
1.2500000	1.687	0.033	12.227	0.019
1.3000000	1.696	0.037	12.261	0.022
1.3500000	1.699	0.041	12.255	0.024

TLP: Collision Scenario (iii)

NATURAL PERIODS : T1= 6.41970 T2= 97.34392

M1= 5.5000 M2= 134.6500

INITIAL VELOCITY= 2.0000 INITIAL ACCELERATION= 0.0

DT= 0.0100000

DT= 0.0005000

TIME	X(SHIP)	X(PLATF)	CONTACT FORCE	FOUNDATION REACTION
0.0500000	0.101	0.000	0.506	0.000
0.1000000	0.201	0.000	1.011	0.000
0.1500000	0.300	0.000	1.513	0.000
0.2000000	0.399	0.000	2.011	0.000
0.2500000	0.496	0.000	2.505	0.000
0.3000000	0.593	0.000	2.993	0.000
0.3500000	0.688	0.001	3.474	0.000
0.4000000	0.781	0.001	3.946	0.000
0.4500000	0.873	0.001	4.409	0.001
0.5000000	0.963	0.002	4.861	0.001
0.5500000	1.051	0.002	5.302	0.001
0.6000000	1.136	0.003	5.730	0.002
0.6500000	1.218	0.003	6.144	0.002
0.7000000	1.298	0.004	6.530	0.002
0.7500000	1.375	0.005	6.877	0.003
0.8000000	1.448	0.006	7.209	0.004
0.8500000	1.519	0.007	7.526	0.004
0.9000000	1.586	0.009	7.826	0.005
0.9500000	1.649	0.010	8.110	0.006
1.0000000	1.709	0.012	8.376	0.007
1.0500000	1.765	0.014	8.623	0.008
1.1000000	1.817	0.016	8.853	0.009
1.1500000	1.865	0.018	9.062	0.010
1.2000000	1.909	0.020	9.253	0.012
1.2500000	1.946	0.023	9.423	0.013
1.3000000	1.984	0.025	9.573	0.015
1.3500000	2.015	0.028	9.702	0.016
1.4000000	2.041	0.031	9.810	0.018
1.4500000	2.063	0.034	9.897	0.020
1.5000000	2.081	0.038	9.963	0.022
1.5500000	2.094	0.041	10.007	0.024
1.6000000	2.103	0.045	10.029	0.026
1.6500000	2.107	0.049	10.030	0.028

TLP: Collision Scenario (iv)

NATURAL PERIODS : T1= 6.72791 T2= 97.34478

M1= 5.5000 M2= 134.6500

INITIAL VELOCITY= 2.0000 INITIAL ACCELERATION= 0.0

DT= 0.0005000

TIME	X(SHIP)	X(PLATF)	CONTACT FORCE	FOUNDATION REACTION
0.0500000	0.101	0.000	0.461	0.000
0.1000000	0.201	0.000	0.920	0.000
0.1500000	0.300	0.000	1.378	0.000
0.2000000	0.399	0.000	1.832	0.000
0.2500000	0.497	0.000	2.283	0.000
0.3000000	0.593	0.000	2.729	0.000
0.3500000	0.689	0.000	3.168	0.000
0.4000000	0.783	0.001	3.587	0.000
0.4500000	0.876	0.001	3.896	0.001
0.5000000	0.966	0.001	4.199	0.001
0.5500000	1.055	0.002	4.495	0.001
0.6000000	1.142	0.002	4.784	0.001
0.6500000	1.227	0.003	5.065	0.002
0.7000000	1.309	0.004	5.338	0.002
0.7500000	1.389	0.005	5.603	0.003
0.8000000	1.466	0.005	5.819	0.003
0.8500000	1.541	0.007	5.976	0.004
0.9000000	1.613	0.008	6.126	0.004
0.9500000	1.682	0.009	6.270	0.005
1.0000000	1.748	0.010	6.408	0.006
1.0500000	1.812	0.012	6.539	0.007
1.1000000	1.872	0.013	6.664	0.008
1.1500000	1.930	0.015	6.782	0.009
1.2000000	1.984	0.017	6.894	0.010
1.2500000	2.035	0.019	6.998	0.011
1.3000000	2.083	0.021	7.095	0.012
1.3500000	2.128	0.023	7.186	0.014
1.4000000	2.170	0.026	7.269	0.015
1.4500000	2.208	0.028	7.335	0.017
1.5000000	2.243	0.031	7.362	0.018
1.5500000	2.274	0.034	7.383	0.020
1.6000000	2.303	0.037	7.405	0.021
1.6500000	2.327	0.040	7.422	0.023
1.7000000	2.349	0.043	7.437	0.025
1.7500000	2.367	0.046	7.448	0.027
1.8000000	2.382	0.050	7.458	0.029
1.8500000	2.393	0.053	7.454	0.031
1.9000000	2.401	0.057	7.468	0.033
1.9500000	2.405	0.061	7.468	0.036

TLP: Collision Scenario (v)

NATURAL PERIODS : T1= 2.71807 T2= 97.85669

M1= 7.0000 M2= 134.6500

INITIAL VELOCITY= 2.0000 INITIAL ACCELERATION= 0.0

DT= 0.0005000

TIME	X(SHIP)	X(PLATF)	CONTACT FORCE	FOUNDATION REACTION
0.0500000	0.101	0.000	3.548	0.000
0.1000000	0.199	0.000	6.774	0.000
0.1500000	0.295	0.000	8.745	0.000
0.2000000	0.388	0.001	10.649	0.000
0.2500000	0.478	0.001	12.470	0.001
0.3000000	0.562	0.002	14.097	0.001
0.3500000	0.642	0.003	14.902	0.002
0.4000000	0.716	0.004	15.650	0.003
0.4500000	0.785	0.006	16.337	0.004
0.5000000	0.848	0.008	16.962	0.005
0.5500000	0.905	0.010	17.522	0.006
0.6000000	0.956	0.013	18.014	0.007
0.6500000	1.000	0.016	18.437	0.009
0.7000000	1.038	0.019	18.790	0.011
0.7500000	1.069	0.022	19.070	0.013
0.8000000	1.093	0.026	19.277	0.015
0.8500000	1.110	0.031	19.410	0.018
0.9000000	1.120	0.035	19.469	0.021
0.9500000	1.124	0.040	19.453	0.024

TLP: Collision Scenario (vi)

NATURAL PERIODS : T1= 2.73801 T2= 97.33621

M1= 5.5000 M2= 134.6500

INITIAL VELOCITY= 2.0000 INITIAL ACCELERATION= 0.0

DT= 0.0005000

TIME	X(SHIP)	X(PLATF)	CONTACT FORCE	FOUNDATION REACTION
0.0500000	0.101	0.000	2.777	0.000
0.1000000	0.199	0.000	5.517	0.000
0.1500000	0.295	0.000	7.534	0.000
0.2000000	0.398	0.001	9.165	0.000
0.2500000	0.476	0.001	10.721	0.001
0.3000000	0.560	0.002	12.186	0.001
0.3500000	0.638	0.003	13.550	0.002
0.4000000	0.710	0.004	14.342	0.002
0.4500000	0.775	0.005	14.824	0.003
0.5000000	0.834	0.007	15.254	0.004
0.5500000	0.885	0.009	15.630	0.005
0.6000000	0.920	0.011	15.949	0.006
0.6500000	0.957	0.014	16.212	0.008
0.7000000	0.997	0.018	16.417	0.010
0.7500000	1.020	0.020	16.563	0.011
0.8000000	1.035	0.023	16.650	0.013
0.8500000	1.042	0.027	16.678	0.016

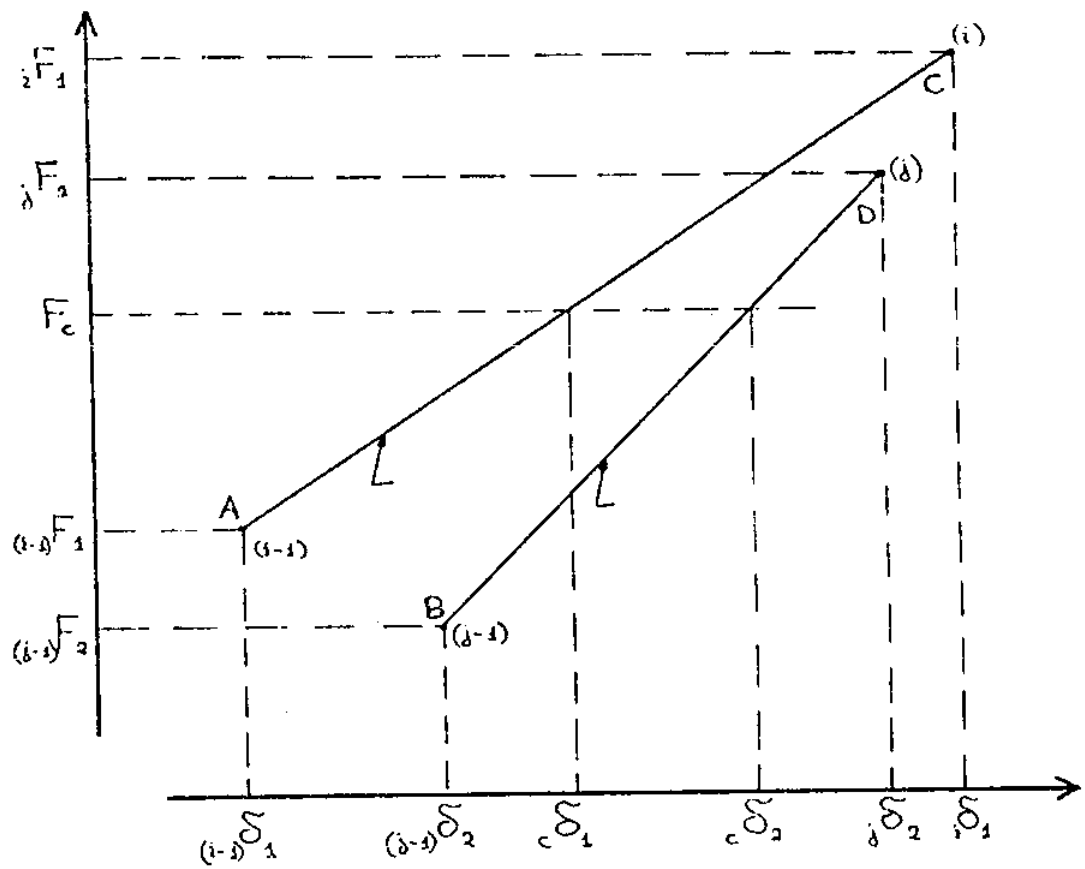

$\delta_c = {}_c\delta_1 + {}_c\delta_2$

FIGURE C1

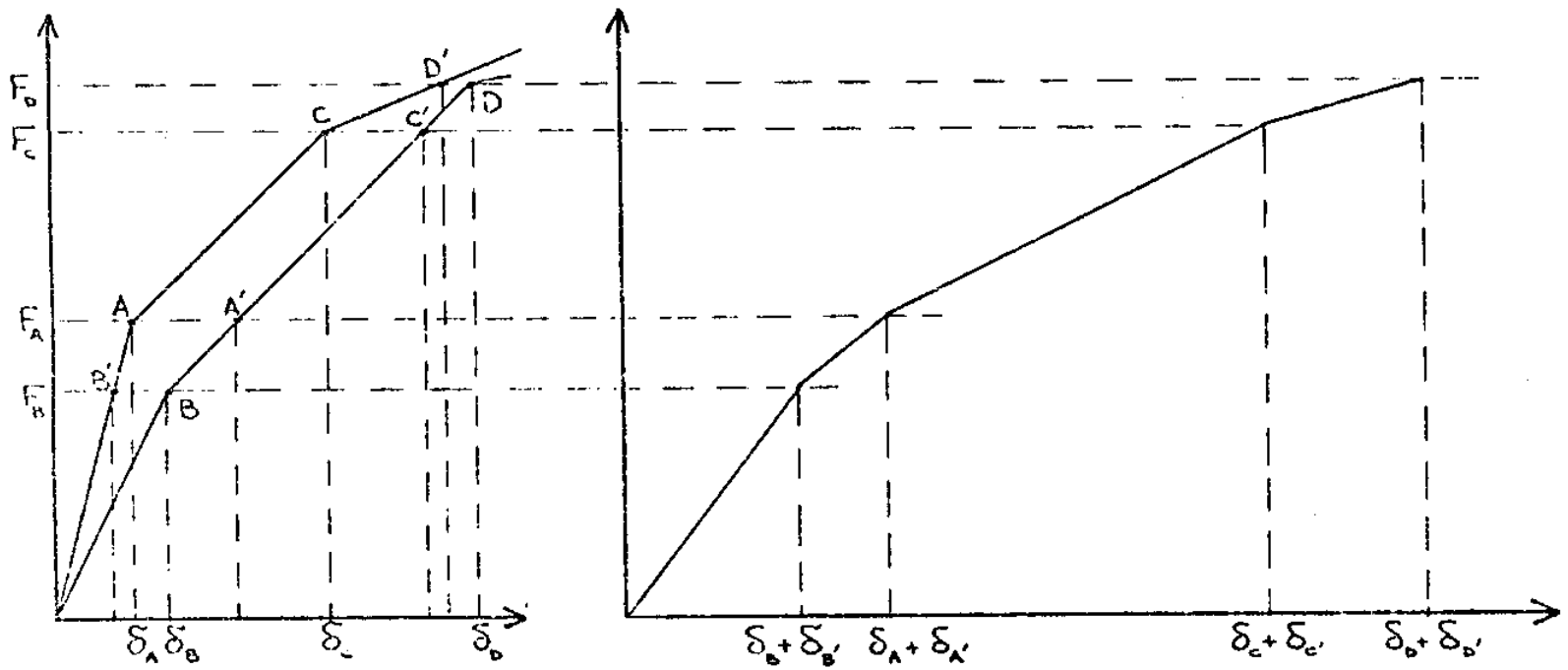

SPRINGS I AND II

COMBINED SPRINGS IN SERIES

FIGURE C2

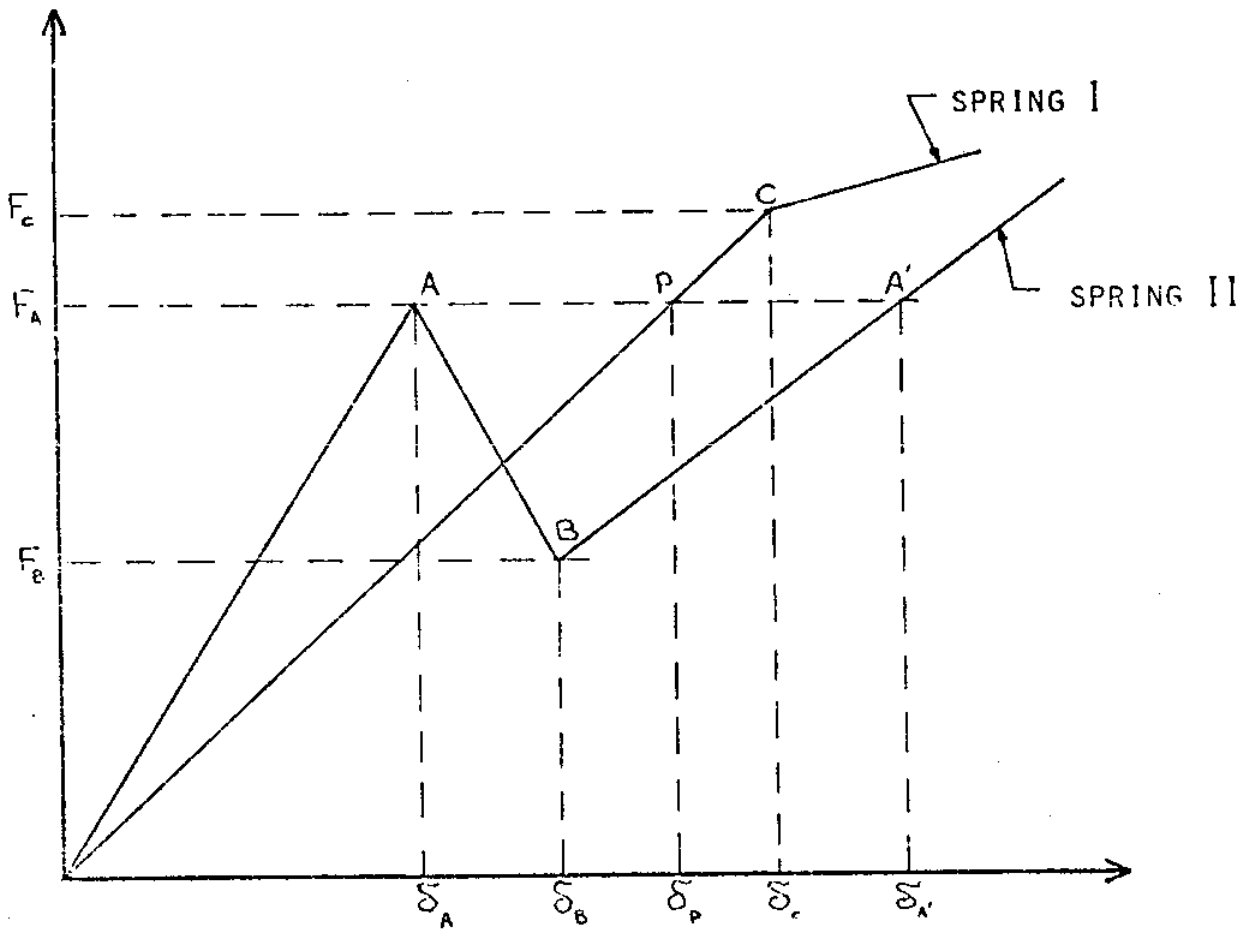
SPRING I
SPRING II
F_c
F_A
F_B
A
B
C
P
A'
δ_A
δ_B
δ_P
δ_C
$\delta_{A'}$

FIGURE C3

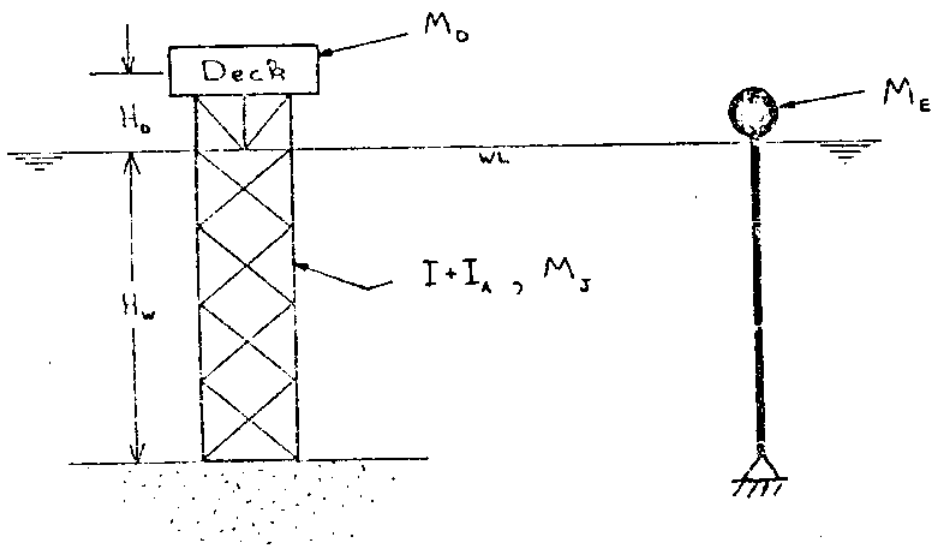

PLATFORM MODEL

FIGURE C4